

Action Spécifique Gaia

SF2A 2008

4 juillet 2008





Table des matières

| | |
|--|------|
| Préface | p 4 |
| Présentations invitées et contributions orales | p 5 |
| Posters | p 55 |





Préface

Ce fascicule rassemble l'ensemble des présentations et posters présentés lors de la Journée AS Gaia de la semaine de la SF2A 2008, ainsi que le résumé de la présentation AS Gaia à la session plénière de la SF2A. Les présentations ainsi que les textes individuels sont disponibles à l'adresse suivante : <http://wwwhip.obspm.fr/gaia/AS/SF2A-2008.html>

La Journée AS Gaia a permis de rassembler une grande partie des scientifiques travaillant sur Gaia en France, que ce soit pour la préparation de l'analyse des données ou pour celle de l'exploitation scientifique future de la mission, de situer la mission Gaia dans le contexte Européen et dans la perspective des progrès spectaculaires de l'astrométrie depuis la fin du 20^{ème} siècle, et de montrer la variété des travaux effectués dans la cadre de l'AS Gaia.

De nombreux aspects des applications scientifiques futures des données Gaia ont été présentés : sur la Galaxie et ses différentes composantes, sur la physique stellaire, mais aussi sur le Système Solaire, la relativité générale, les systèmes de référence, les observations à faire au sol en complément des observations de Gaia, en particulier pour les objets du Système Solaire, et les travaux de modélisation nécessaires à l'interprétation de ces données (atmosphères stellaires, spectres de galaxies, etc.). Différents travaux effectués dans le cadre du Consortium DPAC (Data Processing and Analysis Consortium) ont aussi été exposés : les observations au sol nécessaires à l'analyse des différents types de données qui seront obtenues par Gaia, en particulier pour la calibration des vitesses radiales ; les méthodes développées pour déterminer ces vitesses radiales ; les simulations des observations avec Gaia et des effets des radiations sur ces observations ; les observations astrométriques de WMAP effectuées au sol pour tester précision avec laquelle il est possible de déterminer la position d'un satellite situé à L2.

Félicitations à Géraldine Bourda à qui a été décerné le prix du meilleur poster pour la Session AS Gaia.

Les numéros des pages correspondent à la publication « Proceedings of the Annual meeting of the French Society of Astronomy and Astrophysics », 30 June – 4 July 2008, Paris, SF2A-2008, C. Charbonnel, F. Combes and R. Samadi (eds), disponible en ligne sur l'ADS et sur <http://proc.sf2a.asso.fr>. Lorsque le texte n'est pas disponible, l'abstract seulement est donné ci-après.

Catherine Turon et Frédéric Arenou

Présentations invitées et contributions orales

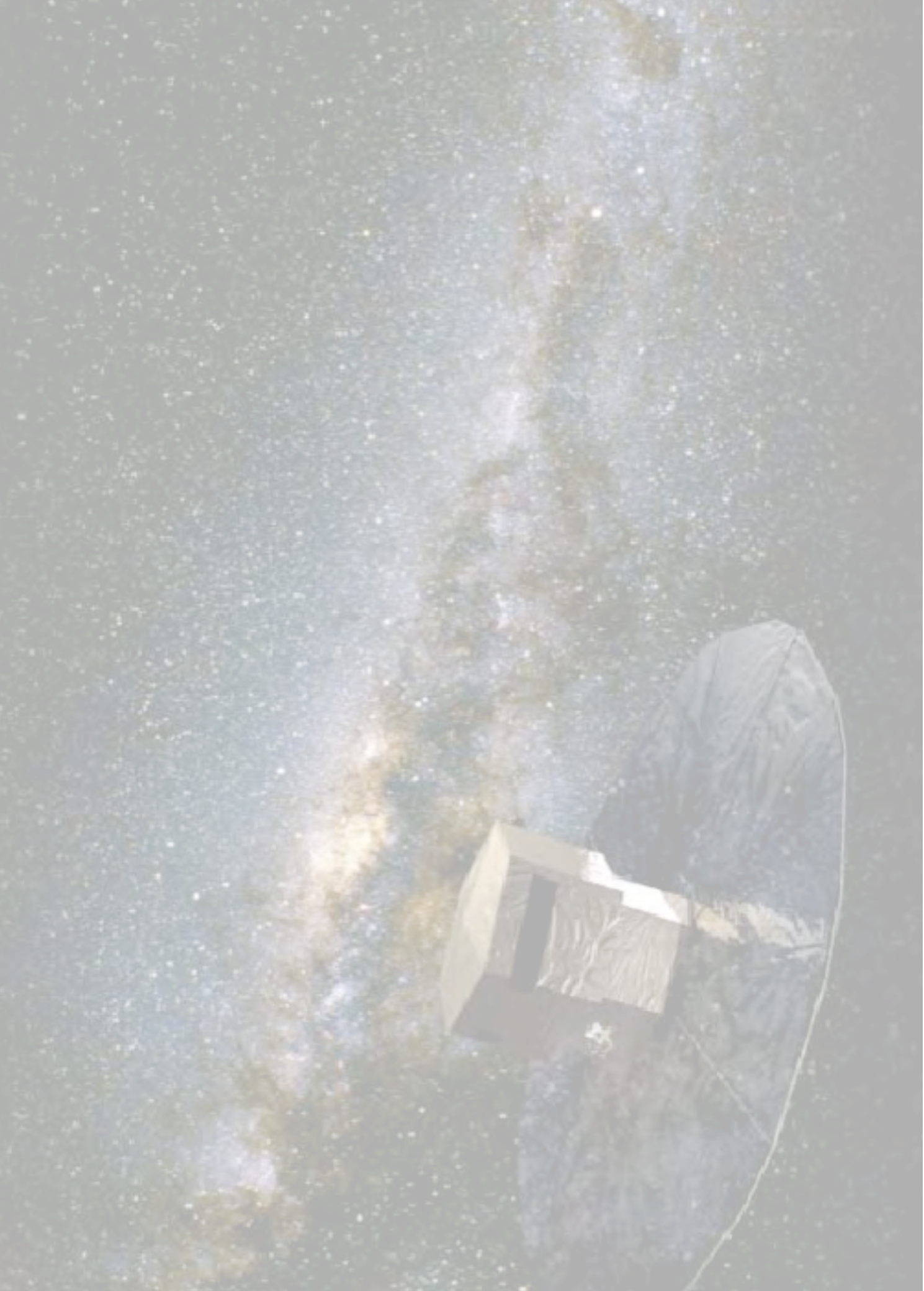
Journée AS Gaia

- Gaia in the European context – C. Turon
- The industrial point of view – X. Moisson
- Astrometry with Gaia in perspective – F. Mignard
- Physical properties of minor bodies of the solar system from Gaia observation – M. Delbò
- 3D hydrodynamical simulations of stellar surfaces : applications to Gaia – L. Bigot & F. Thévenin
- The Gaia satellite: a tool for emission line stars and hot stars – C. Martayan et al.
- A library of synthetic galaxy spectra for Gaia – B. Rocca-Volmerange et al.
- The future of optical reference systems – P. Charlot
- Relativistic aspects of the Gaia mission – C. Le Poncin-Lafitte
- Astrometry with ground based optical telescopes – F. Taris et al.
- Galactic kinematics from RAVE to Gaia-RVS data – L. Veltz et al.
- The galactic bulge as seen in optical surveys – C. Reylé et al.
- The thin and thick galactic disks: migration and lineage – M. Haywood

Présentation invitée

Session plénière

- The Solar System seen by Gaia: new perspectives for asteroid science – P. Tanga



GAIA IN THE EUROPEAN CONTEXT

Turon, C.¹

Abstract. The ESA Gaia mission is placed in the context of the European and worldwide astronomy: What are its main characteristics? What is its place within the ESA Cosmic Vision? What is its place within the Astronet roadmap context? Which actions should be supported or started for taking full benefit of this ambitious mission?

1 Introduction

In the early 90's, the unprecedented success of Hipparcos (see for example Lindegren et al. 1994; Perryman et al. 1995; Perryman et al. 1997) showed how powerful space was for astrometry and what a powerful tool for astrophysics was high accuracy astrometry, and first ideas on how a future astrometry mission could be enhanced with respect to Hipparcos were already discussed. These were including much higher astrometric accuracy, a much larger number of objects observed systematically down to a fainter magnitude, and the possibility to have the radial velocity and an astrophysical characterisation of the observed objects obtained on-board, in parallel with the astrometric measurements. Within the frame of ESA's *Horizon 2000 Plus* long-term scientific programme, a proposal was made for a new mission, Gaia, able to reach 10 μ arcsecond accuracy on positions, trigonometric parallaxes and annual proper motions for some 50 millions stars down to magnitude 15, along with multi-colour multi-epoch photometry of each object (Lindegren & Perryman 1996). The mission finally included in the ESA Science programme in October 2000 is still much more ambitious (Perryman et al. 2001), with the goal to produce a stereoscopic and kinematic census of about one billion stars, down to magnitude 20, throughout our Galaxy, and into the Local Group.

2 The Gaia mission

Gaia, planned to be launched by the end of 2011, is a unique mission thanks to several of its principles: unprecedented astrometric accuracy; three complementary instruments on board, providing parallel astrometric, photometric and spectroscopic observations, i.e. a complete characterisation of the billion objects which will be observed; a largely uniform scanning of the sky surveying all stellar populations over the whole part of the Galaxy observable at optical wavelengths; an on-board systematic detection of all objects down to magnitude 20 (Solar System objects, stars, galaxies, QSOs); a regular sampling over the five years of mission, leading to about 80 observations per object, which will allow photometric and spectroscopic variability analysis and orbit determination for double and multiple stars, giant planets and Solar System objects; global absolute astrometry with extreme accuracy, providing absolute parallaxes for stars of all spectral types, evolutionary status and populations, and absolute proper motions for stars up to the brightest parts of the nearest galaxies of the Local Group. The only parts of the Galaxy which will be poorly observed by Gaia are zones with very heavy extinction in the bulge or some parts of the disc.

The comparison with the Hipparcos performance (Perryman et al. 1997; van Leeuwen & Fantino 2005) gives a flavour of the giant step which will be achieved with Gaia (Perryman et al. 2001): number of stars (1 billion versus 118000), limiting magnitude (20 versus 12.4), astrometric accuracy (best expected accuracy of 8 μ arcsecond for stars brighter than 13 versus 0.2 mas for stars brighter than 5; 0.2 mas accuracy at magnitude 20), astrophysical characterisation (multi-colour photometry down to magnitude 20 and spectra

¹ Observatoire de Paris, GEPI, CNRS UMR 8111, 92195 Meudon, France

down to magnitude 16.5 versus 2 colours down to 12.4), observing programme (on-board systematic detection down to magnitude 20 versus preliminary ground-based star selection). In addition, the sixth dimension in the space parameter, the radial velocity, will be measured on-board for stars brighter than 16.5, in parallel with astrometric and photometric observations. Some 10 million stars will have their distances known to 1%, 100 million to 10% (to be compared with 21 000 with Hipparcos); the photometric accuracy of each of the ~ 80 observations of a star brighter than $V=15$ will be of a few milli-magnitudes in several colours; the radial velocity of stars brighter than 15 will be measured to better than 1 km.s^{-1} ; for stars brighter than $G=16$, the effective temperature will be obtained to better than 5%, their gravity ($\log g$) to 0.2-0.3, their metallicity to 0.2-0.4.

Thanks to this variety of observations, Gaia will contribute to many domains in astronomy: complete census of a large proportion of the Galaxy; characterisation of all stellar populations, both in the Galaxy itself and in the brightest parts of the nearest galaxies of the Local Group; dynamical and chemical evolution of the Galaxy; dynamics of the Galaxy and the Local Group, with a much better knowledge of the distribution of the dark matter at small and large scales; distance scale determination, using various distance candles, and impact on H_0 ; determination of the PPN parameter γ ; stellar structure and evolution; stellar variability; complete census, orbital improvement, and taxonomy of Solar System objects; etc. Finally, it will provide a systematic selection of many specific objects (very metal poor stars, stellar groups and streams, variable stars, double stars or stars with planets, etc.); the distinction between foreground Galactic stars and bright stars in dwarf spheroidal neighbours; the systematic detection of relativistic effects; etc.

3 Gaia within the international and European context

International context

Europe has been a pioneer in developing and launching a satellite entirely dedicated to high accuracy astrometric measurements. The dramatic success of Hipparcos (more than 5000 papers are using its data by mid-2008, among which nearly 2000 refereed) stimulated numerous proposals for similar missions in several countries (Russia, USA, Germany, Japan, Europe). At the moment, only a few are still considered or in development:

- JASMINE (Japan Astrometry Satellite Mission for INfrared Exploration, not totally funded) would be the ideal complement to Gaia as it will operate in the $0.9 \mu\text{m}$ z band. Thereby it will be able to observe deeply in the Galactic centre, the bulge and parts of the disc (not possible with Gaia because of heavy extinction and crowding) with astrometric accuracies similar to Gaia (Gouda et al. 2008). A nano-size satellite (5-cm telescope, 14 kg), Nano-JASMINE, is also being developed in Japan (Kobayashi et al. 2008).
- SIM PlanetQuest (Space Interferometry Mission, NASA-JPL) is a project for an optical interferometer. The goal is to measure the position, trigonometric parallax and proper motion of stars with an accuracy of $4 \mu\text{as}$ down to magnitude 20 (Shao, 2008). A SIM-Light mission is under consideration.
- J-MAPS micro-satellite to be launched by 2011 (15-cm telescope), aim at re-observing all Hipparcos stars (as well as virtually all other stars down to around 14th magnitude) with an accuracy of 1 mas down to 12th magnitude and with reduced accuracy down to 15th magnitude (USNO, Dorland & Gaume 2007).

Gaia in the ESA context

In the last ten years, there has been a festival of Solar System missions launched in the frame of the ESA Science Programme: Soho (Solar observations, with NASA, 1995), Cassini-Huygens (to Saturn and Titan, NASA-ESA, 1997), Cluster (magnetosphere observations, 2000), Mars Express (to Mars, 2003), Smart (to the Moon, 2003), Double-Star (magnetosphere observations, Chinese satellite with ESA collaboration, 2003), Rosetta (to comet Churyumov-Gerasimenko, 2004), Venus Express (to Venus, 2005). The next launches are Chandrayaan-1 (to the Moon, an Indian satellite with ESA collaboration) and Bepi-Colombo (to Mercury, with JAXA, 2013).

The astronomy missions in operation are Hubble (NASA-ESA, 1990), XMM-Newton (observations in X-rays, 1999), and Integral (observations in γ -rays, with Russia, 2002). In addition, ESA is involved in two collaborative missions: AKARI (observations in the IR, JAXA, 2006), and Corot (stellar seismology, exo-planets, CNES, 2006). Herschel (far-IR and sub-mm observations to observe star and galaxy formation) and Planck (map of the Cosmic Microwave Background anisotropies) will be launched in 2009. Gaia is then the only astronomy

mission to be launched before JWST (NASA-ESA, 2013).

Four major questions were identified in the **ESA Cosmic Vision 2015-2025** (Bignami et al., 2005): What are the conditions for planet formation and the emergence of life? How does the Solar System work? What are the fundamental physical laws of the Universe? How did the Universe originate and what is it made of? With its unique capability of surveying all stellar populations, over the whole Galaxy, Gaia will be a major contributor to the first steps of the first and last questions:

- From gas and dust to stars and planets. What are exoplanets and which stars have them?
Gaia will provide unprecedented and complete information on stars of all spectral types, even the rarest, and all evolutionary stages, even the fastest: luminosities, motions, ages, duplicity and chemical characterisation. This will give a detailed picture of which stars form and have been formed where, in each of the component of the Galaxy. Gaia will also make a systematic census of giant planets, delivering insights into the frequency of giant planets as a function of the characteristics of their host stars and their locations in the Galaxy. This will give unique information about the conditions which favour the formation of planets. In addition, since the presence and location of one or several giant planets may severely affect the formation of smaller planets in a system, GAIA will provide important information on the likelihood of finding Earth-like planets orbiting their stars in the habitable zone.
- The Universe taking shape.
Gaia will bring major inputs to the understanding of the formation and history of our own Galaxy by combining positional, kinematics and chemical information: tests of hierarchical structure formation theories and star formation history; detection of disrupted star clusters and satellite debris; firm establishment of the relations between ages, metallicity and kinematics; determination of the dynamical interactions between the bar and the bulge, the disc and the halo, the disc and the warp; etc. It will also provide insights in the distribution of invisible mass, both in our Galaxy and in the Local Group, with an improved determination of galaxy orbits. Finally, the Galaxy will be described in such exquisite detail that it will be possible to use it as a template for the interpretation of observations of external galaxies.

Gaia and ASTRONET Science Vision

ASTRONET was created to develop a comprehensive strategic plan for European astronomy covering the ambitions of all of astronomy, ground and space, and to establish the most effective approach towards answering the highest priority scientific question. The first step was the development of a *Science Vision* identifying the key astronomical questions which may be answered in the next twenty years by a combination of observations, simulations, laboratory experiments, interpretation and theory (de Zeeuw et al. 2007). Four key questions were identified where significant advances and breakthroughs can be expected in the coming two decades: Do we understand the extremes of the Universe? How do galaxies form and evolve? What is the origin and evolution of stars and planets? How do we (and the Solar System) fit in? The recommendations distinguish essential facilities, without which a certain scientific goal simply cannot be achieved, and complementary ones, which would go a long way towards answering the question, but may have their main scientific driver elsewhere.

In this frame, Gaia was considered as an *essential* facility for two main questions:

- How do galaxies form and evolve? Obtain a complete history of our Galaxy early formation and subsequent evolution.
- What is the origin and evolution of stars and planets? Understand the formation and mass distributions of single, binary or multiple stellar systems and stellar clusters. Unveil the mysteries of stellar structure and evolution, also probing stellar interiors. Explore the diversity of exo-planets, in relation with the characteristics of their host stars.

Gaia was also considered as a *complementary* facility for

- How do we fit in? Dynamical history and the composition of trans-Neptunian objects, asteroids and comets.

4 Gaia in 2012

Gaia will provide a huge quantity of unique data which, in addition to being used for themselves, will help the interpretation of many other data: by making our Galaxy a template for the interpretation of external galaxies observed by JWST, VLT, ELT, XEUS, etc; by providing an unprecedented luminosity calibration for

all stellar types from all stellar populations, further observed by the VLT, ELT, JWST, etc; by providing the 3rd dimension and 3-D kinematics to stellar formation areas observed by Herschel, Planck, and Alma; by providing an extremely accurate determination of the PNN parameter γ to be compared with the future results of LISA.

With a systematic census down to magnitude 20 and a complete characterisation of all observed objects, Gaia will be a fantastic tool to select well defined samples in targeted populations, to be further observed with other instruments. Powerful high spectral resolution spectrographs on JWST, VLT, ELT, etc. could be used to study in detail the chemical abundances of statistically significant samples selected from Gaia data: halo stars in a well defined volume; thin and thick disk samples at different distances from the Galactic plane and at different Galacto-radius; stars in streams; stars of a given metallicity; stars in a very rapid evolutionary phase. Gaia will also be able to make systematic statistics of planetary formation versus stellar type, and identify nearby systems with planets, to be further observed in more detail with JWST, ELT, SIM, Darwin, TPF, etc. Last example, Gaia will systematically observe a huge number of asteroids, further targets for observations over longer periods of time, in order to cover larger parts of their orbits.

It is then essential to get prepared for, and in some cases to start in anticipation, these ground-based observations, which will make the difference in the exploitation of Gaia data: spectroscopic observations of exoplanets detected by their astrometric motion; detailed element abundances for unbiased stellar samples; follow-up observations of variable stars, orbital systems, asteroids; etc. The other aspect is to consider spectroscopic and radial velocity observations in complement to those of Gaia for stars fainter than $V=16.5$, for example for halo streams, spiral arms, substructures in the disc or bulge, kinematics in the Local Group, etc.

5 Conclusion

Gaia is planned for launch by the end of 2011, the publication of the final catalogue for 2020. However, some intermediate publications may be expected, especially for photometric and spectroscopic data. To take full advantage of the investment made in the preparatory work on Gaia, and take a leading position in the exploitation of these unique data, thoughts and work have to be devoted *from now on* on several aspects: the development of new statistical methods to use such a mass of data, the improvement of theories and modelling of the Galaxy dynamical and chemical behaviour, the choice of the best methods to use Gaia data for the definition of the optical reference system, the definition - and organisation - of the most adapted follow-up and complementary ground-based or space observations. Finally, in addition to the future use of already existing instrument, it would be extremely valuable to define a multi-object wide-field spectrograph, able to observe simultaneously a few thousands stars, well suited for follow-up and complementary observations of Gaia selected samples. This is supported by the recommendations of the ASTRONET Infrastructure Roadmap (Bode et al. 2008) and by ESA-ESO Working Group Report on Galactic science (Turon et al. 2008). The French - and European - community put a major effort in the preparation of the Gaia data processing. Let us be in the best position to use these data in the many domains where it will provide a complete renewal of the observational basis.

References

- ASTRONET Science Vision 2007, *A Science Vision for European Astronomy*, de Zeeuw P.T. & Molster, F.J. (eds)
 Bignami, G.F., Cargill, P.J., Schutz, B., & Turon, C., 2005, Cosmic Vision, ESA BR 247, A. Wilson ed.
 ASTRONET Infrastructure Roadmap 2008, Bode, M. & Cruz, M. (eds)
 Dorland, B.N. & Gaume, R.A. 2007, AIAA Space 2007 Conf., 18-20 sept. 2007, AIAA 2007-9927
 Gouda, N., Kobayashi, Y., Yamada, Y., et al. 2008, IAU Symp., 248, 248
 Kobayashi, Y., Gouda, N., Yano, T., et al. 2008, IAU Symp., 248, 270
 Lindegren, L., Kovalevsky, J., Høg, E., Turon, C. & Perryman, M.A.C. 1994, ESA Bull., 77, 42
 Lindegren, L., & Perryman, M.A.C. 1996, A&A Suppl., 116, 579
 Perryman, M.A.C., Lindegren, L., Kovalevsky, J., et al. 1995, A&A, 304, 69
 Perryman, M.A.C., Lindegren, L., Kovalevsky, J., et al. 1997, A&A, 323, L49
 Perryman, M.A.C., de Boer, K.S., Gilmore, G., et al. 2001, A&A, 369, 339
 Shao, M. 2008, IAU Symp., 248, 231
 Turon, C., Primas, F., Binney, J., et al. 2008, ESA-ESO Working Group Report on Galactic science
 van Leeuwen, F., & Fantino, E. 2005, A&A, 439, 791

ASTROMETRY WITH Gaia IN PERSPECTIVE

Mignard, F.¹

Abstract. The astrometric accuracy of Gaia is placed in perspective by showing its expected performances in relation with the slow and unsteady historical progress, specifically in two areas: (i) the realisation of the reference frame, (ii) the measurement of trigonometric parallaxes. It appears clearly that both Hipparcos and Gaia are truly epoch-making steps in this age-old quest for accurate star position. No earlier generation of astrometrists has witnessed such a dramatic improvement over so short a period of time.

1 Introduction

With Gaia expected for a launch in less than four years, astrometry will benefit from a new decisive boost into the highest achievable accuracy, recurring just two decades after a similar outstanding landmark with Hipparcos. This will be the (provisionally) final result of a long quest that can be traced back to the origin of position astronomy.

As it stands today, Gaia is a powerful astronomical space project dedicated to high precision astrometry, photometry and spectroscopy. Starting in about 2012, Gaia will survey the whole sky and detect any sufficiently point-like sources brighter than the 20th magnitude with repeated observations over the 5-year mission. The astrometric precision of $25\mu\text{as}$ at 15 magnitude will improve on Hipparcos by nearly two orders of magnitude providing position, proper motions and parallaxes. These observations consist primarily of 1D accurate determination of the image location at the transit time on a frame rigidly attached to the payload together with an estimate of the source brightness. A global adjustment of these elementary observations produces the final astrometric solution with the five astrometric parameters for all the well-behaved stars. This rigid sphere is made inertial through the observations of distant, extragalactic, and non-moving quasars in the visible range.

For astrometry Gaia will be in 2020 the current best astrometric catalogue and the crowning of centuries of painstaking effort by generations of astronomers and instrumentalists to achieve the highest accuracy in pinpointing the stars. In this few pages I attempt to place Gaia in perspective by illustrating the major stages in the construction of reference frames and the measurement of stellar distances.

2 High precision astrometry

It is impossible to trace back the very moment when humankind started recording the position of heavenly bodies, and in the word *recording* we include organized oral transmission as a true mean to hand down a knowledge to posterity. It cannot be doubted however that the daily motion of the celestial sphere, the regular return of the sun in the morning were a shared knowledge within the small groups of humans. Very little is recorded before the apparition of true writing, although several megalithic monuments bear witness of the narrow relationship between the Neolithic man and the cosmos when distinction between science and myths or religion simply did not exist. Whatever the goal of these observations, the monuments can be viewed, at least partly, as astronomical observatories using long baselines to make accurate records of astronomical events from the alignments between markers. In short these early men were the forerunners of astrometry, that branch of astronomy dealing with the determination of the positions, distances and motions of celestial bodies.

This is one the oldest fields of scientific investigations, known for centuries as positional astronomy with social importance for astrology or timekeeping. Until the mid-19th century an astronomer was primarily a man

¹ OCA/Cassiopée, BP404, Nice Cedex

able to describe the celestial sphere and its diurnal rotation to make predictions for the returns of the seasons, the planet wandering or the occurrence of eclipses. As positions and motions are not absolute concepts they can only be described with respect to some reference using a system of coordinates that can be constructed with much freedom.

Astrometry as it is understood today dates back at least to Hipparchus, who compiled in the 2nd century BC the first catalogue of stars visible to him and invented the stellar brightness scale basically still in use today. Hipparchus catalogue has come down to us through Ptolemy who published it in the 2nd century as part of his *Almagest*. (This sequence of events is, and by far, not shared by every historian, but seems to me very probable). This Hipparchus/Ptolemy Catalogue remained the standard star catalogue in the Western and Muslim worlds for over a thousand years, copied and updated by adding the effect of precession to the longitudes, until new observations by Ulugh Begh in Samarkand (early 15th century) and later by Tycho Brahe (late 16th century) led to the production of truly new catalogues of the stars accessible to the unaided eye.

Modern position astronomy, or in short astrometry, was founded by W.F. Bessel (see a short biography in Fricke, 1985) with his *Fundamenta astronomiae*, in which he gave the mean position of 3222 stars observed between 1750 and 1762 by James Bradley at Greenwich. Bessel is also credited and best remembered for the first real measurement of a stellar distance carried out on 61 Cyg in 1838, by which he opened up a totally new window on the scale of the Universe. Apart from the fundamental function of providing astronomers with a

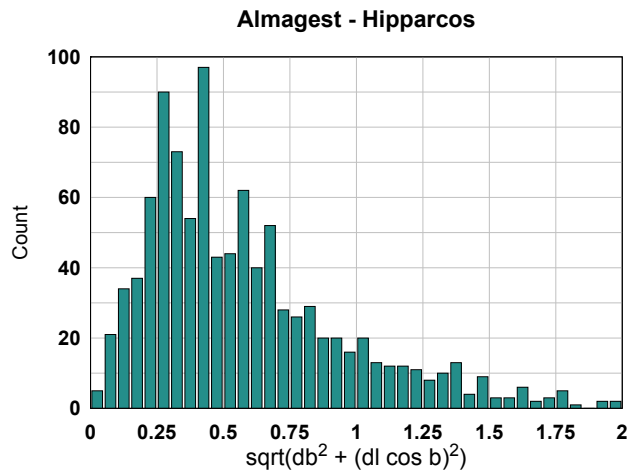


Fig. 1. Accuracy of the *Almagest* star catalogue (in degrees). The histogram is based on a comparison of the positions provided by Ptolemy to those computed with the Hipparcos Catalogue. The date for the precession has been adjusted to give a zero mean in the residuals in longitude.

reference frame to relate their observations, astrometry is also fundamental for fields like celestial mechanics, stellar dynamics and galactic astronomy. In observational astronomy, astrometric techniques help identify stellar objects by their unique motions or predict the orbit of spacecrafts. Astrometry is also involved in creating the cosmic distance ladder because it is used to establish trigonometric reference distances for stars in the Milky Way, that is to say it sets the first rung of the ladder needed to determine the distances of the more distant sources belonging to the next rung. On a more mundane side, astrometry is still instrumental for keeping time, in that the UTC timescale used worldwide in science or for civilian activities is basically the atomic time synchronized to Earth's rotation by means of exact astrometric observations.

Since the early times star catalogues have never ceased to be used to chart the sky and to serve as reference maps to refer the motions of celestial bodies or the positions of fainter stars. As everywhere in science, refinements in the instruments and in computational techniques have been the main source of improvement of the astrometric accuracy from about one half of a degree at the time of Hipparchus to about $0''.05$ for the best ground based measurements of the early 1980s. The improvement in the realisation of the reference frame with fundamental catalogues is clearly visible in the list of Table 1.

Over the last two decades new astrometric techniques like radio interferometry on the ground or global astrometry in space in the visible has brought a considerable improvement with positional accuracy at the

0''001 level. This enormous improvement in few years contrasts with the slow and steady progress which has been the rule for centuries and in the 20th century diverted young astronomers from starting a career in astrometry as they were lured by the nearly monthly breakthroughs in astrophysics.

3 Global space astrometry

The possibility to achieve global astrometry with a spinning satellite doing one dimensional measurements is not a trivial thing and has been the subject of animated discussions, and even challenged, before Hipparcos. The genesis from the initial proposal by P. Lacroute in 1967 to the Hipparcos selection is detailed in Turon & Arenou (2008) with first hand information. The principle which leads to absolute astrometry and nearly absolute parallaxes is still very subtle and deserves attention, all the more as it remains the Gaia baseline.

Table 1. List of the precision astrometry catalogues.

| Year | Name | Number of stars | Comment |
|------|----------------|--------------------|---|
| 1790 | Maskelyne | 36 | zodiacal stars, one epoch |
| 1818 | Bradley/Bessel | 3000 | no PM, nearly fundamental for one epoch |
| 1830 | Bessel | 36 | with PM, + precession |
| 1878 | FK1 | 539 | Start of the FK series |
| 1898 | Newcomb | 1297 | Start of the GC series |
| 1907 | FK2 | 925 | |
| 1937 | FK3 | 873 | 1st IAU supported international RF |
| 1963 | FK4 | 1535 | $\sigma_{1950} \sim 0''.07 - 0''.15$, $\sigma_{2000} \sim 0''.15 - 0''.30$ |
| 1988 | FK5 | 1535 | $\sigma_{2000} \sim 0''.05 - 0''.10$ |
| 1997 | Hipparcos | 100,000 | Quasi fundamental catalogue |
| 1998 | ICRF | 212 ⁽¹⁾ | First extragalactic primary reference frame |

¹ This is the number of defining sources. The full ICRF has now more than 700 sources.

If one knows how the spacecraft rotates, meaning its rigid body attitude is available at any time, then from a local observation of point-source images onto the focal plane and a good time recording, it is clear that the position of each source can be recovered in the same reference frame in which the spacecraft attitude is given. Conversely with an on-board stellar catalogue and a star tracker rigidly connected to the spacecraft, one could know the attitude with great accuracy. In the case of Hipparcos or Gaia neither of the two is initially available (the Input Catalogue of Hipparcos was just a list of program stars, not an astrometric catalogue matching the observing accuracy). There is apparently a vicious loop since ultimately one wishes to determine the position of the stars and to know the spacecraft attitude. In practice this works thanks to the circle closure.

Consider the simpler case of a satellite rotating around a fixed spin axis and stars distributed on the perpendicular great circle, just in one dimension. After one revolution a star transits again in the telescope field of view, and between the two epochs one knows that the satellite has exactly rotated by 360 degrees (within a small amount related to the star proper motion). Since the time is recorded, one knows also the mean rotation rate averaged out over one revolution. But we have many stars at different longitudes on this circle, and each of them produces an average rate at a different time. One sees that it is therefore possible to reconstruct precisely the rotation of the satellite from purely geometrical and kinematical arguments. If one knows from a dynamical modeling that the rotation is smooth and that it can be modeled with few parameters, it becomes easy to fit these parameters. Within a single convention about the origin, one ends up also with the positions of the individual stars on the circle together with their proper motions. With Hipparcos and Gaia one has also the basic angle which tells us that a known rotation has taken place between an observation in the preceding and following field.

Finally the angular distance between pairs of stars will be quickly known if the star density is such that several stars are simultaneously measurable in both fields of view. Even in the simplified 1D celestial *circle* one sees that as soon as the number of arcs is large enough, there is only one way to place the stars, keeping at the end just one degree of freedom for the global rotation (or two if the stars have a proper motion).

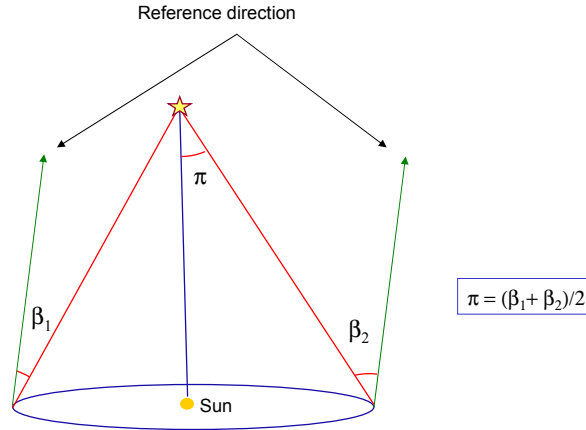


Fig. 2. Principle of measurement of absolute parallaxes. The star parallactic motion is monitored against an absolute reference frame or an absolute direction that can be accessed over the different observations. No other distant star is involved in the process and this should permit to obtain the true parallax of the star. This needs some form of global astrometry to maintain a consistent reference frame over the set of observations.

The same principle extends to the real celestial sphere, although there are several complications arising from the time change of the basic angle. Therefore the attitude reconstruction plays a very important and critical role in the reduction of a space astrometry mission aiming to carry out global astrometry. It is through the attitude reconstruction that the observations from the two fields of view become properly linked. It is therefore not helpful if one field of view contains many more stars than the other. To accommodate this for the Hipparcos mission, an Input Catalogue was created such that the stars were more or less evenly distributed over the sky. For Gaia a dedicated subset of stars will be used to solve for the attitude and the instrument parameters. Then the attitude solution will be used to find the astrometric parameters of the remaining stars.

4 Absolute and relative parallaxes

In many astronomy textbooks the principle of measuring stellar parallaxes is nicely presented, although there is little effort done to draw attention on the difference between relative and absolute parallaxes.

The parallactic effect is the difference in the direction of a distant celestial object as seen from two different viewpoints, that is to say the difference between two unit vectors. In classical astronomy the usual viewpoint was an observing place on the Earth, and the reference point was taken as the centre of the sun or, better, the barycentre of the solar system. Because of the annual motion, the parallactic vector is not constant during the year and the elliptical apparent displacement of the star cannot be incorporated into a linear proper motion. Quite naturally, one adopts as the standard direction of the star that defined in the barycentric frame. The annual parallax, usually referred to as the parallax, is the angle subtended at a star by one astronomical unit and is formally equivalent to the distance to the star. In principle a determination of this angle can be obtained by triangulation as illustrated in Fig. 2 which sketches the variation in the absolute direction of a nearby star. The possibility to do such a measurement implies that a reference direction can be materialised and transported in some way through the different observations while the Earth moves about the Sun. Given the size of the parallax, even for the nearest star, this is very hard to achieve. Typical measurements of this kind were carried out in the early days of the parallax search and later in the XIXth century successfully. The reference direction was either the local vertical (search of Bradley for example) or the spin axis of the Earth (measurement of stellar declination). This was the method used with success by T. Henderson at the Cape from which he determined

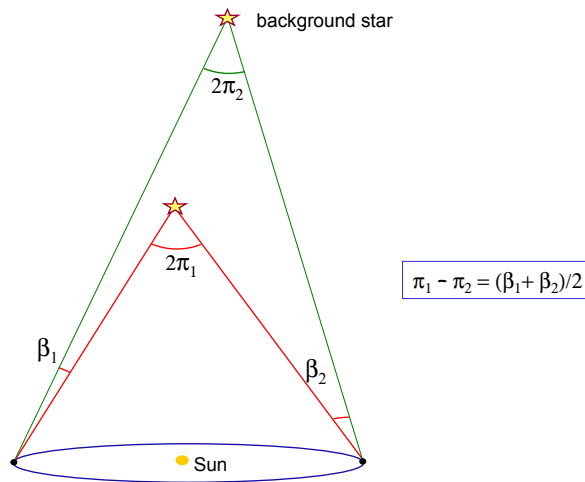


Fig. 3. Principle of measurements of relative parallaxes by referring the parallactic motion of a nearby star to a distant background star. This technique has been first described by Galileo in the *Dialogo* and considered as more promising than the absolute method. By nature it involves small field astrometry and requires an assumption about the distance of the background stars.

the parallax of α centauri in 1839 and later by others with meridian circles or zenithal telescope.

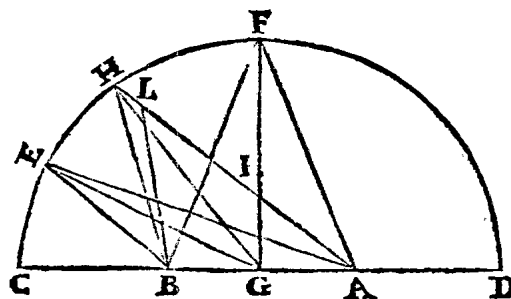


Fig. 4. Original drawing in the *Dialogo* (Third day) where Galileo describes the alteration in star elevation due to the motion of the Earth about the Sun. A and B are two points diametrically opposite on the ecliptic from where stars E, H or F (the latter at the ecliptic pole) are observed at six months interval. Galileo stresses that the change of directions should be visible in the direction of rising or setting of the star and that landscape features, like a remote hill, could be used as the arms of a gigantic quadrant.

In the *Dialogues* Galileo is probably the first to investigate rather deeply the consequences of the annual motion of the Earth on the position of the fixed stars. The qualitative features (i.e. the reflex stellar displacement) have been known for long, but Galileo set himself the objective of ascertaining the observable changes and how to actually do the measurements (Figs. 4- 5).

It took in practice more than 150 years between the first attempts to detect the parallactic motion and its undisputable first measurement by W.F. Bessel in 1838 on the star 61 Cygni. He was shortly followed in publication by F. Struve for Vega and T. Henderson in α Centauri. Work on measuring parallaxes proceeded very slowly with about 20 parallaxes available 10 years later and around 100 at the turn of the century. The number of known parallaxes varies greatly from one author to another since some quote the number found in the early compilation, while other attempt to tell how many *reliable* parallaxes are available at a particular time (Table 2). In the early days, for each star all the published parallaxes are listed and not necessarily discussed.

*perchè io non credo, che le
stelle siano sparse in una sferica superficie egualmente distan-
ti da un centro, ma s'imo, che le loro lontananze da noi siano
talmente varie, che alcune ve ne possano esser 2. e 3. volte più
remote di alcune altre; talchè quando si trouasse co'l Tele-
scopio qualche piccolissima stella, vicinissima ad alcuna delle mag-
giori, e che però quella fusse altissima, potrebbe accadere, che
qualche sensibil mutazione succedesse tra di loro, rispondente
a quella de i pianeti superiori.*

Fig. 5. Original text in the Dialogo (Third day) where Galileo describes the relative parallaxes with reference to the geocentric motion of the planets. The text reads: *I do not believe that the stars are spread over a spherical surface at equal distances from one center; I suppose their distances from us to vary so much that some are 2 or 3 times as remote as the others. Thus if some tiny star were found by the telescope quite close to some of the larger ones, and if that one were therefore very remote it might happen that some sensible alteration would take place among them corresponding to those of the outer planets.* Translation of S. Drake, Univ. of California Press.

Several technics are involved with relative or absolute measurements and very often with scatter larger than the quoted individual precision, when available. In the modern era, the Catalogue entries are based on critical examination of the available values and lead to an adopted value with an estimated accuracy. For example the 4th General Catalogue of Trigonometric Parallaxes contains 15430 determinations of parallaxes for 7888 stars.

Table 2. Progress in the number of available stellar parallaxes.

| Year | Number | Comment |
|------|---------|---|
| 1840 | 3 | Published parallaxes |
| 1850 | 20 | Catalogue of Peters |
| 1888 | 40 | Catalogue of Oudemans |
| 1910 | 100 | of which 52 photog. parall. from Katelyn |
| 1912 | 250 | Catalogue of Bigourdan |
| 1917 | 500 | Catalogue of Walkey |
| 1924 | 1870 | Catalogue of Schlesinger |
| 1930 | 2000 | From here it may include spectroscopic parallaxes |
| 1952 | 5800 | Yale Parallax Catalog (Jenkins) |
| 1965 | 7000 | Yale Parallax Catalog (Jenkins) |
| 1993 | 8000 | Yale Parallax Catalog (van Altena et al.) |
| 1997 | 110,000 | Hipparcos |

References

- van Altena, W. F., Lee, J. T. & Hoffleit, E. D., 1995, The General Catalogue of Trigonometric Stellar Parallaxes, 4th ed., New Haven, Yale Univ. Obs.
- Fricke, W., 1985, Friedrich Wilhelm Bessel, *Astrophysics and Space Science*, 110, 11-19.
- Turon, C. & Arenou, F., 2008, The Hipparcos Catalogue: 10th anniversary and its legacy, in Proc. of IAU Symposium No. 248, W.J. Jin, I. Platais & M. A. C. Perryman, eds.

PHYSICAL PROPERTIES OF MINOR BODIES OF THE SOLAR SYSTEM FROM GAIA OBSERVATIONS

Delbò, M.¹, Tanga, P.¹, Bendjoya, P.², Cellino, A.³, Dell' Oro, A.³, Hestroffer, D.⁴, Mignard, F.¹,
Mouret, S.⁵, Michel, O.² and Ordenovic, C.^{1,5}

Abstract. The space mission Gaia of the ESA has been mainly conceived for stellar astrometry and astrophysics, but it will also represent a milestone for the studies of the physics of the minor bodies in our solar system. More than 200 000 asteroids will be surveyed with repeated observations. Gaia observations will allow the direct measurement of sizes for the largest 1000 asteroids, and the derivation of the masses for about 100 bodies from the measurement of tiny perturbations imparted on smaller asteroids at the epochs of mutual close encounters. Moreover, from Gaia disk integrated photometry it will be possible to derive asteroids' gross shapes and rotation states. This information will be very important to constrain asteroid collisional evolution as well as other processes that are thought to affect the shape and spin vector distributions of multi-km sized asteroids, including the YORP effect. The latter is a radiation pressure effect able to spin up (and down) small asteroids, and possibly cause rotational fission and production of binary systems. Gaia spectroscopic data will allow a new asteroid taxonomy for almost all the observed objects, representing almost two order of magnitude increase in the number of asteroids for which this information is available to date. Because taxonomic classes are related to surface composition and space weathering effects, Gaia data will probe asteroid mineralogy for bodies as small as 5 km in the Main Belt, allowing studies of compositional gradients, dynamical and collisional mixing, space weathering effects and linking to dynamical asteroid families. The derivation of the average densities for about 100 asteroids belonging to a wide variety of taxonomic classes will also allow for the first time to link the taxonomic classification to bulk physical properties and internal macro-porosity, with deep implications for the overall interpretation of surface properties in terms of internal composition, overall structure, and likely thermal histories. Last but not least, the final harvest will also include physical properties of near-Earth asteroids and likely discoveries of objects orbiting at heliocentric distances less than 1 AU.

¹ OCA/Cassiope, BP 4229, 06304 Nice cedex 04, France

² OCA/Fizeau-UMR CNRS 6525, Universit de Nice-Sophia Antipolis, Parc Valrose, 06108 Nice

³ INAF, Osservatorio Astronomico di Torino, 10025 Pino Torinese (TO), Italy

⁴ IMCCE, Observatoire de Paris, UPMC, USTL, CNRS, 77 av. Denfert-Rochereau, 75014 Paris, France

⁵ Helsinki University Observatory, Finland

3D HYDRODYNAMICAL SIMULATIONS OF STELLAR SURFACES : APPLICATIONS TO *GAIA*

Bigot, L. & Thévenin, F.¹

Abstract.

We use 3D time-dependent hydrodynamical simulations to model the photospheres of late type stars in a very realistic way. We apply these simulations to study the 3D line formation in the spectral domain of the spectrometer on board in the space mission *Gaia*.

1 Introduction

The *Gaia* space mission (Perryman et al. 2001) will provide an unprecedented opportunity to map the actual chemical composition of million of stars throughout the Milky Way. Knowing the distances thanks to the astrometric instrument, the photometer on board will provide the fundamental stellar parameters such as the effective temperature, gravity and average metallicity. The Radial Velocity Spectrometer (RVS) will allow a determination of the chemical abundances by observing individual spectral lines (Katz et al. 2004, Wilkinson et al. 2005). Collecting these stellar abundances, it will be then possible to map of the chemical composition of our Galaxy for million of stars (up to $V=12-13$), i.e. to a scale never reached before. The knowledge of this chemical composition of the Galaxy from the disk to the halo will provide information on its formation and history. Regarding the importance of the mission and its goals, it is mandatory to have the best models to extract the physical parameters of the observed stars. It is worth mentioning that these abundances are *not* observed but *interpret* through models. The model atmospheres must therefore be as realistic as possible. The convection plays an essential role in the line forming process and deeply influences the shape, shift and asymmetry of lines in late type stars which will represent most of the stars that will be observed by *Gaia*. To date, most of the abundance determinations are done in 1D *hydrostatic* models in LTE or NLTE. These models have difficulties to fit the shape of the observed lines and more important they require the use of adjustable parameters such as the micro and macro turbulence which are used to mimic the effects of the convection. This is an important source of uncertainties in the diagnostic. This problem can be avoided by using 3D radiative hydrodynamical (RHD) models that naturally account for turbulent motions. Another important aspect of the 3D RHD simulations is that they can correct the convective shifts (few hundreds m/s) of the lines which has to be subtracted to the global lineshifts when determining the stellar radial velocities. A realistic modelling of stellar atmospheres is therefore crucial for a better interpretation of future data.

In this paper, we present preliminary work which consists in using state-of-the-art 3D RHD simulations to calculate synthetic line profiles in the wavelength region of *Gaia*/RVS. We first focus on the Ca II triplet and then discuss the use of these models to derive accurate radial velocities, corrected from convective lineshifts.

2 The 3D modelling of the stellar atmospheres

Realistic modelling of the solar and stellar surfaces has been developed since the early eighties by Nordlund and coworkers (Nordlund 1982, Stein & Nordlund 1989, Nordlund & Dravins 1990, Stein & Nordlund 1998, Asplund et al. 2000). They found great success in reproducing observed constraints such as granulation topology, spectral lines, helioseismic data. In the present work, we use a code that solves the equations for mass, momentum and internal energy in a conservative form, for fully 3D compressible flow on a staggered mesh (Nordlund &

¹ Université Nice Sophia Antipolis, Observatoire de la Côte d'Azur, BP 4229, 06304, Nice cedex 4

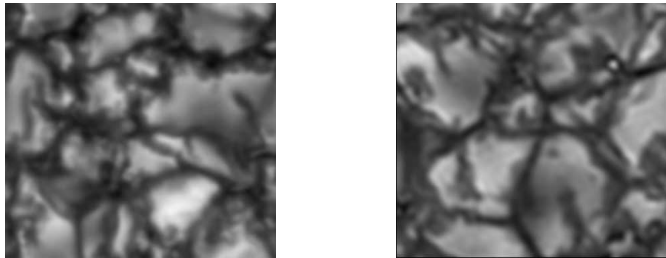


Fig. 1. Comparison between synthetic disk-center emergent intensity (left panel) and the observed equivalent (Right panel) made at the Solar Swedish Telescope (SST). Each panel represents an area of 6000×6000 kms. (Left) Synthetic image obtained by a 3D RHD simulation (Bigot, unpublished) with a grid resolution of $512^2 \times 384$ (11.6 kms horizontal). The synthetic image is smoothed by an Airy function that mimics the PSF of the SST. (Right) G-band (4305 Å) image obtained at the SST using adaptative optics and speckle reconstruction. This image (unpublished) is kindly provided by J. Hirzberger. Data of the same observations may be found in Wiehr et al. (2004) and Hirzberger & Wiehr (2005). The resolution is $0.041''$ (30kms).

Galsgaard 1995). The code uses 6th order finite differences and 5th order interpolation. The time advance is done by a 3rd order Runge-Kutta scheme. Horizontal boundary conditions are periodic whereas top and bottom boundary conditions are transmitting. We use ghost zones at the top and the bottom of the domain in order to use the same spatial derivative scheme at the boundaries and in the interior. The code is stabilized by numerical diffusion of the Von Neumann and Richtmyer type in the momentum and energy equations. The Uppsala's equation-of-states and opacities are used (Gustafsson et al. 1975 + updates). The radiative transfer is solved by using wavelength binning technique (Nordlund 1982).

Each model is defined by the entropy at the bottom of the simulation domain, the gravity and the chemical composition. We note that the effective temperature is not an input in our model but rather an output fluctuating around a mean value. For each stellar model, the time sequence spans several hours, enough to cover several convective turn-overs. An illustration of the realism of the 3D RHD simulation is shown in Fig. 1.

In order to calculate synthetic spectra, we extract from the 3D RHD simulation a run of about 1 hour, with snapshots stored every 10 min. For each of them, the radiative line transfer was solved with long characteristics using a Feautrier scheme. Pure LTE (no scattering) is assumed. We use the most recent quantum mechanical calculations of hydrogen collisions with neutral species (Barklem & O'Mara 1997, Barklem et al. 1998) to account for Van der Waals broadening. This is a great improvement compared with the traditional Unsöld recipe since we no longer need an enhancement factor. The disk-center or disk-integrated intensities are computed for each grid point at the surface. The 2D time-dependent surface intensity profiles are then spatially and temporally averaged before comparison with observations.

3 Applications to *Gaia*/RVS

There are several advantages to use 3D RHD simulations in stellar abundance and radial velocity determinations. These simulations lead to a very good fit of the observed lines in shape, depth, shifts and asymmetry as shown by Asplund and coworkers in a series of papers (e.g. Asplund et al. 2000, 2004) and by Bigot & Thévenin (2006) for the RVS spectral domain. Moreover, on the contrary to hydrostatic models, the 3D hydrodynamical ones naturally account for turbulent motions and therefore do not need the use of the traditional micro and macro turbulence. These adjustable quantities, which are unavoidable in 1D hydrostatic models, lead to some uncertainties in the diagnostic of stellar parameter determinations, in particular for abundance determinations.

Another important advantage is the possibility to calculate the convective shifts of the spectral lines. These shifts are of the order of a few hundreds m/s to a few km/s for late type stars. Since the RVS aims at determining the stellar radial velocities (V_{rad}) of the Galaxy, it is particularly important to use these simulations to subtract the doppler shifts coming from the hydrodynamic motions *inside* the star. The precision expected for *Gaia*/RVS will be of the order of 1km/s (up to $V=15$ depending on spectral type).

In the following sections we apply these 3D hydrodynamical simulations to two cases of interest for *Gaia*/RVS which are the fit of the Ca II triplet and the convective shift correction for radial velocity determination.

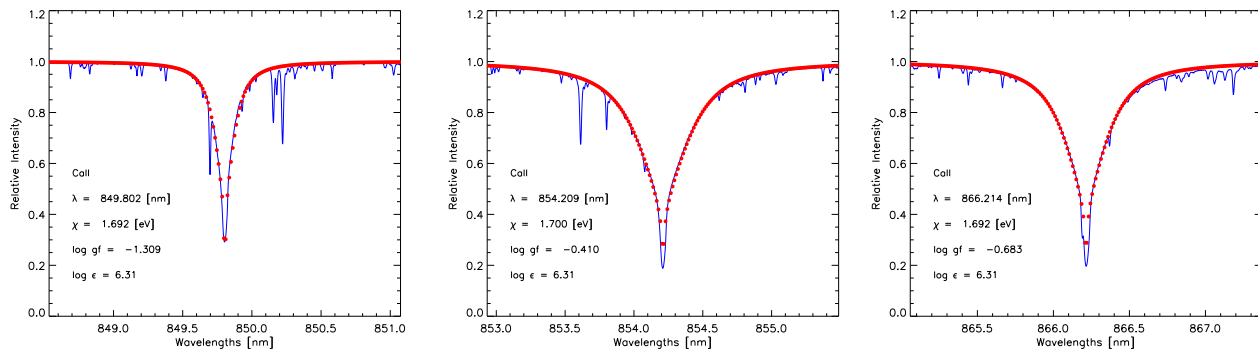


Fig. 2. Fits of the synthetic (●) disk-center Ca II triplet with solar spectrum (full line). The central depression is not well fitted since the line cores are formed in non-LTE conditions.

3.1 The calcium II triplet

The RVS spectral domain has been chosen mainly for the presence of the calcium II triplet ($\lambda = 849.802, 854.209, 866.214$ nm). This strong triplet will be visible in most stars, even in metal poor stars. We then pay a special attention to the calculation of synthetic profiles for these three lines (Bigot & Thévenin, 2008). In this work, we decided to fit the solar Ca II triplet by fixing the abundance of calcium ($[Ca/H]=6.31$) and by adjusting the oscillator strengths ($\log gf$) whose values provided by database such as VALD (Kupka et al. 1999) are often badly known. The fit of these three lines is shown in Fig. 2. For such simulations we used a grid resolution of $253^2 \times 163$. The synthetic profiles were convolved with a Gaussian function representing the instrumental profile of the solar FTS ($\lambda/\delta\lambda \approx 500000$). The calculated profiles are shifted to take into account the gravitational redshift (633 m/s). Since the core of these lines is formed in the chromosphere and might suffer from NLTE effects, we only fit the wings of the Ca II triplet. The derived values (-1.309, -0.410, -0.683) are very close to quantum mechanical calculation of Meléndez et al. (2007) : -1.356 , -0.405, -0.668, respectively. This good agreement, without adjustable parameters, is in favor of the realism of our simulations.

3.2 The convective shift corrections

The primary goal of the RVS is to determine the radial velocities of stars. In order to have an accurate V_{rad} , one must correct the contribution of the convective shift. The amplitude of these lineshifts depends on the location of the formation of the line and on the star itself. We calculate a series of line profiles for different stars : α Cen B (K dwarf), sun and α Cen A (G dwarfs), Procyon (F star) and the metal poor star HD 84937. For this work, we used in all cases a grid resolution of $128^2 \times 96$. An investigation of convective shifts for late type stars was first made by Dravins & Nordlund (1990) but with a much lower resolution than ours. We focus for this exercise on the Ca II triplet and Fe I lines. The latter were selected to be non blended lines and to cover the spectral domain of the RVS (Bigot & Thévenin 2006).

As seen in Fig. 3ab the Fe I lines are blueshifted. This is due to the fact that they are formed deeply into the atmosphere where most of the light is emitted from the bright ascending granules. This is the case of most of the Fe I lines of our sample, with some exceptions like Fe I 868.86 nm. The convective shifts for Fe I lines range from a few hundreds m/s for α Cen B up to about 1 km/s for Procyon. The amplitude of the shift increases when going from K dwarfs to earlier type star such as Procyon, as a consequence of the more vigorous convective motions : $V_{\text{rms}} = 1.4$ km/s for α Cen B and 4.1 km/s for Procyon.

As seen in Fig. 3c the Ca II triplet lines are redshifted. This is a consequence of the fact that these lines are formed well above the photosphere ($\tau < 0.1$). This is an overshoot region where the granulation is reversed: The largest fluctuations of temperature correspond to the descending flows (see e.g. Cheung et al. 2004 for a numerical investigation of this property.). The amplitude of the convective shift is larger than for Fe I lines.

4 Conclusion

The 3D RHD simulations are very helpful for the stellar abundance and radial velocity determinations. The main advantage lies in the fact that these simulations reproduce the stellar surfaces with a great realism. Since

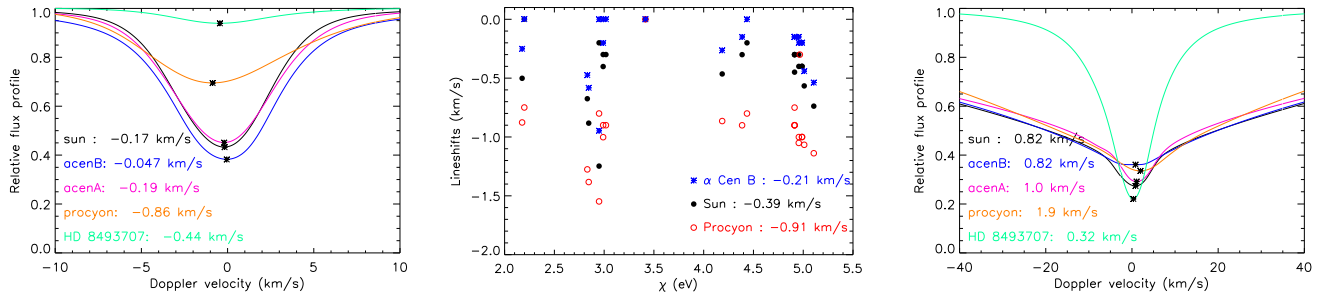


Fig. 3. (Left) Flux profiles of the Fe I at 851.407 nm for different stars. The lineshifts are indicated in each case. (Middle) Convective blueshifts of some Fe I lines of interest for the RVS (Bigot & Thévenin, 2006) as function of the excitation potential for three different stars: α Cen B, the Sun and Procyon. The convective shift increases as the star is hotter. (Right) The same as left panel but for the Ca II line at 854.209 nm. In that case, the convection leads to a redshift.

all the dynamics is naturally taken into account, they do not need to use adjustable free parameters that generally pollute the diagnostics in stellar physics. We have shown that these simulations can be useful for *Gaia*/RVS to get accurate line profiles and even more important for the RVS they allow corrections of the convective shifts to the determination of radial velocities. The amplitude of these lineshifts for late type stars can be of the order of the accuracy expected for the radial velocities, i.e. ~ 1 km/s. In a future work, we will explore these corrections to more stars throughout the HR diagram.

Acknowledgments

We thank Å. Nordlund for providing his code. L. Bigot thanks the organizers of the session "Action Spécifique Gaia" for the invitation to present this work during the "Journées de la SF2A 2008".

References

- Asplund, M., Nordlund, Å., Trampedach, R., Allende Prieto, C., & Stein, R. F. 2000, *A&A*, 359, 729
 Asplund, M., Grevesse, N., Sauval, A. J., Allende Prieto, C., & Kiselman, D. 2004, *A&A*, 417, 751
 Barklem, P. S., & O'Mara, B. J. 1997, *MNRAS*, 290, 102
 Barklem, P. S., O'Mara, B. J., & Ross, J. E. 1998, *MNRAS*, 296, 1057
 Bigot, L., & Thévenin, F. 2006, *MNRAS*, 372, 609
 Bigot, L., & Thévenin, F. 2008, *Journal of Physics Conference Series*, in press
 Cheung, M. C. M., Schessler, M., & Moreno-Insertis, F. 2004, *A&A*, 461, 1163
 Dravins, D., & Nordlund, Å. 1990, *A&A*, 228, 184
 Dravins, D., & Nordlund, Å. 1990, *A&A*, 228, 203
 Gustafsson, B. et al. 1975, *A&A*, 42, 407
 Hirzberger, J., & Wiehr, E. 2005, *A&A*, 438, 1059
 Katz, D., Munari, U., Cropper, M., Zwitter, T., Thévenin, F., David, M., Viala, Y., et al. 2004, *MNRAS*, 354, 1223
 Kupka, F., Piskunov, N., Ryabchikova, T. A., Stempels, H. C., & Weiss, W. W. 1999, *A&AS*, 138, 119
 Meléndez, M., Bautista, M. A., & Badnell, N. R. 2007, *A&A*, 469, 1203
 Nordlund, Å. 1982, *A&A*, 107, 1
 Nordlund, Å., & Dravins, D. 1990, 228, 155
 Nordlund, Å., & Galsgaard, K. 1995, <http://www.astro.ku.dk/> kg
 Perryman, M. A. C., de Boer, K. S., Gilmore, G., Hög, E., Lattanzi, M. G., et al. 2001, *A&A*, 369, 339
 Stein, R.F., & Nordlund, Å. 1989, *ApJ*, 342, L95-98
 Stein, R.F., & Nordlund, Å. 1998, *ApJ*, 499, 914
 Wiehr, E., Bovelet, B., & Hirzberger, J. 2004, *A&A*, 422, L63
 Wilkinson, M. I., Vallenari, A., Turon, C., Munari, et al. 2005, 359, 1306.

THE GAIA SATELLITE: A TOOL FOR EMISSION LINE STARS AND HOT STARS

Martayan, C.^{1,2}, Frémat, Y.¹, Blomme, R.¹, Jonckheere, A.¹, Borges, M.³, de Batz, B.², Leroy, B.⁴, Sordo, R.⁵, Bouret, J.-C.⁶, Martins, F.⁷, Zorec, J.⁸, Neiner, C.², Nazé, Y.⁹, Alecian, E.¹⁰, Floquet, M.², Hubert, A.-M.², Briot, D.², Miroshnichenko, A.¹¹, Kolka, I.¹², Stee, P.¹³, Lanz, T.¹⁴ and Meynet, G.¹⁵

Abstract. The Gaia satellite will be launched at the end of 2011. It will observe at least 1 billion stars, and among them several million emission line stars and hot stars. Gaia will provide parallaxes for each star and spectra for stars till V magnitude equal to 17. After a general description of Gaia, we present the codes and methods, which are currently developed by our team. They will provide automatically the astrophysical parameters and spectral classification for the hot and emission line stars in the Milky Way and other close local group galaxies such as the Magellanic Clouds.

1 Introduction: The Gaia space mission

The Gaia space mission will be launched in 2011/2012. It will orbit at the anti-solar L2 point. Its lifetime is expected to be 5 years. Onboard, there are 3 different instruments: ASTRO, which will provide astrometric measurements (parallaxes, proper-motions) for all stars down to V magnitude 20 with an accuracy 200 times better than Hipparcos. There are 2 spectrophotometers BP/RP (R~100, 320–660nm and 650–1000nm) and a low/medium resolution spectrograph called the Radial Velocity Spectrometer (R=5000 to 11500, 847-874nm, designed for GK stars). This last one will provide spectra for stars till V magnitude equal to 17, and will be used to determine the radial velocity of the stars (see Viala et al. 2008). It is expected that 1 billion of stars will be observed by Gaia, on average 70 times in 5 years (but only 40 times for the RVS). Among them, using the IMF from Kroupa (2001), it is estimated that there are, at maximum, 68 million of hot stars (HS), and 6 million of emission line stars (ELS). Due to the huge quantity of data (200 teraBytes by year), all the data-reduction and the scientific analysis must be performed automatically via new software based on java programming language.

¹ Royal Observatory of Belgium, 3 avenue circulaire 1180 Brussels, Belgium

² GEPI, Observatoire de Paris, CNRS, Université Paris Diderot; 5 place Jules Janssen 92195 Meudon Cedex, France

³ Fizeau, Observatoire de la Côte d'Azur, France

⁴ LESIA, Observatoire de Paris, 5 place Jules Janssen 92195 Meudon Cedex, France

⁵ Padova Astronomical Observatory, Italy

⁶ Laboratoire d'Astrophysique de Marseille, France

⁷ GRAAL-Université Montpellier 2, France

⁸ Institut d'Astrophysique de Paris, France

⁹ Institut d'Astrophysique de Liège, Belgium

¹⁰ RMC Kingston, Canada

¹¹ University of North Carolina at Greensboro, USA

¹² Tartu Observatory, Estonia

¹³ Fizeau, Observatoire de la Côte d'Azur, France

¹⁴ Dpt of Astronomy, University of Maryland, USA

¹⁵ Observatoire de Genève, Switzerland

2 Introduction: Hot stars and Emission Line Stars

The hot stars are defined as stars with effective temperature higher than 7500K. They concern main sequence OBA stars but also Supergiant O stars, etc. The emission line stars are the stars with emission lines in their spectra (in the RVS domain but also in others parts of the spectrum). From time to time, some ELS exhibit emission lines in the UV-Visible part of the spectrum but not in the RVS domain, in which CaII triplet and/or Paschen lines are present. This is the case for example of the late-type Be stars. More generally, ELS can be found everywhere in the HR diagram, they range from hot to cool stars and from young to evolved stars. As examples, one can cite the WR, LBV, Oe, Of, Be, supergiant Oe to Ke, PNe, HBe/Ae, B[e], Mira Ceti e, TTauri, UV Ceti, Flare stars, etc.

With Gaia, we shall obtain for these stars:

- with ASTRO: the proper motions and distances,
- with the BP/RP spectrophotometry: the ELS detection (for example in $H\alpha$), the stellar photometric classification, and photometric fundamental parameters.
- With the RVS spectrograph: the ELS detection, the radial velocity, the spectroscopic fundamental parameters, the stellar spectral classification.
- An indice of the spectroscopic and photometric variability of the stars because they will be observed several times during the 5 years of the mission.
- Indications about potential behaviour differences between HS and ELS from our Galaxy and close local group galaxies, because the bright stars of these galaxies, which correspond mainly to hot stars, will be observed by Gaia.

Combining these informations, we shall determine:

- 3D static and dynamic maps. These 2 maps allow to study the open cluster membership, the site of origin of the stars, the site of formation, and then to characterize the stars.
- The fundamental parameters and spectral classification of stars and where possible the parameters of the disks.
- Statistical links between the lines (amount of emission between $H\alpha$ and Pa for example).
- With the distance, one can provide statistical relation between M_v and spectral types and find potential outliers among OB stars. This deviation could be interpreted in term of fast rotation effects (see Lamers et al. 1997).
- The interstellar reddening of the stars to correct their photometry. The remaining reddening will be interpreted as due to circumstellar matter/disk (Be, HBe/Ae stars).
- Previously unknown ELS (Be, WR), in case of Be stars, the Be phenomenon is transient and a Be star could be seen like a B star at one epoch and several years after seen like a Be star (due to the disk variability).
- The evolutionary status of Be stars. It will be possible to compare the status determined spectroscopically and photometrically via dereddened absolute magnitudes.
- An index on the deviation from the expected behaviour of WR stars.
- The correct classification of B[e] stars. 50% of them are currently badly or not classified: SgB[e], PN[e], HB[e] because their distance is not yet known.
- The percentage of binarity. This is an important issue to understand the behaviour of some stars: what is the rate of binaries among Be stars? 75% according to McSwain & Gies (2005) or 30% according to Porter & Rivinius (2003)? What is the rate of binaries among hot stars? 60% for O stars according to Sana (2008), 30% according to Porter & Rivinius (2003) for B stars.

3 Algorithms and methods

In this section, we briefly present the methods of algorithms currently developed in order to obtain the astrophysical parameters of the stars and reach the goals enumerated above. They are elaborated in Coordination Unit 6, in the Coarse Characterization of Sources scientific module (managed by C. Martayan), in Coordination Unit 8, in the Extended Stellar Parametrizer scientific module (managed by Y. Frémat), in the Hot Stars scientific module (managed by R. Blomme), and in the Emission Line Stars scientific module (managed by C. Martayan).

3.1 Photometric detection of ELS and pre-classification of HS/ELS

The first possibility to detect the ELS and to pre-classify the HS is to use photometric colour-colour or colour-magnitude diagrams. To do that, with the BP/RP spectrophotometry, it is possible to obtain magnitudes in different filters similar to the classical Johnson or Geneva filters and draw the corresponding diagrams. Among them, to detect the ELS, the CMD (R- $H\alpha$ vs. V-I) could be very useful as shown by Keller et al. (1999). Note that due to the low resolution, only stars with strong emission in $H\alpha$ could be detected.

It is also possible to do the same kind of study with the RVS. We computed magnitude-filters in the RVS, defined in areas with CaII lines or Pa lines or both, and in the continuum. The magnitudes are then normalized to the size of the filters. Theoretical magnitudes are computed in filters where there are Pa+Ca lines (filter PaCa) and only one single Pa line (filter PaS that corresponds to the Pa14 line, which is the alone Pa line not blended with CaII lines in the RVS domain). Then the difference between the theoretical magnitude and the observed magnitude in the 2 filters are obtained ($PaCa_{th}-PaCa_{obs}$ and $PaS_{th}-PaS_{obs}$). The difference between 2 filters in the continuum is also determined in order to have an index on the slope of the spectrum and split the stars by categories (hot/cool stars). The first tests on simulated spectra (from CU2 team) for Be, WR stars and normal stars (from O to M stars) show that with the PaCa diagram, the ELS with strong or medium emission in the RVS are detected (above a threshold defined by the upper limit of the normal stars). We also used observed spectra both for ELS and HS from various ground-based spectrographs, which are correctly pre-classified with these diagrams (ELS or absorption). With the PaS diagram, we pre-classify the stars in spectral-types because the filter PaS allows to know whether the star contains or not Pa lines and then whether the star is a hot star or not).

3.2 Fundamental parameters determination

The fundamental parameters determination for hot stars is performed using grids of NLTE models with winds. The observed spectrum is fitted with theoretical ones using the Simplex downhill method (Nelder & Mead 1965). First tests based on 1089 synthetic spectra with noise added, T_{eff} , $\log g$, V_{sini} randomly chosen were performed. They indicate that in case of B stars, 61% of T_{eff} are determined with an error bar of 10%, 65% of $\log g$ are determined with an error-bar of $\pm 0.25dex$ ($\pm 6\%$), 66% of V_{sini} are determined with an error-bar of $\pm 50\%$. In case of O stars, the error-bars are greater than for B stars, because the lines in the RVS spectra are weak. Due to its design, for HS the RVS displays only hydrogen lines (Pa lines) and from time to time weak HeII lines, which implies a poor precision on the V_{sini} . Full results are detailed in Frémat et al. (2007, 2008 in preparation), and Martayan et al. (2008). Moreover, the parameters derived for the HS will be useful for improving the galaxy models, in which there is a lack of HS population.

The same method of minimization/determination could be used to fit the emission lines with theoretical models to obtain parameters for the stellar winds and/or circumstellar matter/disks. Another technique for classical Be stars can use the relation between the strength of emission in $H\alpha$ and Pa lines. However, it is necessary to remove the amount of emission due to CaII lines in the Ca–Pa blends. Using data from Briot (1981), we obtained an interpolated distribution of cleaned Pa emission in the RVS domain using the Pa14 line as beginning point.

3.3 Spectral classification

There are different possibilities to spectroscopically classify the stars. The first one is to use the T_{eff} - $\log g$ plane and calibrations, which link fundamental parameters to spectral types (Zorec 1986, Bouret et al. 2003). The second one is to use the equivalent widths of the lines and calibrations from Andrillat et al. (1995), and

Carquillat et al. (1997). However, to do that, we have to detect the presence of a line, to determine the parameters of the lines (the wavelength, the intensity in emission or absorption, the equivalent width). For detecting the lines, we developed different algorithms based on local signal to noise ratio variations, the local slope variation, and by gaussian fitting (see Viala et al. 2008, Frémat et al. 2007). In case of high signal to noise ratio (better than 20), the different methods provide good lines detection. In case of bad signal to noise ratio (lower than 20), from time to time wrong lines are detected. The automatic identification is currently tested. It is based on a cross-correlation of the theoretical and observed wavelength -differences between consecutive lines. The EWs, FWHM, I, are then determined and added to the tables of observed lines and identified lines. Details will be given by Martayan et al. (in preparation).

3.4 Classification with neural networks approach

We explore also other kind of classification methods based on the neural network approach or on the decision tree via the WEKA library. These algorithms need training samples of spectra for each kind of stars in order to teach the neural networks. Then, they are tested with tests samples in order to determine the reliability of their automatic classification. Finally, after having defined the rates of good/bad classification, they are used in the true data. Currently, the first tests based on magnitude in filters (defined above) provide an excellent classification of stars, but the 1000 spectra used here are synthetic noise-free ones and we need more true observed spectra for each kind of object (ELS, HS) to correctly supervise the learning of the neural networks.

An important issue for these methods as well as for the other algorithms currently developed is to obtain in the near future enough observed spectra to test and improve them before the launch of Gaia. In addition, it will be useful for a more complete scientific analysis of the stars to have a dedicated telescope/instrument (probably a multi-objects spectrograph) for the follow-up of the Gaia targets.

4 Conclusion

The Gaia satellite is one of the most ambitious space mission of the next decades. It will provide some astrophysical parameters for 1 billion of stars and among them for several million of hot stars and emission line stars both in the Milky Way and close local group galaxies. They will allow to elaborate 3D static and dynamic maps, statistical studies, giving new clues about the behaviour of the stars (origin, evolution, variability, binarity). Different methods and algorithms are currently developed by our team in order to detect and identify the lines, to determine the fundamental parameters of the stars, and also to provide their spectral classification.

C.M. acknowledges funding from the ESA/Belgian Federal Science Policy in the framework of the PRODEX program (C90290). C.M. thanks the SOC of the Gaia session for the invitation to present a talk and the AS-Gaia France for the financial support.

References

- Andrillat, Y., Jaschek, C. & Jaschek, M., 1995, A&A, 299, 493
- Bouret, J.-C., Lanz, T., Hillier, D. J., Heap, S.R ., et al., 2003, ApJ, 595, 1182
- Briot, D., 1981, A&A, 103, 5
- Carquillat, M. J., Jaschek, C., Jaschek, M., Ginestet, N., 1997, A&AS, 123, 5
- Frémat, Y., Barrado, D., Barro, L., Jonckheere, A., et al., 2007, GAIA-C8-SP-OPM-BL-001-02
- Keller, S. C., Wood, P. R. & Bessell, M. S., 1999, A&AS, 134, 489
- Kroupa, P., 2001, MNRAS, 322, 231
- Lamers, H. J., Harzevoort, J. M., Schrijver, H., Hoogerwerf, R., et al., 1997, A&A, 325, 25
- Martayan, C., Barrado, D., Barro, L., Blomme, R., et al., 2008, GAIA-C8-SP-OPM-BL-001-04
- McSwain, M. V. & Gies, D. R., 2005, ApJS, 161, 118
- Nelder, J. A. & Mead, R., 1965, the Computer Journal, 7.4, 308
- Porter, J. M. & Rivinius, T., 2003, PASP, 115, 1153
- Sana, H., 2008, IAUS, 250, 554
- Viala, Y., Blomme, R., Dammerdji, Y., Delle-Luche, C., et al., 2008, GAIA-C6-SP-OPM-YV-004
- Zorec, J., 1986, PhD thesis, Université Paris VII

A LIBRARY OF SYNTHETIC GALAXY SPECTRA FOR GAIA

Rocca-Volmerange, B.¹, Tsalmantza, P.² and Kontizas, M.³

Abstract. An extended library of synthetic spectra of galaxies is built for training and testing the classification system (SVM) of GAIA. The final aim is to derive astrophysical parameters for all the unresolved galaxies observed by the satellite with the low resolution prism spectrometer. Predictions of the evolutionary code PÉGASE give the basic templates by spectral types and their corresponding astrophysical parameters (star formation rates, initial mass function, metallicity, ages and others). The new library is a largely extended sample from basic templates, tested for classification. In the future, a peculiar attention will be focused on a selection of the main astrophysical parameters. Moreover we keep in mind ambitious objectives to make coherent the interpretation of low resolution data with high resolution spectra obtained with the RVS.

1 Introduction

Gaia will obtain observations of several million of unresolved galaxies over the whole sky, down to the 20th magnitude. This is an exceptional opportunity to access to statistical samples of galaxy data with a rare accuracy, every source being observed up to 70 times by Gaia. The main objectives are to use the low resolution spectroscopic observations to classify and determine the main astrophysical parameters of all the unresolved galaxies. The method rests on a set of galaxy templates by spectral types produced by the spectrophotometric evolutionary code PÉGASE (<http://www2.iap.fr/pegase>). The comparison of the model predictions with observed data is done with the SDSS colour-colour diagrams. The model templates are extended to the complete coverage of observations by varying the main physical parameters. The final part is to simulate Gaia observations and to train classification and parametrization algorithms.

1.1 The new extended library

The new library (Tsalmantza et al. 2008) corresponds to 28885 synthetic spectra at redshift zero covering four Hubble type of galaxies respecting resolution and wavelength domains of the low resolution prism spectrometer. It is an improved version of the synthetic library (Tsalmantza et al. 2007). The first improvements are to add scenarios of starburst galaxies to cover the blue part of the SDSS colour-colour diagrams. The second improvement is to shorten the time-scales of star formation rates for elliptical galaxies to fit the reddest part of the diagrams. The comparison of model predictions with SDSS data in the g-r/r-i diagram is shown on Fig.1. The new library is also found in good agreement with LEDA (Paturel et al. 1997) photometric observations.

Tsalmantza et al. (2008) also presents a detailed comparison of synthetic spectra of the new library with flux calibrated spectra of the Kennicutt's atlas (Kennicutt, 1992) for similar types. Normalization, conversion to rest frame and spectra rebinning were done for such a comparison.

1.2 Classification and Parametrization

The Support Vector Machines (SVMs) are trained and tested on an extremely large number of synthetic spectra derived from the new library for three G-band magnitude values $G=15$, $G=18.5$, $G=20$. Extinction by our

¹ Institut d'Astrophysique de Paris, 98bis Bd Arago, F-75014 Paris, France

² Max-Planck-Institut für Astronomie, Königstuhl 17, 69117 Heidelberg, Germany

³ Department of Astrophysics Astronomy & Mechanics, Faculty of Physics, University of Athens, GR-15783, Athens, Greece

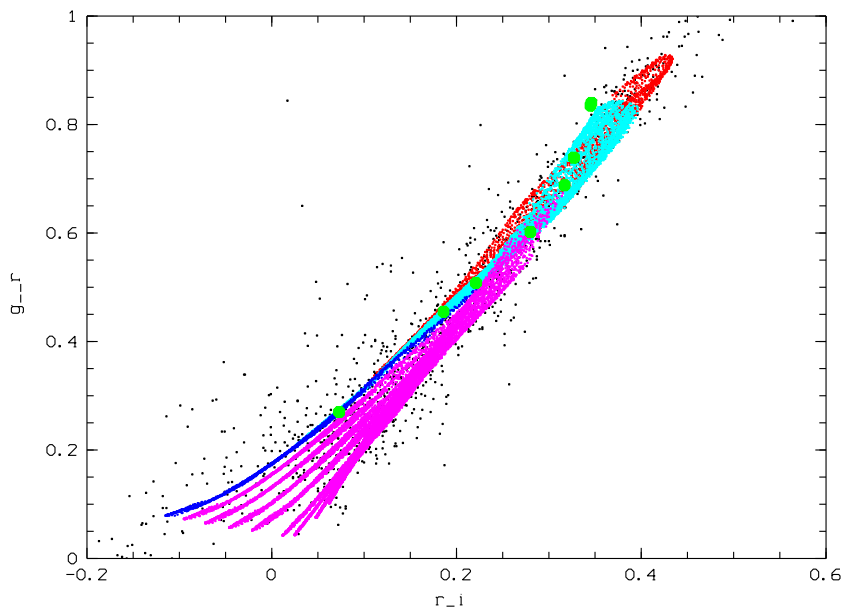


Fig. 1. Model predictions for the four galaxy types: irregular(blue), starburst(magenta), spirals(light blue) and early type galaxies (red). Observations (black dots) are from the SDSS data sample. Examples of the classical PÉGASE models for various types are also shown (green dots).

Galaxy, various noises (Poisson, CCD readout) are taken into account. Regression tests by galaxy types allow to test the classification of SVMs. Regression of redshifts are also performed by comparing predicted versus true z values for the test set. The first results of classification and parametrisation of the second library are very satisfying.

1.3 Conclusion

The new library gives a satisfying comparison to observations of colours and spectra at low resolution. The training of SVMs with the extended library gives good results for galaxy types, redshift and Galaxy reddening. Improvements are required for the extraction of the astrophysical parameters. Synthetic models might suffer any degeneracy for the extremely extended training library. The best solution will be in the future to extract only a few number of the main physical parameters, representative of the morphology and evolution by type at all redshifts. Moreover a new exploration is in progress by building the high-resolution spectra library for the RVS instrument which will allow to coherently link the interpretation of resolved observations of nearby galaxies with the unresolved galaxy samples at higher redshifts.

References

- Fioc, M., & Rocca-Volmerange, B. 1997, A&A, 326, 950
- Kennicutt, R.C. Jr 1992, ApJS, 79, 255
- Paturel, G., Andernach, H., Bottinelli, L., et al. 1997, A&AS, 124, 109
- Tsalmantza, P., Kontizas, M., Bailer-Jones, C.A.L., Rocca-Volmerange, B., et al. 2007, A&A, 470, 761
- Tsalmantza, P., Kontizas, M. & Rocca-Volmerange et al. 2008, submitted

THE FUTURE OF OPTICAL REFERENCE SYSTEMS

Charlot, P.¹

Abstract. Optical reference frames have been traditionally limited in astrometric accuracy compared to radio reference frames which have long reached a sub-milliarcsecond accuracy. The next decade holds promises for big changes in this area with the launch of the Gaia space astrometric mission which unlike Hipparcos will be able to observe several hundred thousands of extragalactic objects with an astrometric accuracy of a few tens of microarcseconds. After reviewing the current status of optical and radio reference frames, this paper draws prospects for building the Gaia optical frame and its alignment with the current International Celestial Reference Frame (ICRF) which is based on radio-interferometric measurements.

1 Introduction

The extragalactic reference system is defined based on the positions of active galactic nuclei (AGN), a class of objects located at the center of distant active galaxies and characterized by extremely compact and bright emission on milliarcsecond (mas) scales. These sources show various observational properties over the whole electromagnetic spectrum, ranging from radio to γ -ray energies, most of which are explained by unified theories of active galactic nuclei. According to the standard representation (Urry & Padovani 1995), illustrated in Fig. 1a, the key elements of a radio-loud active galactic nucleus are a central supermassive black hole, an accretion disk, a broad-line region (fast-moving gas clouds) surrounded by a dusty torus region, an extended narrow-line region (slow-moving gas clouds), and a pair of relativistically out-flowing jets emitting synchrotron radiation which originate within a few tens of Schwarzschild radii from the black hole.

The inner compact radio structure (usually called the source core) detected by Very Long Baseline Interferometry (VLBI) arrays, originates at the base of the jet where the optical depth is approximately unity. Orientation has a major influence on the observed AGN properties since relativistic beaming strongly amplifies kinematics and brightness for jets that are pointed towards us while it attenuates these for jets that are pointed away from us. As a result, most sources show a one-sided morphology with a dominant core component on VLBI scales (Figs. 1b & c) due to sensitivity limitations and selection effects. The most suitable sources for defining a celestial reference frame are those that are the most compact on these scales. Due to their cosmological distances, such extragalactic sources show no transverse motion and therefore define a quasi-inertial system in a kinematical way, i.e. the system is non-rotating with respect to a local inertial frame.

2 The current IAU fundamental frame

The official IAU reference frame in use since 1 January 1998 is the International Celestial Reference Frame (ICRF), which is currently based on the VLBI positions of 717 extragalactic radio sources (Fig. 2). Of these, 608 sources are from the original ICRF (Ma et al. 1998), built from geodetic/astrometric VLBI data obtained between 1979 and 1995. The ICRF source categorization comprised 212 well-observed *defining* sources (which served to orient the axes of the frame), 294 less-observed *candidate* sources, and 102 *other* sources showing coordinate instabilities. The accuracy in the individual ICRF source positions has a floor of 250 microarcseconds (μ as), while the axes of the frame are stable to about 20 μ as in orientation (Fig. 2). Since then the position of the non-defining sources has been improved and the frame has been extended by 109 *new* sources in ICRF-Ext.1 and ICRF-Ext.2 using additional data acquired in the period 1995–2002 (Fey et al. 2004a).

¹ Laboratoire d'Astrophysique de Bordeaux, Université de Bordeaux, CNRS, 2 rue de l'Observatoire, BP 89, 33271 Flouirac Cedex, France

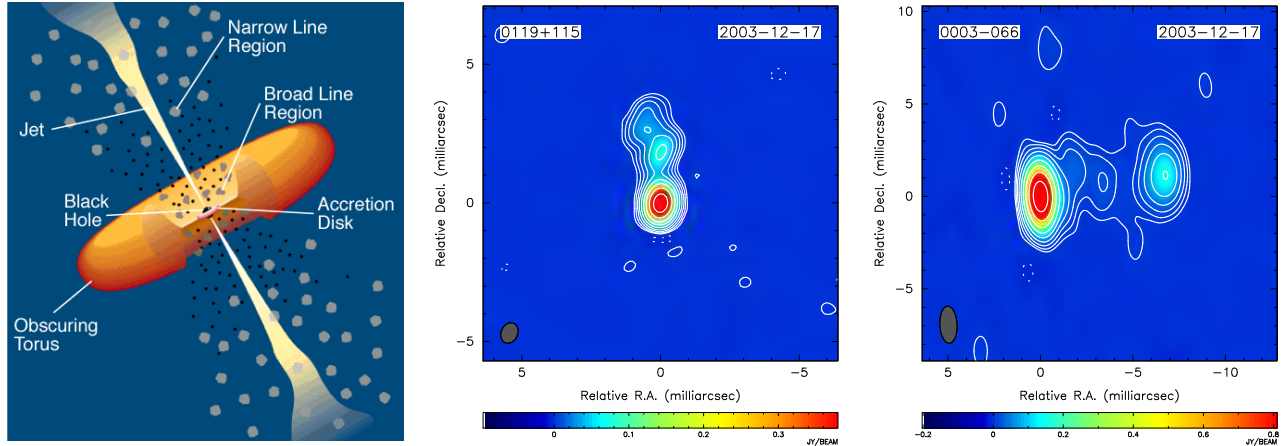


Fig. 1. *Left panel:* Schematic view of the key elements of an active galactic nucleus (credit: C. M. Urry & P. Padovani). *Middle/right panels:* VLBI images at 8.6 GHz for two ICRF sources (0003–066 and 0119+215) observed on 2003/12/17.

Continued VLBI observation of the ICRF sources is essential to maintain the viability and integrity of the frame on the long term because the intensity and VLBI morphology of extragalactic objects evolve in unpredictable ways. Densification of the frame through the identification and observation of new high-quality sources is equally important to facilitate routine differential phase-referenced astrometry, e.g. for spacecraft navigation, and to control any local deformations of the frame which might be caused by tropospheric propagation effects or apparent source motions due to variable intrinsic VLBI structure. The VLBA Calibrator Survey (VCS) provides single-epoch VLBI images and astrometric positions at the milliarcsecond level for approximately 3500 additional sources (Petrov et al. 2008 and references therein). This survey forms the basis for the ICRF densification north of -45° declination. Increasing the density of sources further south has been more difficult because of the limited number of VLBI antennas in the southern hemisphere. Dedicated programs have now been initiated (Fey et al. 2004b, 2006), which should improve the situation, but progress is slower than for the northern sky.

At the IAU XXVIth General Assembly in Prague (August 2006), the community decided to engage in the realization of the successor of the ICRF, to be presented at the next IAU General Assembly in 2009. The motivation for generating this new celestial frame is to benefit from recent improvements in VLBI modeling (e.g. for the troposphere) and to take advantage of the wealth of VLBI data that have been acquired since the time the ICRF was built. A specific issue to be addressed is whether and how to incorporate the VCS sources in this new realization. Another major issue is the revision of the source categorization, in particular the choice of the defining sources. Such a revision is necessary because some of the original ICRF defining sources were found to have extended structures (Fey & Charlot 2000) or position instabilities (e.g. MacMillan 2006), and are therefore improper for defining the celestial frame with the highest accuracy.

3 Towards the Gaia optical frame

The most comprehensive optical catalog available to date is the Large Quasar Astrometric Catalog (LQAC) recently compiled by Souchay et al. (2008). This catalog comprises 113666 objects, an increase of 25% compared to the previous compilation by Véron-Cetty & Véron (2006) which reported only about 85000 objects. The construction of the LQAC was guided by the aim of reporting the most accurate position for every identified quasar, as available through 11 major optical catalogs from which the LQAC was derived. Among these, the largest contributing catalog was the DR5 release of the Sloan Digital Sky Survey which comprises about 75000 quasars (Schneider et al. 2007). In addition to source position estimates, the LQAC also provides redshift and photometric information when available as well as estimates of absolute magnitudes. It is anticipated that the LQAC will be updated on an annual basis by adding newly-discovered quasars with the goal of obtaining the most complete and the most precise optical catalog of quasars by the time Gaia is launched in 2011.

The Gaia space astrometric mission will survey all stars and quasars down to an apparent magnitude of 20 (Perryman 2002). Position accuracies will range from a few tens of microarcseconds at magnitude 15–18 to about $200 \mu\text{as}$ at magnitude 20. Based on current estimates from local surveys, it is expected that 500 000 such

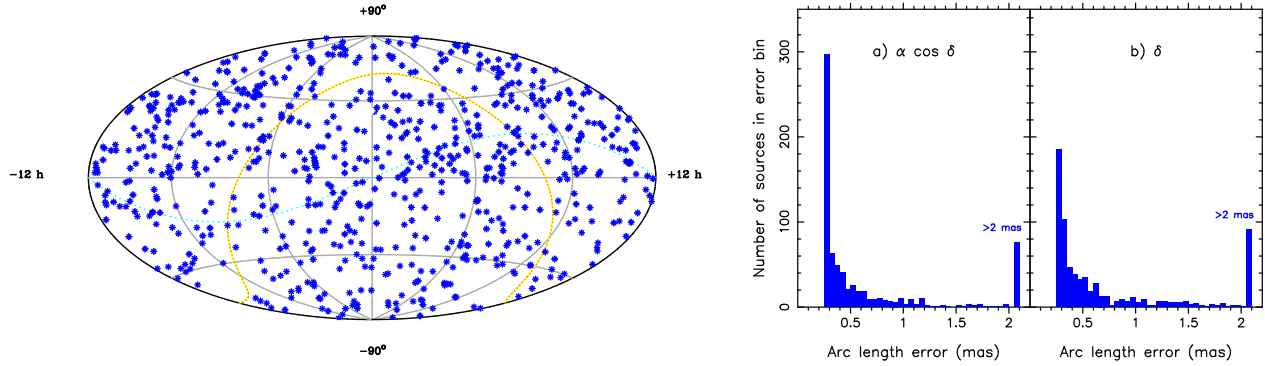


Fig. 2. *Left panel:* Distribution of the current 717 ICRF sources on an Aitoff equal-area projection of the celestial sphere. *Right panel:* Histogram of source position errors in (a) right ascension and (b) declination.

quasars should be detected; unlike Hipparcos, Gaia will thus be able to construct a dense optical reference frame *directly* in the visible wavebands. Initial simulations showed that the residual spin of the Gaia reference frame could be determined to $0.5 \mu\text{s}/\text{yr}$ with a *clean sample* of 10 000 defining sources (Mignard 2002). In practice, the ultimate accuracy of the frame may be limited by random instability of the sources which may show extended and variable structure on these spatial scales, similar to that observed at radio wavelengths (Fey & Charlot 2000). Despite this limitation, the Gaia reference frame should surpass the current ICRF, both in accuracy and in source density. Hence, it is likely that the realization of the fundamental celestial frame will be brought back to visible wavebands in about 10 years when the Gaia catalog is published, although the VLBI reference frame should remain for specific applications such as the monitoring of the Earth’s rotation.

4 Issues in realizing the Gaia frame

Prior to acquiring data, simulations will be essential in order to determine how to best use the thousands of quasars that will be detected by Gaia for realizing the celestial frame. In particular, it will important to study the impact of the lack of sources in the galactic plane and more generally the effect of the distribution of the sources on the quality of the frame. Another important parameter to decide on is the magnitude limit of the sources to consider for inclusion in the clean sample that will define the Gaia frame. Should this magnitude be strictly limited to a value of 18 as originally anticipated (Mignard 2002) or should this criterion be relaxed in order include more sources at the expense of coordinate accuracy? In this respect, the actual magnitude distribution in the LQAC should be quite useful to determine the best compromise between having more sources of lesser astrometric quality or less sources of higher astrometric quality. One should also note that these objects may vary in magnitude, especially the blazar-type objects (a class of objects with jets oriented close to the line of sight) which can show changes of several magnitudes over short time scales (see Fig. 2b). Such variability needs to be investigated as it may affect the choice of the Gaia-defining sources and the quality of the frame.

During the construction process for the Gaia frame, an essential element will be its alignment with the current ICRF in order to maintain consistency with the International Celestial Reference System (Arias et al. 1995) when the transition from radio to optical wavelengths is made. Such alignment, to be obtained with the highest accuracy, requires a large number of sources common to the two frames. A study by Bourda et al. (2008a) revealed that only 10% of the current ICRF sources may be used for this purpose when considering the source magnitude and their VLBI position accuracy and compactness. This prompted the development of new VLBI observing program, targeted to weaker sources, in order to identify further high-quality sources for this alignment (Bourda et al. 2008b). Also to be investigated in this framework is the registration between the VLBI and Gaia positions since the spatial location of the radio and optical emission may differ due to opacities in the quasar jets. Kovalev et al. (2008) showed that on average the optical-radio *core shifts* in a sample of 29 ICRF objects are at the level of $100 \mu\text{as}$, which is significant considering the expected accuracy of the Gaia catalog and that foreseen for the ICRF by 2015–2020. Such effects would thus have to be accounted for when aligning the two frames. On the other hand, the differences between the optical and radio positions may provide a direct measurement of such core shifts, which would be of high interest for probing AGN jet properties.

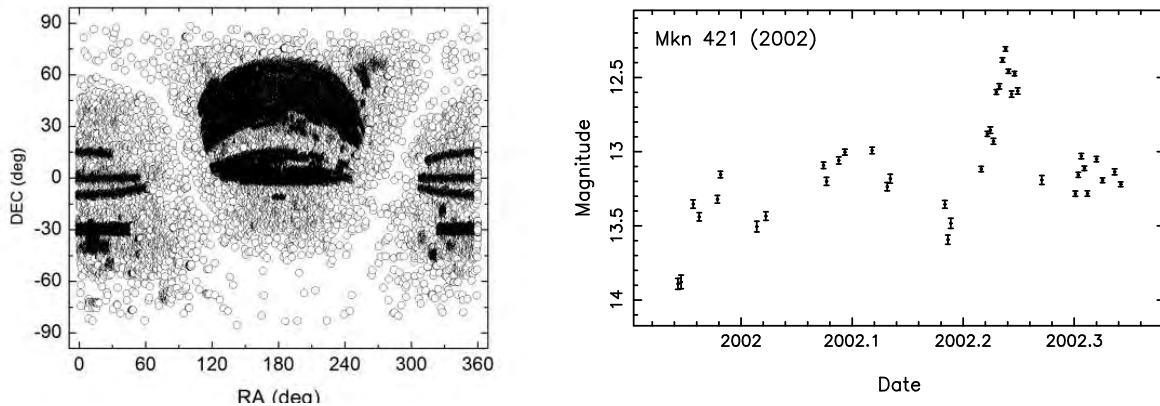


Fig. 3. *Left panel:* Distribution in equatorial coordinates of the 113666 quasars in the Large Quasar Astrometric Catalogue (reproduced from Souchay et al. 2008). *Right panel:* Optical variability of the BL Lac object Mkn 421 (corresponding to the ICRF source 1101+384) on scales of a few months in 2002.

5 Conclusion

The Gaia space astrometric mission will realize for the first time a highly-accurate extragalactic reference frame directly at optical wavelengths. This future frame will surpass the current radio-based ICRF both in accuracy (a few tens of microarcseconds in the individual source positions) and in the number of objects (500 000 sources). Simulations are necessary in order to determine the best strategy for constructing the frame (number of defining sources, sky distribution, magnitude limit) and assess the impact of limiting factors such as photometric variability. Particular attention should be paid to the alignment of the future Gaia frame with the current ICRF in order to maintain continuity in the International Celestial Reference System. Ultimately, comparisons of radio and optical positions may bring new insights into the physical properties of AGN jets.

References

- Arias, E. F., Charlot, P., Feissel, M., & Lestrade, J.-F. 1995, *A&A*, 303, 604
- Bourda, G., Charlot, P., & Le Campion, J.-F. 2008a, *A&A*, 490, 403
- Bourda, G., Charlot, P., Porcas, R., & Garrington, S. T. 2008, in *Proceedings of the Fifth International VLBI Service for Geodesy and Astrometry General Meeting*, St. Petersburg, Russia, March 3–6, 2008 (in press)
- Fey, A. L., & Charlot, P. 2000, *ApJS*, 128, 17
- Fey, A. L., Ma, C., Arias, E. F., Charlot, P., Feissel-Vernier, M., Gontier, A.-M., Jacobs, C. S., Li, J., & MacMillan, D. S. 2004a, *AJ*, 127, 3587
- Fey, A. L., Ojha, R., Jauncey, D. L., Johnston, K. J., Reynolds, J. E., Lovell, J., Tzioumis, A. K., Quick, J. F. H., Nicolson, G. D., Ellingsen, S. P., McCulloch, P. M., & Koyama, Y. 2004b, *AJ*, 127, 1791
- Fey, A. L., Ojha, R., Quick, J. F. H., Nicolson, G. D., Lovell, J., Reynolds, J. E., Ellingsen, S. P., McCulloch, P. M., Johnston, K. J., Jauncey, D. L., & Tzioumis, A. K. 2006, *AJ*, 132, 1944
- Kovalev, Y. Y., Lobanov, A. P., Pushkarev, A. B. & Zensus, J. A. 2008, *A&A*, 483, 759
- Ma, C., Arias, E. F., Eubanks, T. M., Fey, A. L., Gontier, A.-M., Jacobs, C. S., Sovers, O. J., Archinal, B. A., & Charlot, P. 1998, *AJ*, 116, 516
- MacMillan, D. S. 2006, in *International VLBI Service for Geodesy and Astrometry 2006 General Meeting Proceedings*, ed. D. Behrend & K. D. Baver, NASA/CP-2006-214140, 274
- Mignard, F. 2002, in *Gaia: A European Space Project*, ed. O. Bienaymé & C. Turon, EAS Publ. Ser., 2, 327
- Perryman, M. A. C., in *Gaia: A European Space Project*, ed. O. Bienaymé & C. Turon, EAS Publ. Ser., 2, 3
- Petrov, L., Kovalev, Y. Y., Fomalont, E. B., & Gordon, D. 2008, *AJ*, 136, 580
- Schneider, D. P., Hall, P. B., Richards, G. T. et al. 2007, *AJ*, 134, 102
- Souchay, J., Andrei, A. H., Barache, et al. 2008, in *Proceedings of the Fifth International VLBI Service for Geodesy and Astrometry General Meeting*, St. Petersburg, Russia, March 3–6, 2008 (in press)
- Urry, C. M., & Padovani, P. 1995, *PASP*, 107, 803
- Véron-Cetty, M.-P., & Véron, P. 2006, *A&A*, 455, 773

RELATIVISTIC ASPECTS OF THE GAIA MISSION

Le Poncin-Lafitte, C.¹

Abstract. Given the extreme accuracy reached in future global space astrometry, a mission such that GAIA will need a global relativistic modeling of observations. Outlining the importance of having a consistent relativistic approach all the way through the data analysis, we present also why GAIA observations will lead, in return, to an improvement of some General Relativity tests much beyond the current level.

1 Introduction

In 2000 the International Astronomical Union has adopted a general relativistic framework for modeling high-accuracy astronomical observations. Two fundamental systems have been fixed: the Barycentric Celestial Reference System (BCRS) and the Geocentric Celestial Reference System (GCRS). The BCRS has been defined in such a way that it is covering the Solar System and observed sources. It is mainly very useful for the modeling of the dynamics of the solar system bodies and/or probe as well as the description of light propagation between light sources and an observer. The coordinate time of the BCRS is called the Barycentric Coordinate Time (TCB). It is however possible to use a scaled TCB for practical purpose, the so-called Dynamical Barycentric Time (TDB). The GCRS has been constructed in order that all gravitational fields generated by other bodies are seen as tidal potentials. The coordinate time of the GCRS is called Geocentric Coordinate Time (TCG). A scaled version of TCG exists and is called Terrestrial Time (TT) which is directly related to the International Atomic Time (TAI). The CGRS is suitable for the modeling of all physical processes in the immediate vicinity of the Earth. In addition, a local reference system, GCRS-like, can be constructed for any massless bodies, *i. e.* an observing satellite, and it is convenient to model any physical processes in the local vicinity of the satellite (Klioner 2004). By using this set of three relativistic reference systems, it is possible to draw a consistent relativistic scheme for the modeling of all kind of GAIA observations, as illustrated in Fig. 1.

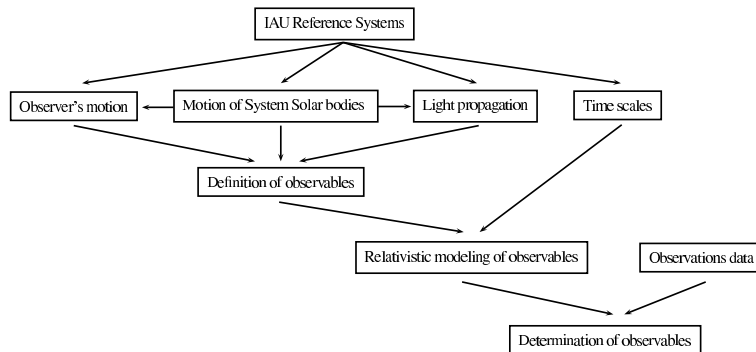


Fig. 1. Principles of relativistic modeling of astronomical observations.

¹ Observatoire de Paris, SYRTE CNRS/UMR 8630, 61 Avenue de l'Observatoire, F75014 Paris, France

2 modeling of the motion of the satellite/ Solar System bodies

It is well known that the equation of motion are ordinary differential equations of second order which can be solved numerically. The principal relativistic effects in the mass-monopole approximation for the gravitating bodies are the so-called Einstein-Infeld-Hoffmann equations of motion which can be written as follow

$$\begin{aligned}
a_E^i = & - \sum_{B \neq E} G M_B \frac{r_{EB}^i}{r_{EB}^3} + \frac{G}{c^2} \sum_{B \neq E} M_B \frac{r_{EB}^i}{r_{EB}^3} \left\{ \sum_{C \neq B} \frac{G M_C}{r_{BC}} + 4 \sum_{C \neq E} \frac{G M_C}{r_{EC}} \right. \\
& \left. + \frac{3}{2} \frac{(r_{EB}^j \dot{x}_B^j)^2}{r_{EB}^2} - \frac{1}{2} \sum_{C \neq E, B} G M_C \frac{r_{EB}^j r_{BC}^j}{r_{BC}^3} - 2 \dot{x}_B^j \dot{x}_B^j - \dot{x}_E^j \dot{x}_E^j + 4 \dot{x}_E^j \dot{x}_B^j \right\} \\
& + \frac{1}{c^2} \sum_{B \neq E} G M_B \frac{r_{EB}^j}{r_{EB}^3} \left\{ 4 \dot{x}_E^j - 3 \dot{x}_B^j \right\} (\dot{x}_E^i - \dot{x}_B^i) - \frac{1}{c^2} \frac{7}{2} \sum_{B \neq E} \frac{G M_B}{r_{EB}} \sum_{C \neq E, B} G M_C \frac{r_{BC}^i}{r_{BC}^3} + \mathcal{O}(c^{-4}),
\end{aligned} \tag{2.1}$$

where capital latin subscripts B , C and E enumerate massive bodies, M_B is the mass of body B , $\mathbf{r}_{EB} = \mathbf{x}_E - \mathbf{x}_B$, a dot signifying time derivative with respect to TCB.

Of course, on the first hand, modern planetary ephemerides use Eq. (2.1) as a basic one and they are usually distributed in TDB time scale. On the other hand, one of the most controversial question is relativistic time scales and their relations. Indeed, one consequence of relativity is that the relation between one moment of time from one reference system to another can be constructed if and only if the spatial positions of the event are specified. A particular case is the transformation from TCG to TCB at the geocenter, which reads

$$\frac{dT_{CG}}{dT_{CB}} = 1 + \frac{1}{c^2} \alpha(TCB) + \frac{1}{c^4} \beta(TCB) + \mathcal{O}\left(\frac{1}{c^5}\right), \tag{2.2}$$

with

$$\alpha(TCB) = -\frac{1}{2} v_E^2 - \sum_A \frac{G M_A}{r_{GA}}, \tag{2.3}$$

$$\begin{aligned}
\beta(TCB) = & -\frac{1}{8} v_E^4 + \frac{1}{2} \left(\sum_A \frac{G M_A}{r_{EA}} \right)^2 + \sum_A \left(\frac{G M_A}{r_{EA}} \sum_{B \neq A} \frac{G M_B}{r_{AB}} \right) \\
& + \sum_A \frac{G M_A}{r_{EA}} \left[4 \mathbf{v}_A \cdot \mathbf{v}_E - \frac{3}{2} v_E^2 - 2 v_A^2 + \frac{1}{2} \mathbf{a}_A \cdot \mathbf{r}_{EA} + \frac{1}{2} \left(\frac{\mathbf{v}_A \cdot \mathbf{r}_{EA}}{r_{EA}} \right)^2 \right],
\end{aligned} \tag{2.4}$$

where capital latin subscripts A , B and C enumerate massive bodies, E corresponds to the Earth, $\mathbf{v}_E = \dot{\mathbf{x}}_E$ and $\mathbf{a}_E = \ddot{\mathbf{x}}_E$.

Let us also stress that TDB has been redefined by the last IAU general assembly as a fixed linear transformation of TCB. It means that each planetary ephemeride, usually distributed in TDB, "realizes" the transformation (2.2). Since the official time scale chosen to process the GAIA data is TCB, It will be then natural to have an access to the transformations $TT \rightarrow TDB$ and back from the ephemeride used in the processing itself. Taking into account that it is not very complicated to do a Chebyshev polynomials representation of the numerical integration of Eq. (2.2), one can expect that in the future, GAIA mission is a good opportunity to lead the ephemeride providers to construct consistent relativistic four-dimensional planetary ephemerides.

3 modeling of positional observations

First of all, the equation of light propagation relative to the BCRS should be derived and solved. It can be seen that five vectors are needed (see Fig. 2): \mathbf{s} is the unit observed direction, \mathbf{n} is the unit vector tangential to the light ray at the moment of observation, σ is the unit vector tangential to the light ray at $t = -\infty$, \mathbf{k} is the unit coordinate vector from the source to the observer and \mathbf{l} is the unit vector from the Solar System barycenter to the light source. The modeling (GREM, Klioner 2003) consists then in a sequence of transformations between these vectors:

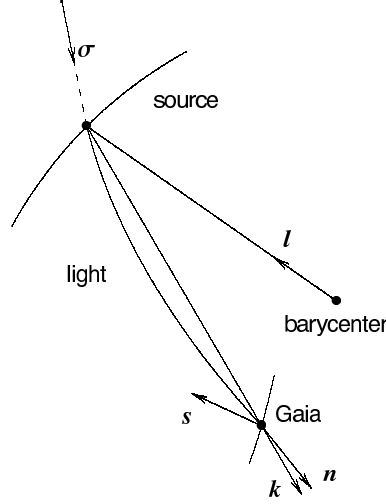


Fig. 2. Vectors used in the modeling of light propagation.

- a) aberration: this step converts the observed direction to the source \mathbf{s} into the coordinate velocity of the light ray \mathbf{n} at the event of observation,
- b) light deflection for source at past infinity: the vector \mathbf{n} is converted into σ ,
- c) light deflection for finite sources: this step converts σ into the coordinate direction \mathbf{k} going from the source to the observer,
- d) parallax: \mathbf{k} is converted into \mathbf{l} going from the Solar System barycenter to the source,
- e) proper motion: this step gives a description of the time dependence of \mathbf{l} caused by the motion of the source with respect to the Solar System barycenter.

The most complicated part of the modeling lies on the description of light deflection. To reach the microarc-second accuracy, it is needed to take into account the effects of monopole field of major celestial bodies as well as the quadrupole field of giant planets and gravitomagnetic fields due to the translational motion of deflecting bodies.

4 Synchronization of the onboard clock

Another important aspect is the conversion of BCRS time intervals $dTCB$ into the corresponding GAIA proper time intervals dTG . The general form of this transformation is similar to Eq. (2.2), but has to be calculated along the worldline of GAIA. It reads

$$\frac{dTG}{dTCB} = 1 + \frac{1}{c^2}\alpha'(TCB) + \frac{1}{c^4}\beta'(TCB) + \mathcal{O}\left(\frac{1}{c^5}\right), \quad (4.1)$$

with

$$\alpha'(TCB) = -\frac{1}{2}v_G^2 - \sum_A \frac{GM_A}{r_{GA}}, \quad (4.2)$$

$$\begin{aligned} \beta'(TCB) = & -\frac{1}{8}v_G^4 + \frac{1}{2} \left(\sum_A \frac{GM_A}{r_{GA}} \right)^2 + \sum_A \left(\frac{GM_A}{r_{GA}} \sum_{B \neq A} \frac{GM_B}{r_{AB}} \right) \\ & + \sum_A \frac{GM_A}{r_{GA}} \left[4\mathbf{v}_A \cdot \mathbf{v}_G - \frac{3}{2}v_G^2 - 2v_A^2 + \frac{1}{2}\mathbf{a}_A \cdot \mathbf{r}_{GA} + \frac{1}{2} \left(\frac{\mathbf{v}_A \cdot \mathbf{r}_{GA}}{r_{GA}} \right)^2 \right], \end{aligned} \quad (4.3)$$

where all quantities, indexed with capital latin subscript G , refer to the satellite. GAIA will be observable from Earth ground stations several hours per day. During all visibility periods, the clock of GAIA will be synchronized with the ground. Essentially, GAIA onboard clock will generate some time packet OBT_k , which differs from the "ideal" proper time TG because technical errors of the clock, and this information will be sent to the ground station which will produce a time tag in Universal Coordinate Time UTC_k . The whole story is to be able to give a relation between all pairs $(OBT_K; UTC_K)$ and the corresponding relativistic pairs (TG_K, TCB_k) . One possible approach is illustrated in Fig. 3 where numerous time scales and relativistic transformations are involved.

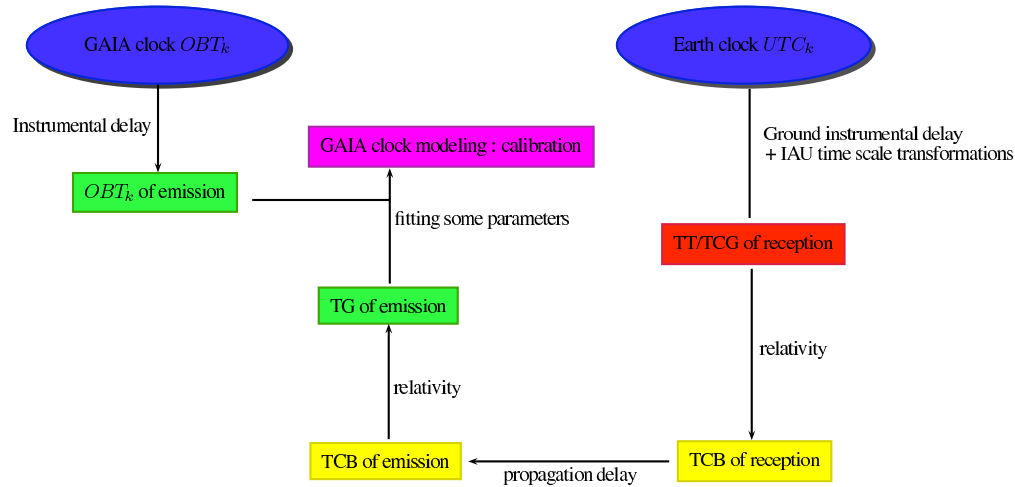


Fig. 3. Relativistic scheme of onboard clock synchronization

5 Testing General Relativity?

Because the standard reduction modeling of GAIA is deeply based on General Relativity basic principles, GAIA data can be used to test many aspects of relativity itself. It is difficult to describe here all possible tests, so let us only give the main contributions of GAIA to fundamental physics:

- the PPN parameter γ will be measured with an accuracy between 10^{-6} and 5×10^{-7} in a wide range of angular distances from the Sun which constitutes a complete test of light deflection in Solar System,
- the PPN parameter β will be measured with an accuracy close to 10^{-4} from the observations of asteroids (Hestroffer et al. 2007),
- local gravitational light deflection due to giant planet will be measured: the monopole deflection, the deflection due to translational motion of the planets and the deflection due to the quadrupole field of Jupiter (GAREX experiment of Crosta & Mignard 2006, Le Poncin-Lafitte & Teyssandier 2008).

References

- Crosta, M.-T., Mignard, F. 2006, *Classical and Quantum Gravity*, 23, 4853
 Hestroffer, D., Mouret, S., Berthier, J., Mignard, F., Tanga, P., 2008, *IAU Symposium*, 248, 266
 Klioner, S. A., 2003, Technical report on the implementation of the GAIA relativistic model, available from the GAIA document archive
 Klioner, S. A., 2004, *Physical Review D*, 69, 124001
 Le Poncin-Lafitte, C., Teyssandier, P., 2008, *Physical Review D*, 77, 044029
 Soffel, M., et al., 2003, *Astronomical Journal*, 126, 2687

ASTROMETRY WITH GROUND BASED OPTICAL TELESCOPES

Taris, F.¹, Bouquillon, S.¹, Souchay, J.¹, Andrei, A.H.² and Albert-Aguilar, A.¹

Abstract. Astrometry with ground based optical telescopes is a newly developed theme in the SYRTE department of the Paris observatory. It recovers some activities like: - the observation of the WMAP probe with optical telescopes for the future astrometric monitoring of GAIA, - the realization of an ecliptic catalog of quasars (using the CFHT images), - the link between radio and optical positions of quasars. In the case of WMAP we will detail more particularly the observations made with the ESO 2.2 m telescope and with the 105 cm telescope of the Pic du Midi. Our goal is to be able to obtain the position of GAIA on its orbit with an uncertainty of 150m in position and 2.5 mm/s in velocity. For that purpose, the telescope of the Pic du Midi could be used as a main observing station when GAIA will be launch. We will give the firsts results obtain for the astrometric reduction of the images of WMAP obtain with these two telescopes. We also present the CFHT-LS project. We will use the images of the Very Wide survey to realize an astrometric catalog of quasars. The goal of this project is to obtain the position of quasars with an uncertainty around 10mas up to the 25th magnitude. It will permit to densify the GAIA catalog.

1 Introduction

In the domain of astrometry, SYRTE is involved in the realization of the International Celestial Reference Frame (ICRF) which is necessary to know with optimal precision the location of all the bodies in the Universe. One of the tasks consists in establishing the coordinates of quasars as accurately as possible. These quasars are assumed to provide fixed (quasi-inertial) directions in space, which make it possible to determine the coordinates of moving objects: stars in galactic rotation, planets and asteroids rotating around the sun etc... Because of the increasing number of sources in the catalogues of quasars, it is necessary to make their intercomparison as well as the analysis of the extremely accurate observation data obtained by very long baseline interferometry (VLBI) in the radio domain, or by CCD images in the focal plan of large telescopes at optical wavelengths. Another research theme is the link between the International Celestial Reference System and the dynamical system represented by the trajectories of the mobile bodies in the solar system. At SYRTE, the analysis of lunar laser ranging data, of pulsar chronometry, and the use of optical observations lead to the determination of this link.

2 Astrometry with optical telescopes at SYRTE-OP

Since january 2007 a team of SYRTE-OP is particularly involved in the field of astrometry with ground based optical telescopes. Some points of interest are currently under development: - The realization of an ecliptic catalogue of quasars, - the link between the dynamical reference system and the ICRF through the observation of asteroids, - the link between radio and optical positions of quasars and their photometric vs astrometric variability, - the observation of WMAP to prepare the GAIA mission. The two next subsections show the telescopes and softwares used to obtain images and analyse them.

¹ Observatoire de Paris, SYRTE, CNRS UMR 8630, 61 av. de l'observatoire, F75014, Paris, France

² Observatorio Nacional/MCT, Observatorio do Valongo/UFRJ, Brasil

2.1 The telescopes

Up to now three ground based optical telescopes have been used to obtain images both for quasars and WMAP. The larger one is the 3.6m optical/infrared telescope TCFH (Telescope Canada France Hawaii). The observatory is located atop the summit of Mauna Kea, a 4200 meter dormant volcano, located on the island of Hawaii (USA). The MEGACAM camera, a set of 36 CCD, was used together with the telescope (see 4.1). The second one is the 2.2m Telescope of the European Southern Observatory at La Silla (Chile). It has been in operation since 1984. The telescope is a Ritchey-Chretien design mounted on an equatorial fork mount. The telescope is at a geographical location of 70d44'4"543 W 29d15'15"433 S and an altitude of 2335 metres. It was used with the Wide Field Imager (WFI), a focal reducer-type camera at the Cassegrain focus and with a field of view of 34'x33'. The last and small one is the 1.05m Telescope of the Pic du Midi (France). It is located in the south-west of France by 42d56'10".9N, 00d08'32".6E and 2877m in altitude. In 1963 that telescope was used in collaboration with the National Aeronautics and Space Administration (NASA) to prepare the Apollo missions for moon landing.

2.2 Tools for reduction/analysis of observations

Softwares used to reduce and analyse images can be divided in two sets. The home made softwares have been built for astrometric reduction, linking of independant CCD of a large camera (MEGACAM, WFI...), quasars identification, differential astrometry. The automatization of these softwares is scheduled for large catalogue realization. The other set is made of known softwares (IRAF or TERAPIX suite, see 4.3). Sextractor, Scamp, Swarp were used to obtain a file with the position of the detected object on the CCD and to control that the equatorial coordinates obtain by the home made softwares were consistent.

3 WMAP for GAIA

3.1 Preparing the GAIA mission

The requirements, due to astrometric reasons, about the position and velocity of the spacecraft on its orbit are very stringent. It has been shown (Perryman 2005, Mignard 2005) that the uncertainty must be, at most, 150m (20mas) and 2.5 mm/s (1mas/h) respectively. The classic Doppler and ranging techniques can only deliver 6 km and 8 mm/s. To achieve that high level of requirements the only usable technique is the Ground Based Optical Tracking (GBOT). GAIA's location roundabout the L2 Lagrange point is approximately 1.5 million km from the Earth, facing roughly opposite of the sun. It's visual magnitude would be approximately 18 (this value can be off by a huge amounts). In order to prepare the GBOT of GAIA, the Wilkinson Microwave Anisotropy Probe (WMAP) has been chosen. That probe is also located around the L2 Lagrange point and its magnitude (roughly 19) is very near from the expected magnitude of GAIA. WMAP is then a reasonable model for the brightness and observability of GAIA. The precise astrometric position of WMAP has been provided by Dale Fink, Navigator of WMAP Spacecraft Control Team at NASA.

3.2 ESO 2.2m + WFI

Sebastien Bouquillon (SYRTE-OP), Ricky Smart (INAF/OATo, Torino) and Alexandre Andrei (Observatorio Nacional, Rio de Janeiro) have used the 2.2m telescope of the European Southern Observatory at La Silla, Chile, to take several images of NASA's WMAP satellite in its orbit. Sextractor (Terapix) or Daophot (IRAF) have been used to obtain the (x,y) positions of the sources on the CCD. The standard deviation of the difference between the computed and the observed positions gives the best available information about the standard deviation of WMAP. Results obtained with three independant softwares are given here:

| | Home made | TERAPIX | IRAF |
|------------|-----------|---------|---------|
| Right asc. | 70.1mas | 70.5mas | 69.7mas |
| Dec. | 80.8mas | 77.0mas | 72.2mas |

3.3 T105 Pic du Midi (France)

The astrometric reduction has been done with the same three independant softwares that for the ESO CCD. A plate solution was determined with a second order polynomial in x and y leading to the following residuals:

| Time of observ. | sigma(alpha) | sigma(delta) |
|-----------------|--------------|--------------|
| 23h05m33s | 64mas | 48mas |
| 23h09m00s | 65mas | 61mas |
| 23h12m25s | 65mas | 57mas |

The results obtain were compared with the theoretical ephemeride supplied by Dale Fink. Moreover the brightness of WMAP has been calibrated with respect to the UCAC2 reference stars (UCAC2 stars are not photometric standards). The results are as follows:

| Time of observ. | diff(alpha) | diff(delta) | mag(+/-1sigma) |
|-----------------|-------------|-------------|------------------|
| 23h05m33s | 21.104" | 3.234" | 18.620(+/-0.249) |
| 23h09m00s | 21.297" | 3.141" | 18.661(+/-0.257) |
| 23h12m25s | 21.530" | 3.231" | 18.757(+/-0.251) |

The difference between the observed position and the ephemeride is relatively large but quite constant. This can be due to the ephemeride itself (constant offset), to the inaccuracy of the position of the telescope (10m), to the time synchronisation of the Pic du Midi (0.1s) or to other effect...

The fluctuation of the magnitude can be explained by the ambient condtions (extremely difficult conditions with light diffusion through clouds, moon's age of 11 and bad seeing). The rapid changes in object brightness due to varying illumination of spacecraft must also be taken into account.

4 The CFHT-LS

Canada and France have joined a large fraction of their dark and grey telescope time for a large project, the Canada-France-Hawaii Telescope Legacy Survey (CFHTLS). More than 450 nights over 5 years will be devoted to the survey using the wide field imager MegaPrime equipped with MegaCam. The three main entities serving the Canadian and French communities are 1) the CFHT for the data acquisition, pre-processing and calibration, 2) the Canadian Astronomy Data Centre (CADC) for all activities related to the archiving and release of the various data products to the communities, and 3) Terapix (based in Paris) for the data resampling and stacking, fine astrometric calibration, and source catalogs generation.

4.1 TCFH-MEGAPRIME/MEGACAM

The telescope itself has been described above (see 2.1). MegaPrime is the wide-field optical imaging facility at CFHT. The wide-field imager, MegaCam (built by CEA, France), consists of 36 2048 x 4612 pixel CCDs (a total of 340 megapixels), covering a full 1 degree x 1 degree field-of-view with a resolution of 0.187 arcsecond per pixel to properly sample the 0.7 arcsecond median seeing offered by the CFHT at Mauna Kea. The new prime focus upper end includes an image stabilization unit and a guide/autofocus unit with two independent guide CCD detectors.

4.2 CADC

The Canadian Astronomy Data Centre (CADC) serves the Canadian and French communities for all activities related to the archiving and release of the various data products.

4.3 Terapix

TERAPIX (Traitement Elementaire, Reduction et Analyse des PIXels de megacam) is an astronomical data reduction centre dedicated to the processing of extremely large data flows from digital sky surveys. TERAPIX is located at IAP (Institut d'Astrophysique de Paris). Its primary tasks are: - to develop image processing and pipeline software for MegaCam; - to develop and provide tools for handling of large CCD images; - to operate the final reduction pipeline to produce calibrated images and catalogues of MegaCam images over the next 5 years; - to provide technical assistance and computing facilities for MegaCam and WIRCam users.

4.4 The three surveys

The Canadian and French scientific agencies have decided to set up the CFHTLS observational program. It consists of three observational programs: - The CFHT-LS "very wide": 1300 square degrees over the ecliptic area and focussed on the Trans-Neptunian and Kuiper Belt observations. - The CFHT-LS "wide": covering 170 square degrees over three large fields located at high galactic latitude, in "dust-free" areas of the sky. The wide survey will be focussed on large-scale structure of the Universe, cosmological weak lensing, clusters of galaxies, quasars as well as stellar proper motions in the Galaxy. - The CFHT-LS "deep": covering four uncorrelated 1 square degree patches (i.e., one MegaCam field) in "dust-free" areas of the sky. The deep survey will be optimised for the detection of light-curve measurements of Type Ia supernovae and the study of very high redshift galaxies.

5 Observations with TCFH

Six of the QSO quasars densest (on average 25 QSOs up to $R=21$) SDSS DR5 regions were selected for two band optimum photometry observation using MEGACAM to obtain the largest at this date, statistically significant and coherent sample of the magnitude, size, and astrophysics of the host galaxies of the quasars. The DR5 regions guarantee a high number of galaxy and stellar comparison objects. In parallel it furnishes ugriz magnitudes for all and spectral information for many ones. Two fields in the ecliptic plane complied the density threshold and will additionally enable one to obtain a direct comparison between the ICRF and the dynamical system represented by field asteroids. Bright cusps on the GAIA QSOs PSF will give rise to astrometric jitter. This program will give practical templates and constraints for the definition of the QSO Initial Catalogue for GAIA. The detailed luminosity profile of the host galaxy so obtained can be combined to the DR5 data in order to contribute to the understanding of their morphology, star formation history and dust distribution. The observations of the semester 08A obtained at TCFH are up to now under investigation.

Other observations in the public domain will be used to transfer the astrometric precision of the GAIA catalogue to faint objects, up to the 25th magnitude, in the ecliptic fields, with the help of the CFHT-LS VW survey. In return it will permit us to densify the GAIA catalogue.

6 Conclusion

Since January 2007 a team of SYRTE-OP is particularly involved in the field of astrometry with ground based optical telescopes

In the frame of the GBOT-GAIA, first observations of WMAP have been done with the 2.2m ESO and 1.05m Pic du Midi telescopes. For that late telescope we propose to use it as a main observing station when GAIA will be launched. Preliminary results show that it is possible to obtain the position of WMAP with the uncertainty of the UCAC2 stars. Hence when the GAIA early-catalogue will be accessible to the GBOT community the uncertainty about the GAIA position could be better than 20 mas. It will permit to reach the very stringent requirements of the GAIA mission.

Observations of the CFHTLS will be used to transfer the astrometric precision of the GAIA catalog for faint objects, up to the 25th magnitude, in the ecliptic fields, with the help of the Very Wide survey. In return it will permit us to densify the GAIA catalog.

References

- Perryman, M. 2005, GAIA-CA-TN-ESA-MP-012-2
- Mignard, F. 2005, GAIA-FM-023
- Andrei, A. H., et al. 2008, these proceedings

GALACTIC KINEMATICS FROM RAVE TO GAIA-RVS DATA

Veltz, L.¹, Bienaymé, O.², Steinmetz, M.¹, Zwitter, T.³, Watson, F. G.⁴, Binney, J.⁵,
Bland-Hawthorn, J.⁶, Campbell, R.¹, Freeman, K. C.⁷, Gibson, B.⁸, Gilmore, G.⁹, Grebel, E. K.¹⁰,
Helmi, A.¹¹, Munari, U.¹², Navarro, J. F.¹³, Parker, Q. A.¹⁴, Seabroke, G.¹⁵, Siebert, A.², Siviero,
A.^{12,1}, Williams, M.¹ and Wyse, R. F. G.¹⁶

Abstract. RAVE data has provided new results on Galactic kinematics like the kinematical decomposition of the Galactic disk. This decomposition permits to identify the different components of the disk and to characterize them in terms of scale height and scale length. With the data provided by Gaia and in particular the RVS, we will have a completely renewed view of the Galaxy. The precision of the RVS will permit to undertake a precise analysis of the kinematics of the Galactic disks. This knowledge will provide significant clues to constrain the scenarios of the Galactic disk formation.

1 Introduction

The hierarchical formation scenario is a great success in describing the formation of the large-scale structure of the universe. But, the detailed mechanisms of formation of individual galaxies are still an open question. Some answers to this question rely on the knowledge of the position, the kinematics and chemical composition of the stars of the Milky Way. Therefore, in 2000, ESA has approved the Gaia mission that will provide the 6-D (position-velocity) information for 50 millions stars in the Galaxy. The expected launch of the Gaia satellite is planned for 2011. As a precursor in the spectroscopic area, an international cooperation called "RAVial Velocity Experiment" (RAVE) has started in 2003 a survey of one million stars in the southern sky hemisphere (Steinmetz 2003). There has been already two data releases. The first release contains about 25 000 radial velocity measurements (Steinmetz et al. 2006). The second data release contains about 25 000 radial velocity measurements more and 20 000 stars for which the stellar parameters ($[M/H]$, $\log g$, T_{eff}) have been determined (Zwitter et al. 2008). The spectroscopic acquisition techniques differ between RAVE and the Gaia Radial Velocity Spectrometer (RVS), although they have almost the same resolution and wavelength range.

¹ Astrophysical Institute Potsdam, An der Sternwarte 16, 14482 Postdam, Germany

² Observatoire Astronomique de Strasbourg, 11 rue de l'Université, 67000 Strasbourg, France

³ University of Ljubljana, Department of Physics, Jadranska 19, 1000 Ljubljana, Slovenia

⁴ Anglo-Australian Observatory, Coonabarabran, NSW 2357, Australia

⁵ Rudolf Peierls Centre for Theoretical Physics, 1 Keble Road, Oxford, UK

⁶ School of Physics, University of Sydney, NSW 2006, Australia

⁷ Research School of Astronomy & Astrophysics, Mount Stromlo Observatory, Cotter Road, Weston ACT 2611, Australia

⁸ Centre for Astrophysics, University of Central Lancashire, Preston, UK

⁹ Institute of Astronomy, University of Cambridge, Madingley Road, Cambridge, UK

¹⁰ Astronomisches Rechen-Institut, Zentrum für Astronomie der Universität Heidelberg, Mönchhofstraße 12-14, 69120 Heidelberg, Germany

¹¹ Kapteyn Astronomical Institute, University of Groningen, P.O. Box 800, 9700 AV Groningen, Netherlands

¹² Osservatorio Astronomico di Padova - INAF, Sede di Asiago, 36012 Asiago, Italy

¹³ Department of Physics and Astronomy, University of Victoria, P.O.Box 3055, Victoria, Canada

¹⁴ Department of Physics, Macquarie University, NSW 2109, Australia

¹⁵ Planetary & Space Sciences Research Institute, The Open University, Milton Keynes, UK

¹⁶ Department of Physics and Astronomy, Johns Hopkins University, 3400 N. Charles Street, Baltimore, USA

The RAVE spectra are obtained with the multi-fiber spectrograph 6dF (Watson et al. 2000) on the UK Schmidt telescope at the Anglo-Australian Observatory. Each field is observed during five exposures of 600 seconds. The RVS is an integral field instrument on board of the Gaia satellite that will not use fibers (Katz et al. 2004). The observation will be done in a time delay integration scan mode. Each spectrum will be exposed for 4 seconds.

The 6dF spectrograph and RVS are medium resolution instruments with $R = 7500$ and 11500 , respectively. The spectra have a near infrared wavelength range between $[8470 - 8740]$ Å for Gaia-RVS and $[8410 - 8795]$ Å for RAVE. This wavelength range and resolution have three main advantages (Munari 1999, 2003). They present the lowest possible contamination by telluric absorptions that will facilitate the pre- and post- Gaia mission observations from the ground. According to the Galaxy model, the largest number of stars that will be observed by Gaia will have an energy distribution that peaks in this wavelength range due to their spectral type or the interstellar extinction. In this wavelength range, the presence of the CaII triplet lines for cool stars, the Paschen lines for hot stars and metallic lines will be useful to determine accurately radial velocity and chemical abundances.

2 A model of Galactic kinematics

In order to analyze the spectroscopic data in combination with the photometric information and proper motion, we have developed a self-consistent model of the Galactic disk. The disk is describe as sum of 20 isothermal stellar components with a vertical velocity dispersion σ_{zz} ranging from 10 to 70 km.s⁻¹. The distribution function of each component is built from three elementary functions describing the vertical density ρ_i , the kinematic distribution f_i (3D-gaussians) and the luminosity function ϕ_{ik} .

We define $\mathcal{N}(z, V_R, V_\phi, V_z; M)$ to be the density of stars in the Galactic position-velocity-absolute magnitude space:

$$\mathcal{N} = \sum_{ik} \rho_i(z) f_i(V_R, V_\phi, V_z) \phi_{ik}(M), \quad (2.1)$$

where the index i differentiates the stellar components and the index k the absolute magnitudes used to model the luminosity function.

We insert this model in the generalized equation of stellar statistics giving:

$$A(m, \mu_l, \mu_b, V_r) = \int N(z, V_R, V_\phi, V_z; M) z^2 \omega dz. \quad (2.2)$$

To determine $A(m)$, the apparent magnitude count, together with the marginal distributions of the proper motion μ_l and μ_b and the distributions of radial velocities for any direction and apparent magnitudes.

Assuming the stationarity of the density distribution, the consistency between the vertical velocity $\sigma_{zz,i}$ and density $\rho_i(z)$ distributions for each stellar component i is ensured by the following expression:

$$\rho_i(z) = \exp(-\Phi(z)/\sigma_{zz,i}^2) \quad (2.3)$$

where $\Phi(z)$ is the vertical gravitational potential at the solar Galactic position.

For the vertical gravitational potential, we use the recent determination obtained by Bienaymé et al. (2006). The vertical potential is defined at the solar position by:

$$\Phi(z) = 4\pi G \left(\Sigma_0 \left(\sqrt{z^2 + D^2} - D \right) + \rho_{\text{eff}} z^2 \right)$$

with $\Sigma_0 = 48 M_\odot \text{pc}^{-2}$, $D = 800 \text{pc}$ and $\rho_{\text{eff}} = 0.07 M_\odot \text{pc}^{-3}$.

The kinematical model is given by shifted 3D gaussian velocity ellipsoids. For simplicity, we assume that the $\sigma_{RR}/\sigma_{\phi\phi}$ ratio is the same for all the stellar components. The velocity ellipsoids are inclined along the Galactic meridian plane. The main axis of velocity ellipsoids are set parallel to confocal hyperboloids as in Stäckel potentials. The focus is set to $z_{\text{hyp}}=6 \text{kpc}$ on the main axis giving them realistic orientations (see Bienaymé 1999).

The luminosity function of each stellar component is modeled with n different kinds of stars according to their absolute magnitude:

$$\phi_i(M) = \sum_{k=1,n} \phi_{ik}(M) = \frac{1}{\sqrt{2\pi}\sigma_M} \sum_{k=1,n} c_{ik} e^{-\frac{1}{2}\left(\frac{M-M_k}{\sigma_M}\right)^2}$$

where c_{ik} is the density for each type of star (index k) of each stellar component (index i).

3 Results

We have adjusted the density of each stellar component to a sample of stars extracted from the 2MASS catalogue for the photometric data, the UCAC2 catalogue for proper motion and RAVE for the radial velocity. These stars are selected in color with $J-K = [0.5-0.7]$. In this color interval, we have defined 4 types of stars: Stars with a mean absolute magnitude $M_K = -1.61$ are identified to be the red clump giants ($k = 1$), with $M_K = -0.89$ and $M_K = -0.17$ are first ascent giants stars ($k = 2 - 3$) and with $M_K = 4.15$ for dwarfs ($k = 4$). We neglected sub-giant populations with an absolute magnitude M_K between 0.2 and 2. We adopt $\sigma_M = 0.25$ for each kind of stars on the luminosity function.

Adjusting the Galactic kinematical model to star counts, proper motions and radial velocities histograms, we obtained a kinematical decomposition of the Galactic disk (Fig. 1 left). The kinematical decomposition exhibits three main structures. We propose to identify the first one with vertical velocity dispersion $\sigma_W = [10-25] \text{ km s}^{-1}$ with the thin disk, the second with $\sigma_W = [30-45] \text{ km s}^{-1}$ with the thick disk. The decomposition shows a clear separation between the thin and thick components. For the third component with $\sigma_W = [60-70] \text{ km s}^{-1}$, the kinematical information is missing. This component could be a 'hot' kinematically thick disk or the halo.

From the kinematical decomposition, the scale height of the thin and thick disk could be determined independently by fitting an exponential on the density $\rho(z)$ (Fig. 1 right). We find a scale height for stellar components with $\sigma_W = [10-25] \text{ km s}^{-1}$ (thin disk) of $225 \pm 10 \text{ pc}$, for stellar components with $\sigma_W = [30-45] \text{ km s}^{-1}$ (thick disk) of $1048 \pm 36 \text{ pc}$ and the density ratio of thick to thin disk stars to be 8.7% at $z=0 \text{ pc}$. Our values are in agreement with previous determinations like the ones of Cabrera-Lavers et al. (2005) who have obtained a scale height of $267 \pm 13 \text{ pc}$ and $1062 \pm 52 \text{ pc}$ for the thin and thick disks respectively.

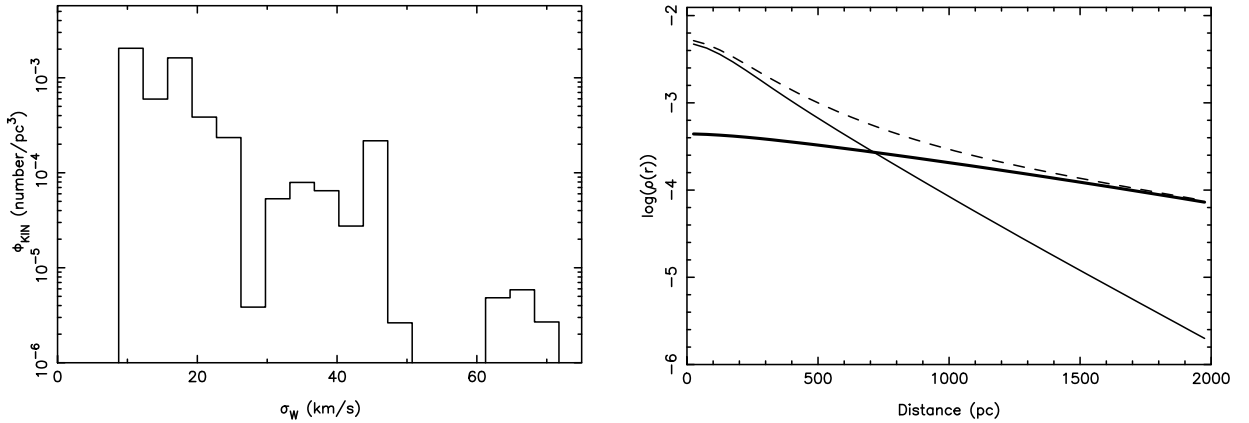


Fig. 1. Left: Kinematical decomposition of the Galactic disk. **Right:** The logarithm of the vertical stellar density $\rho(z)$ towards the the North Galactic Pole (dashed line) and its thin and thick disk decomposition (respectively thin and thick lines).

From our model, the solar motion relative to the LSR and the asymmetric drift were also determined. We obtained a value of $u_{\odot} = 8.5 \pm 0.3 \text{ km s}^{-1}$, $w_{\odot} = 11.1 \pm 1.0 \text{ km s}^{-1}$ and a thick disk lag is $V_{\text{lag}} = 33 \pm 2 \text{ km s}^{-1}$ relative to the LSR. v_{\odot} was fixed to $= 5.2 \text{ km s}^{-1}$, otherwise we could not measure the asymmetric drift.

By looking at latitude $|b| > 20^{\circ}$, we measure a radial scale length of $2.5 \pm 0.4 \text{ kpc}$ for the thin disk and $3.5 \pm 1.0 \text{ kpc}$ for the thick disk. There is no consensus on the values of the scale length of the values of the scale length of the thin and thick disk, but our values are in relative agreement, for example, with Ojha (2001) who finds $2.8 \pm 0.3 \text{ kpc}$ for the thin disk and $3.7_{-0.5}^{0.8} \text{ kpc}$ for the thick disk.

4 Conclusions

The fact that the decomposition of the Galactic disk reveals the kinematical separation of the thin and the thick disk puts some constraints on the scenarios of the Galactic disk formation. The thick disk could not have been created by a continuous ‘heating’ mechanism like the diffusion due to molecular clouds or spiral arms.

The scientific use of the RAVE data has already permitted us to obtain a lot of results on Galactic structure and kinematics: constrains on the local Galactic escape speed (Smith et al. 2007), absence of the Sgr stream near the Sun (Seabroke et al. 2008), scale height of the thin and thick disk (Veltz et al. 2008), vertical tilt of the ellipsoid (Siebert et al. 2008). With the accuracy and number of stars that will be observed by Gaia, the future is very promising for the analysis of the structure and kinematics of the disk. All these new informations will help to improve our understanding of the formation and evolution not only of the Milky Way but also the galaxies in general.

Acknowledgments

Funding for RAVE has been provided by the Anglo-Australian Observatory, by the Astrophysical Institute Potsdam, by the Australian Research Council, by the German Research Foundation, by the National Institute for Astrophysics at Padova, by The Johns Hopkins University, by the Netherlands Research School for Astronomy, by the Natural Sciences and Engineering Research Council of Canada, by the Slovenian Research Agency, by the Swiss National Science Foundation, by the National Science Foundation of the USA, by the Netherlands Organisation for Scientific Research, by the Particle Physics and Astronomy Research Council of the UK, by Opticon, by Strasbourg Observatory, and by the Universities of Basel, Cambridge, and Groningen. The RAVE web site is at <http://www.rave-survey.org>.

References

- Bienaymé, O. 1999, *A&A*, 341,86
Bienaymé, O., Soubiran, C., Mishenina, T. V., Kovtyukh, V. V. & Siebert, A. 2006, *A&A*, 446, 933
Cabrera-Lavers, A., Garzn, F., & Hammersley, P. L. 2005, *A&A*, 433, 173
Katz, D., Munari, U., Cropper, et al. 2004, *MNRAS*, 354, 1223
Munari, U. 1999, *Baltic Astronomy*, 8, 73
Munari, U. 2003, editor, *ASPC: "GAIA Spectroscopy: Science and Technology"*, 298
Ojha, D. K. 2001, *MNRAS*, 322, 426
Seabroke, G. M., Gilmore, G., Siebert, A., et al. 2008, *MNRAS*, 384, 11
Siebert, A., Bienaymé, O., Binney, J., et al. 2008, *arXiv0809.0615*
Smith, M. C., Ruchti, G. R., Helmi, A., Wyse, R. F. G., & Fulbright, J. P., et al. 2007, *MNRAS*, 379, 755
Steinmetz, M 2003, *ASPC: "Gaia Spectroscopy: Science and Technology"*, 298, 381
Steinmetz, M., Zwitter, T., Siebert, A., et al. 2006, *AJ*, 132, 1645
Veltz, L., Bienaymé, O.; Freeman, K. C., et al. 2008, *A&A*, 480, 753
Watson, F. G., Parker, Q. A., Bogatu, G., et al. 2000, *Proc. SPIE*, 4008, 123
Zwitter, T., Siebert, A., Munari, U., et al. 2008, *AJ*, 136, 421

THE GALACTIC BULGE AS SEEN IN OPTICAL SURVEYS

Reyl , C.¹, Marshall, D. J.², Schultheis, M.¹ and Robin, A. C.¹

Abstract. The bulge is a region of the Galaxy of tremendous interest for understanding galaxy formation. However measuring photometry and kinematics in it raises several inherent issues, such as severe crowding and high extinction in the visible. Using the Besan on Galaxy model and a 3D extinction map, we estimate the stellar density as a function of longitude, latitude and apparent magnitude and we deduce the possibility of reaching and measuring bulge stars with Gaia. We also present an ongoing analysis of the bulge using the Canada-France-Hawaii Telescope.

1 Introduction

Observing towards the bulge gives measures for a large number of individual stars that are the tracers of the Galactic formation and evolution. A detailed study of the bulge is necessary to understand its structure, dynamics and formation. The bulge of the Milky Way is the only one where the parameters in the six dimensions of phase space can be determined, as well as elemental abundances, on a star by star basis. Its detailed observation is thus very useful to test different scenarios of galactic bulge formation.

The bulge has been explored by a few ground based surveys, for example DENIS, 2MASS and microlensing surveys (OGLE, MACHO, DUO, EROS-2 and MOA) in the visible and the infrared, and from space by Spitzer in the mid infrared. The interstellar matter distributed in the plane is a major obstacle to the observation of the stars in the direction of the bulge and the Galactic center, particularly in the visible.

Gaia will give unprecedented view of the Galaxy, but it is often stated that, due to the wavelength coverage of instruments, it will be hardly usable for bulge studies. However, estimations of what Gaia will effectively see in the bulge is worthwhile to do before launch. We have investigated this question using a population synthesis model and a realistic 3D map of the extinction in the inner Galaxy. Studies of the bulge from ground before Gaia are also possible. We present an on-going survey of the bulge undertaken with Megacam aimed at producing good photometry and proper motions for a substantial number of clump stars.

2 Interstellar extinction

Extinction is so clumpy in the Galactic plane that it determines for a great part the number density of stars, more than any other large scale galactic structure. Thus, it is possible to extract information about the distribution of the extinction from photometry and star counts. Marshall et al. (2006) have shown that the 3D extinction distribution can be inferred from the stellar colour distributions in the 2MASS survey. Using stellar colours in $J - K_S$ as extinction indicators and assuming that most of the Galaxy model prediction deviations on small scales from observed colours arises from the variation of extinction along the line of sight, they built a 3D extinction map of the galactic plane. The resulting 3D extinction map furnishes an accurate description of the large scale structure of the disc of dust.

¹ Observatoire de Besan on, Institut UTINAM, Universit  de France-Comt , BP 1615, 25010 Besan on Cedex, France

² D partement de Physique et Centre Observatoire du Mont M gantic, Universit  Laval, Qu bec, G1K 7P4, Canada

3 The bulge density law from DENIS and 2MASS

The DENIS survey has produced specific observations in the direction of the bulge. Picaud & Robin (2004) used these data in 94 low extinction windows with $|l| < 10^\circ$ and $|b| < 4^\circ$ and the Besancon population synthesis model to determine shape parameters of the bulge as well as constraints on its age and luminosity function.

Using the 3D extinction map described above and the Galaxy model thus constrained, it is possible to perform a realistic comparison of the number of stars from the Galactic model with the number of observed stars in the 2MASS data (Fig. 1). The comparison points to significant discrepancies. In particular the bulge as defined by Picaud & Robin (2004) discrepant from the data at $4 < |b| < 10$, probably because the bulge shape was determined from a more restricted area in latitudes. A better adjustment of all 11 parameters characterizing the bulge over the whole 2MASS data set towards the bulge is ongoing.

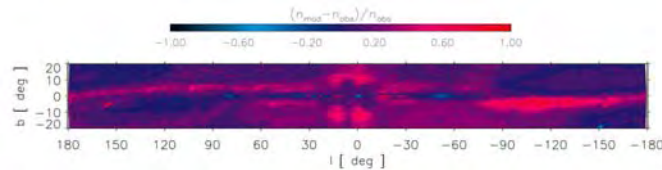


Fig. 1. Comparison between predicted star counts from the Galaxy model and 2MASS data. The colours code the relative difference $(n_{mod} - n_{obs})/n_{obs}$, n_{mod} and n_{obs} being star counts per square degree to magnitude $K_S=12$ for the model and the data respectively. It varies from a factor of two excess in modeled star counts (in red) to a factor of two deficiency in modeled star counts (in dark blue). Regions where the Galaxy model overestimates or underestimates the density of stars clearly appear.

4 The bulge with MegaCam

We started a photometric and astrometric survey of the bulge with MegaCam at CFHT. We observed 22 fields covering $-5^\circ < l < +5^\circ$, $-1^\circ < b < +1^\circ$, in the r' , i' , and z' bands. The observations are made at two epochs, separated by 3 years and have just been completed.

This survey provides unprecedented observations of the red clump very close to the Galactic plane. It will bring constraints on the luminosity function of the bulge. Moreover, a detailed extinction map with a very high spatial resolution can be obtained, using theoretical isochrones, such as the map obtained with Spitzer data (Schultheis et al., submitted). Proper motions will also be measured. We expect to get a precision of 1 mas yr^{-1} , corresponding to a velocity of 18 km s^{-1} at the bulge distance. 6 of the fields have also Giraffe observations (PI Babusiaux). In these fields we will get the 3 components of the velocity, as well as metallicity, allowing us to investigate the kinematics/metallicity relation.

Fig. 2 shows the colour-magnitude diagram for one field, in different parts of the CCDs mosaic. It shows how patchy and variable the extinction is. The red clump is clearly visible in some parts of the image, whereas it is not detected in other more extinguished parts.

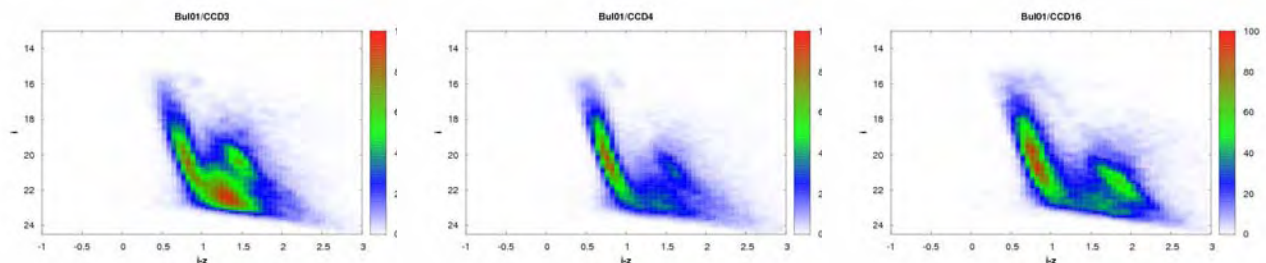


Fig. 2. i' versus $i' - z'$ diagram in 3 CCDs of one of the bulge fields.

5 The bulge with Gaia

Gaia will provide accurate positional, radial velocity, and photometry measurements for 1 billion of stars, that is about 1% of the Milky Way stellar content. Each star will be observed about one hundred times during the time of the mission, allowing the determination of proper motions. It comprises an astrometric instrument, photometers (GRP and GBP) and a spectrometer (RVS). The limit magnitude is $G=20^1$, except for the RVS ($G=17$). Detection problems may occur for these low spatial resolution instruments if the observed field is crowded. The estimated crowding limit is 600 000 stars deg^{-2} on the astrometric fields and photometers, and 40 000 stars deg^{-2} on the spectrometer.

Observations of bulge stars will strongly depend on the extinction and on the crowding. If the extinction is too high, the number of stars will be low (no crowding) but conversely the bulge stars would be out of reach, as they would be too faint. If the extinction is low (like in Baade’s window), bulge giants on the red clump are bright enough to be reached, but the crowding will limit the number and/or the quality of their measurements. Of course the number of stars in the bulge also strongly depends on latitudes and longitudes.

We use the Galaxy model together with the Marshall et al. (2006) extinction map to address the following question: is there a combination of parameters (extinction, latitude) in the galactic bulge where the extinction is large enough to avoid crowding and not too high to allow bulge star measurements with Gaia instruments? The results of the simulations are shown in Fig. 3 for the astrometric fields and in Fig. 4 for the spectrometer. The left panel shows the density of bulge stars at the limiting G magnitude of the instrument, as a function of longitude and latitude. The blue contour depicts the density at which crowding occurs. The green contour shows a iso-density of 100 bulge stars deg^{-1} , value at which we consider that the number of bulge stars starts to be significant. The right panel shows the absolute magnitude M_V of the intrinsically faintest bulge stars reached at the limiting G magnitude.

In the astrometric fields, a large part of the bulge will be visible, mainly in the Northern hemisphere, where extinction is higher. That corresponds to a number of 23 million bulge stars over an area of 220 deg^2 . Even still, in the Southern hemisphere bulge stars brighter than the limiting magnitude $G=20$ will be detected. Turn-off stars ($M_V \sim 4$) and even main sequence stars are observable at high latitudes. At lower latitudes, including regions very close to the Galactic plane, the absolute magnitude of the bulge stars is $M_V \sim 1$ to 2, and these stars are mainly clump giants. In the spectrometer (Fig. 4) where the crowding is a much more dramatic issue, there are unextended regions where the extinction is high enough to make the crowding low but still not too strong to mask completely bulge stars. About 30 000 bulge stars over 9.7 deg^2 are predicted to be observed, in regions around $b = 1$ to 2° . They are clump giants.

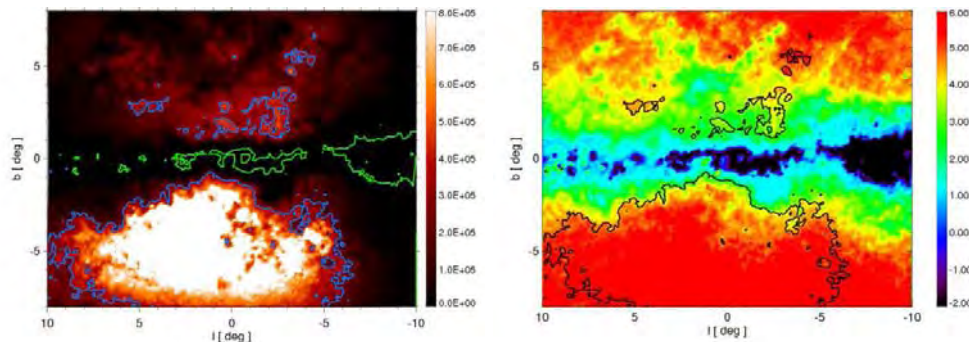


Fig. 3. Left: Density of the bulge in the Gaia astrometric fields at the limiting magnitude $G=20$, as a function of latitude and longitude. The blue contour shows the iso-density of 600 000 stars deg^{-2} , which is the crowding limit in the astrometric fields. The green contour shows the iso-density of 100 stars deg^{-2} . Right: Absolute magnitude M_V of bulge stars just reached at the limiting magnitude $G=20$.

There will be opportunities for Gaia to access reliable measurements in the Galactic bulge, photometry and astrometry, parallaxes, and proper motions, in nearly all the bulge regions. These regions strongly depend on the

¹ G is the photometric band used by the GAIA sky mappers. It is close to the V magnitude for stars with $V - I = 0$

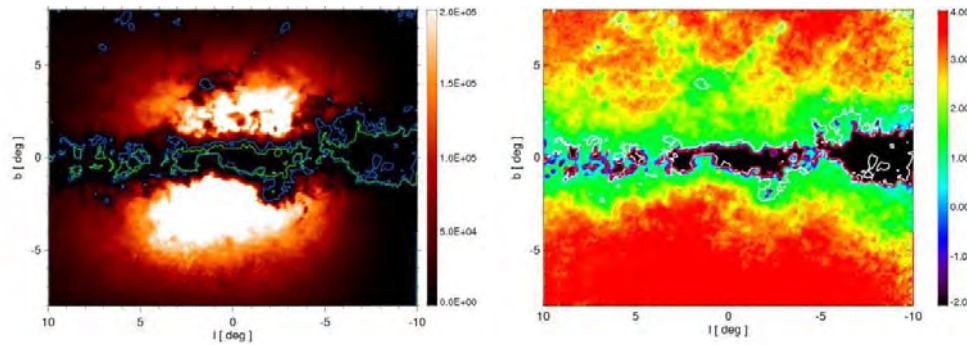


Fig. 4. Same as Fig. 3 for the RVS (limiting magnitude $G=17$ and crowding limit of $30\,000$ stars deg^{-2}).

assumed extinction. However, if the extinction maps do not suffer from systematics, there should be accessible windows well spread in longitude quite close to the dust lane in the Galactic plane. Observable bulge stars will also be spread in depth well inside the bulge. At low latitudes in the dense dust lane, most of the bulge stars will be too faint (due to extinction) to be reached. However in a few fields close to the Galactic plane in windows of lower extinction, stars in the giant clump should be observed. In any event, the position of the fields given here should be taken with caution because of the extreme sensitivity of the computation to the extinction which is not known to better than about 2 magnitudes in the most obscured regions. Putting together observations of the different instruments including RVS, Gaia should produce a detailed survey of bulge giants in terms of photometry as well as kinematics. Detailed analysis of these data sets should allow us to put strong constraints on the bulge structure and history.

6 Conclusion

Thanks to new photometric and astrometric surveys, the bulge structure can be revealed, bringing important constraints on the galaxy formation and evolution scenarii. We presented here several studies using such data set. Other available data are worthwhile to be analysed, such as the 49 OGLE-II fields for which proper motions have been measured Sumi et al. (2004). A preliminary analysis of these data with the Galaxy model shows that the bulge rotation can be constrained with these data.

Furthermore, radial velocities and metallicities data are available in the bulge directions (Ibata & Gilmore 1995; Minniti et al. 1996; Tiede & Terndrup 1999; Rich et al. 2007). The analysis of these data will allow us to refine the kinematical parameters of the bulge, as well as bulge metallicity. Finally, we showed that Gaia should give a detailed survey of bulge stars, down to the main sequence, in terms of photometry but also kinematics, including regions very close to the Galactic plane..

References

- Ibata, R. A. & Gilmore, G. F. 1995, MNRAS, 275, 605
- Marshall, D.J., Robin, A.C., Reylé, C., Schultheis, M., Picaud, S. 2006, A&A 453, 635
- Minniti, D., Liebert, J., Olszewski, E. W., & White, S. D. M. 1996, AJ, 112, 590
- Picaud, S., & Robin, A. C. 2004, A&A, 428, 891
- Rich, R. M., Reitzel, D. B., Howard, C. D., & Zhao, H. 2007, ApJ, 658, L29
- Robin, A.C., Reylé, C., Derrière, S., & Picaud S. 2003, A&A, 409, 523. Erratum 2004, A&A, 416, 157
- Sumi, T., et al. 2004, MNRAS, 348, 1439
- Tiede, G. P., & Terndrup, D. M. 1999, AJ, 118, 895

THE THIN AND THICK GALACTIC DISKS : MIGRATION AND LINEAGE

Misha Haywood¹

Abstract. Our understanding of the local constraints of the chemical evolution of the Galaxy have significantly changed in the recent years. This includes new results on the link between the two disks and on the two main constraints of galactic chemical evolution - the distribution of metallicities and the age-metallicity relation - and their new interpretation when radial migration of stars is properly taken into account. I discuss most recent advances on these three points.

It is argued that the so-called G dwarf problem cannot constrain infall because, starting with an initial metallicity of -0.2 dex, the thin disk could not have formed stars with 1/3 of solar abundance. Given this initial metal content, the problem is not to explain why there are so few metal-poor stars, but more likely to explain why there are so few metal-rich ones, for which infall could bring a correct answer. As a consequence of the conclusive link, or parenthood, that relates the thin and thick disks, the picture that emerge is that the thick disk appears to have been the main episode of chemical enrichment in the Galaxy. The Gaia perspective is evoked.

1 Introduction

Our understanding of local constraints (within 100 pc of the Sun) of the chemical evolution of the Galaxy have significantly changed in the recent years. This is due to both new accurate spectroscopic data and from the in depth analysis of the Hipparcos catalogue and complementary data (Nordström et al., 2004), giving access to the full 3D space velocities of solar neighbourhood stars. Several recent studies (Haywood (2008), Roškar et al. (2008), Schoenrich & Binney (2008)) have pointed out the importance of analysing both kinematic and chemical data in order to interpret key features, leading to a new understanding to the main constraints of the disk galactic chemical evolution. This includes new results on the link between the two disks, and the two main constraints of galactic chemical evolution, the age-metallicity relation and the distribution of metallicities. I review most recent advances on these three subjects.

2 Linking the thick and thin disks

2.1 Radial migration & the homogeneity of chemical species in the disk

Empirical evidences that radial mixing is effective have been found in solar neighbourhood data (Haywood, 2008). The study of the metallicity and orbital characteristics of thin disk stars sampled locally shows that the low and high metallicity tails of the thin disk are populated by objects which origins are in the outer and inner disk, and brought to the solar radius by radial migration. One possible mechanism giving rise to this mixing has been identified in Sellwood & Binney (2002), and its impact on the local kinematics and chemistry has been studied thoroughly by Schoenrich & Binney (2008). Signatures of this mixing is detected on the kinematic and orbital behaviour of thin disk stars, which show systematic trends as a function of metallicity. Metal-poor stars of the thin disk have guiding centres larger than the mean of solar neighbourhood stars (Fig. 1b), corresponding to V space velocities systematically higher than the LSR (Fig. 1a). Metal-rich stars have a symmetrical behaviour (Fig. 1c). This is best interpreted as corresponding to the inward and outward shift of stars that migrate from the outer and inner disk.

¹ GEPI, Observatoire de Paris, F-92195 Meudon Cedex, France

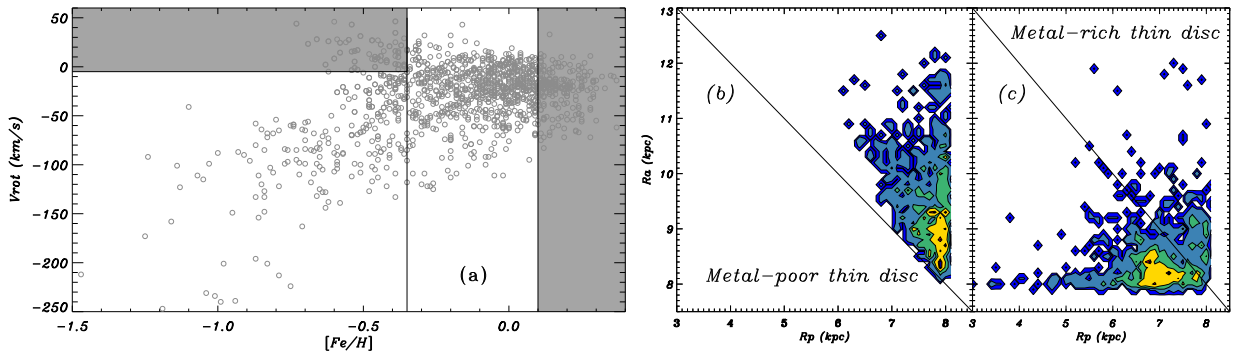


Fig. 1. (a) V_{rot} - $[Fe/H]$ plot for a sample of stars with accurate metallicities. (b) and (c) are the density distribution in the (pericentre, apocentre) space for stars as selected by the 2 boxes of plot (a) in the GCS catalogue.

Evidences are now accumulating that chemical evolution proceeds essentially from homogeneous ISM at all times in the disk, as testified by meteoritic presolar grains (Nittler, 2005), spectroscopic measurements through the ISM (Cartledge et al. 2006), and abundance ratios. Allowing for the effect of radial mixing as being responsible for most of the dispersion measured on stellar metallicities, it implies that thin disk stars born at the solar galactocentric radius have a rather restricted range of metallicities - within $[-0.2$ to $+0.2]$ dex.

It means that although the ISM is well mixed at a given radius, giving rise to similar relative abundance ratios of chemical species at all radii, the absolute level of enrichment (the metallicity) is mainly a function of galactic radius, much less a function of time. Radial migration of stars produced some amount of mixing in the disk, and thereby increased the dispersion in metallicity, while the relative ratios, being a slow function of metallicity, have remained relatively homogeneous. Given the small age-dependence of the metallicity at the solar neighbourhood, the widening of the metallicity interval due to radial mixing and present measurements of the radial metallicity gradient suggest that the radial variation of metallicity is 3 to 4 times more important than its local temporal evolution.

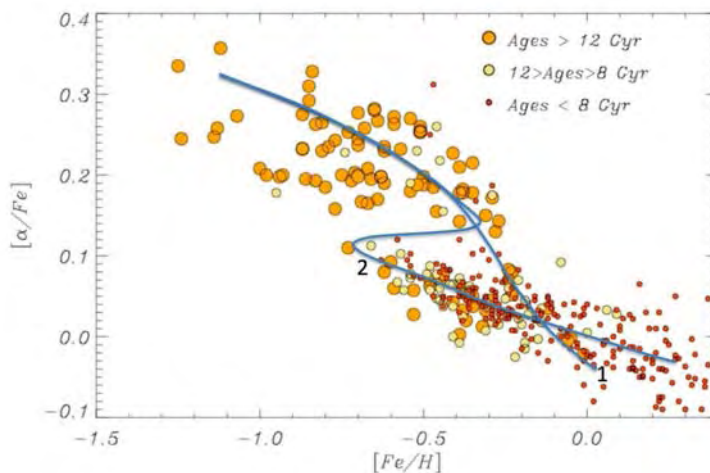


Fig. 2. Linking the thick and thin disks through α -element abundances. It has been suggested that the hiatus in metallicity could have resulted from an infall episode of gas that would have diluted metals in the ISM at the end of the thick disk formation (2). Orbital parameters of solar neighbourhood stars suggest on the contrary that the thin disk outside the metallicity interval $[-0.2, +0.2]$ dex are objects brought to the solar radius by radial migration. It suggests that the local thin disk at solar metallicities could be the continuation and the end point of a sequence (1) starting near $[Fe/H] = -1.2$ dex, or lower. Samples from Reddy et al., 2003, 2006 and Gilli et al. (2006)

2.2 *The parenthood between the two disks*

The accurate abundance patterns now available on local stars give the best indication so far of a continuity, or parenthood, between the thin and thick disks. The hiatus in metallicity (see Fig. 2) between thick disk stars (at $[\text{Fe}/\text{H}]=-0.2$ dex, $[\alpha/\text{Fe}]=0.18$ dex) and thin disk stars (at $[\text{Fe}/\text{H}]=-0.7$ dex, $[\alpha/\text{Fe}]=0.1$ dex) interpreted as the signature of an infall episode in standard chemical evolution (curve (2) on Fig. 2) is in fact best understood by taking into account the kinematic behaviour of the stars. The thin disk metal-poor stars, responsible for the hiatus, have a mean rotational component and a corresponding guiding centre greater than the mean disk population (Haywood, 2008) at the solar neighbourhood. This is best interpreted as testifying the outer disk origin of these stars (Haywood, 2008b, Schoenrich & Binney, 2008). If this interpretation is correct, these stars are outliers to the local thin disk chemical evolution, and the hiatus is not resulting from the local chemical evolution, but is a consequence of the radial redistribution of stars in the disk due to migration. The local evolution can then be seen to proceed continuously from high $[\alpha/\text{Fe}]$ and low metallicities to low $[\alpha/\text{Fe}]$ and solar metallicities (curve 1 on Fig. 2). In the $([\alpha/\text{Fe}], [\text{Fe}/\text{H}])$ plane, the thick disk seem to develop a sequence, while stars endemic of the thin disk at solar galactocentric radius are almost restricted to a point (nearly centred on the sun), at the end of, but possibly separated from, the thick disk sequence.

2.3 *Inconsistencies in the description of the thick disk*

Chemical data of stars kinematically labeled as thick disk in the solar vicinity seem to confirm a high degree of homogeneity, as is apparent in different studies (see in particular Fuhrmann 2008, Nissen & Schuster 2008), pointing to a well-defined population. What poses a problem however is its kinematic definition. Fig. 3 shows an histogram of V space velocity values from the work of Soubiran & Girard (2005). Stars flagged as thick disk members according to probability membership based on mean kinematic properties are given as the smaller histogram. One of these properties is the rotational lag, which in the case of the thick disk is standardly assumed to be 40-50 km/s. The plot shows that the thick disk selected in Soubiran & Girard (2005) is more likely to rotate with a mean lag of 80 km/s. Similar values are found on all kinematically defined thick disk samples from solar neighbourhood stars. Notice that this is near to the value found by Arifyanto & Fuchs (2006), making it unclear if thick disk parameters are polluted by an unknown stream or if Arifyanto & Fuchs (2006) have been pointing to the 'correct' thick disk. More generally, it must be clarified how the several streams that have been found on solar neighbourhood stars (Helmi et al. (2006), Arifyanto & Fuchs (2006)) are linked to the thick disk or even if they could be part of the thick disk.

The thick disk age in the solar neighbourhood is not better known. For example, Bernkopf & Fuhrmann (2006) advocates that the thick disk stars form a coeval population resulting from a single burst of star formation 12 Gyrs ago. Enlarged samples however seems to indicate a substantial evolution, as demonstrated in Bensby et al. (2004), Haywood (2006) and below. Obviously this point needs to be clarified, and echoes the more general challenge of identifying stars that truly make up this population.

3 **Age-metallicity relations in the thick and thin disks**

3.1 *How to correlate age and metallicity: biases in action*

Depending on the selection that is made to choose local stars, samples will include various amount of migrants from the outer or inner disk, or stars of the thick disk, and will therefore represent the local evolution accordingly. This is illustrated in Fig. 4, which shows the sample of Edvardsson et al. (1993) overplotted on our age-metallicity distribution from Haywood (2008). The sample of Edvardsson et al. (1993) was designed to be representative of the range of local metallicities, but has been often used to estimate the age-metallicity relation. The ages of the two samples were derived using the same procedure described in Haywood (2008). The sample of Edvardsson et al. is known to have provided the basis for claims of a real correlation between age and metallicity (Pont & Eyer, 2004). The age-metallicity relation evidenced in these studies stems from three different effects. The first one is the inclusion of thick disk objects. Non-differentiating the thick and thin disk stretches the relation across the two populations (down to -0.8 dex) and artificially creates a correlation that is mostly nonexistent within the thin disk. The inclusion of thin disk stars without taking account their radial origin also extends the metallicity range outside its normal interval by including metal-poor stars from

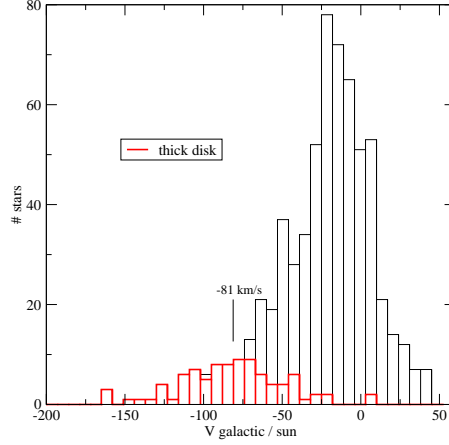


Fig. 3. Histogram of velocities in the direction of galactic rotation for the sample of Soubiran & Girard (2005). The histogram with mean at -81 km/s is representing stars flagged as thick disk using kinematic membership probability in their catalogue.

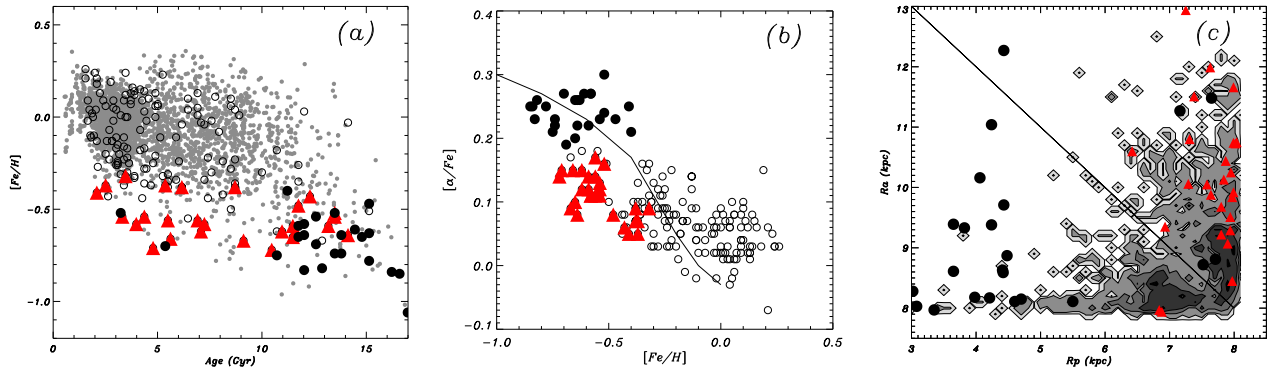


Fig. 4. (a) Stars from Edvardsson et al. (1993), overlaid to our age-metallicity distribution (small grey dots). Triangles are thin disk stars with $V > 5$ km/s, $[Fe/H] < -0.3$ dex and $[\alpha/Fe] < 0.18$ dex. Large black dots are thick disk object with the condition that $[\alpha/Fe] > 0.18$ dex. The age-metallicity distribution of the sample of Edvardsson et al. (1993) is heavily weighted towards metal-poor stars, due to the fact that it is biased against old solar-metallicity or metal-rich stars, and contains both thin disk stars from the outer disk and thick disk objects, which have not contributed to the thin disk local evolution. The apparent correlation between age and metallicity that has been obtained from this sample (Pont & Eyer, 2004) is essentially due to the combination of these 3 effects. (b) Position of these two groups in the $([\alpha/Fe], [Fe/H])$ diagram, and (c) on the (R_p, R_a) distribution.

the outer disk. Finally, Edvardsson et al. (1993) acknowledge that their selection excluded old metal-rich star, also contributing to enhance the correlation.

3.2 The thick disk as the main episode of galactic chemical enrichment

Figure 5 illustrates the different pace at which metal enrichment occurred in the galactic thin and thick disks. Metallicity has changed by about 0.3 dex in 8-10 Gyrs in the thin disk, or a factor of 2 of increase in Z . This is to compare with a factor 10 increase in 3-4 Gyr in the thick disk, and implies that most chemical enrichment in the solar neighbourhood have preceded the thin disk. Evidences are becoming more acute for a thick disk playing

a central role in the building of the Milky Way. Most recently, Nissen & Schuster (2008) presented new data on solar vicinity stars at lower metallicities ($[\text{Fe}/\text{H}] < -0.6$ dex), showing that two distinct components (accreted and dissipative) that make up the halo. One is clearly the continuity of the thick disk at lower metallicities, possibly making a single dissipative component of the Galaxy, the other shows distinct lower abundances of α elements with a pattern that resembles closely the one observed on dwarf spheroidals. On the contrary, if stars of the thick disk are of external origin, we are left with a gap of about 1.2 dex between the metallicity of the halo and that of the old thin disk. It would also imply that the Milky Way would have been relatively exceptional in the sense of having negligible star formation activity for several Gyrs when the universe was having its most intense phase of star formation.

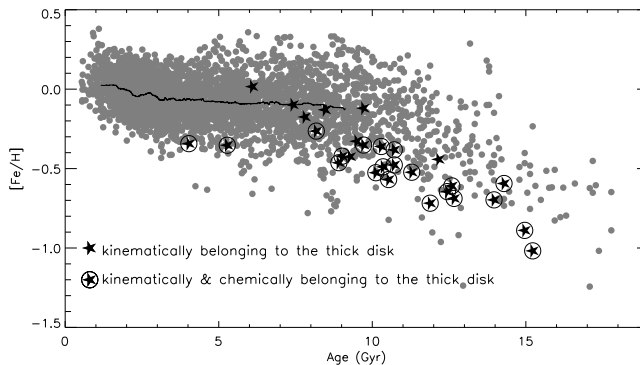


Fig. 5. Age-metallicity distribution for stars in the solar vicinity. Continuous curve is the mean metallicity of thin disk stars as a function of age. Star symbols are objects kinematically known has belonging to the thick disk (see Haywood (2006)). Symbols within circles have the additional condition that $[\alpha/\text{Fe}] > 0.18$ dex. The age of these objects has been derived taking into account their α -element content, which explains why they have systematically lower ages than stars of the same metallicities in the main sample (grey dots).

4 The new 'G dwarf problem', or the lack of metal-rich stars born at solar galactocentric radius

Contrary to what is stated in Prantzos (2008), Haywood (2006) didn't argue that the solar neighbourhood behaved like a closed box, but that its metallicity distribution, if the thick disk contribution is taken into account, is similar to a close-box distribution. It does only imply that the argument that infall-must-have-occurred-because-the-MDF-is-not-closed-box is fake, but does not imply that infall did not occur. Given the difficulties that classical modelling have to go beyond the unfruitful dilemma infall *vs* closed-box model, it is encouraging that new models (Brook et al. (2007), Schoenrich & Binney (2008), Roškar et al (2008)) combining dynamical and chemical evolution have had more success to account for local distributions as resulting from a mix of both kind of processes.

How does radial mixing affects the local metallicity distribution? Radial mixing has the effect of enlarging the range of observed metallicities at the solar radius, amounting to an approximate 10% of the stars, either metal-poor or metal-rich. As mentioned above, stars that are truly endemic of the solar galactocentric radius, have a range of metallicities of $-0.2 < [\text{Fe}/\text{H}] < 0.2$ dex in the thin disk, while the thick disk has $[\text{Fe}/\text{H}] < -0.2$ dex. How does it impact on the interpretation of the local metallicity distribution? The 'G-dwarf' problem, in its classical form, concerns the lack of stars with 1/3 of metals of the peak population (which is at $[\text{Fe}/\text{H}] \approx 0$), or $[\text{Fe}/\text{H}] \approx -0.45$ dex. Clearly, *there are no such stars stemming from the local evolution (at solar galactocentric radius) in the thin disk*, because at this metallicity, stars all reside in the thick disk. Since the metallicity was already -0.2 dex at the end of the thick disk phase, there is no point questioning why the thin disk has not formed stars more metal-poor than this limit. Therefore, there is no *metal-poor* G-dwarf problem in the thin disk, while there may be one in the thick disk. Unfortunately, there is no statistically meaningful sample of thick disk stars in the solar vicinity to test this prediction.

In 1974, B. Tinsley already pointed out the problem posed by the slow enrichment rate in the galactic thin disk: "Although disk-population stars of all ages have considerable dispersion in Z , the mean value is

only a very slowly increasing function of birth epoch". Considering an initial gas disk with surface density at the solar galactocentric radius of $40 M_{\odot} \cdot \text{pc}^{-2}$, mean initial metallicity -0.2 dex, mean star formation rate $4 M_{\odot} \cdot \text{pc}^{-2} \cdot \text{Gyr}^{-1}$, yield 2% and return gas fraction of 30%, it is expected that the present metallicity in the disk at the solar radius, would be about $+0.5$ dex, when at most 0.2 dex is observed (higher metallicities are due to contamination from the inner disk). Arguably, all these quantities are very uncertain, but still, there may be a 'G-dwarf', metal-rich problem, to which infall could be solution, as already noted by Tinsley. In other words, infall is not necessary to explain the absence of metal-poor dwarfs in the thin disk, but may be required to explain why so few metal rich stars have formed at the solar radius.

5 Gaia prospect

The vast majority of the stars Gaia will observe are disk stars. Accurate age determinations should be achievable within 2 kpc for a typical G-type main sequence star and 3 kpc for an old subgiant. The age-scale itself should also benefit from a drastic improvement in stellar physics that are expected from the availability of numerous fine calibrators that will map the entirety of the HR diagram, both from Gaia itself and present or forthcoming asteroseismology studies and complementary data. It is therefore expected that several millions of stars with accurate age determination will be available for the kind of studies that are achievable today only on a few hundreds of objects in the solar vicinity (within 50-100 pc). It implies that, complemented with high resolution, high SN spectroscopic data, a detailed map of the interface between the thick and thin disk populations should be obtainable, not only in the solar neighbourhood but also radially on several kpc. Moreover, the continuity that is lacking between local and in situ samples of the thick disk should help to characterize the properties of this population. Concerning the thin disk, particularly important will be the availability of radially distributed samples to understand the intricacy of chemical and dynamical processes as outlined here. Realistic simulations of the thin disk evolution including radial redistribution of stars and gas are just coming out in recent studies (see Roškar et al. 2008, Schoenrich & Binney 2008), and give us insights of what this complexity could be.

References

- Arifyanto M. I. & Fuchs B., 2006, *A&A*, 449, 533
 Bensby T., Feltzing S., Lundström I., 2004, *A&A*, 421, 969
 Bernkopf, J. & Fuhrmann, K., 2006, *MNRAS* 369, 673
 Brook, C. et al., 2007, *ApJ* 658, 60
 Cartledge et al., 2006, 641, 327
 Edvardsson B., et al., 1993, *A&A*, 275, 101
 Fuhrmann K., 2008, *MNRAS* 384, 174
 Gilli, G., et al, *A&A* 449, 723
 Haywood, M., 2006, *MNRAS*, 371, 1760
 Haywood, M., 2008, *MNRAS* 388, 1175
 Helmi, A. et al., 2006, *MNRAS* 365, 1309
 Nissen, P.E. & Schuster, W.J., 2008, *astro-ph*, 0807.3831
 Nordström B., Mayor, M., Andersen, J., et al., 2004, *A&A*, 418, 989
 Nittler, L. R., 2005, *ApJ* 618, 281
 Pont F., Eyer L., 2004, *MNRAS*, 351, 487
 Prantzos, N., 2008, *astro-ph* 0809.2507
 Reddy B. E., Tomkin J., Lambert D. L., Allende Prieto C., 2003, *MNRAS*, 340, 304
 Reddy B. E., Lambert D. L., Allende Prieto C., 2006, *MNRAS*, 367, 1329
 Roškar, R. et al., 2008, *ApJ* 684, 79
 Schoenrich, R. & Binney, J., 2008, *astro-ph*
 Sellwood J. A. & Binney J. J., 2002, *MNRAS*, 336, 785
 Soubiran C. & Girard P., 2005, *A&A*, 438, 139
 Tinsley B. M., 1974, *ApJ*, 192, 629

THE SOLAR SYSTEM SEEN BY GAIA: NEW PERSPECTIVES FOR ASTEROID SCIENCE

Tanga, P., Delbò, M. and Mignard, F.¹

Abstract. The Gaia astrometric mission of the European Space Agency, to be launched at the end of 2011, will perform a 5-years satellite survey of the whole sky at an unprecedented level of astrometric accuracy. Designed to explore the Galaxy, Gaia will indeed provide observations of small Solar System objects brighter than $V \sim 20$, including some small planetary satellites, comets, trans-neptunian objects and asteroids. This last category will be, by far, the most populated, since we can expect to receive data for $\sim 250\,000$ objects. The observations of Gaia will provide will not only include astrometric measurements, but also multi-band photometry, thus resulting in the most accurate and homogeneous data set available on both Main Belt Asteroids and Near Earth Objects. In the frame of the Gaia Data Processing and Analysis Consortium, a specific effort is devoted to prepare the Solar System data reduction pipeline that will extract the relevant scientific information from raw observations. Impressive achievements are expected, concerning both the improvement of orbit accuracy and the physical properties of asteroids. While these results, obtained on Gaia data alone, will represent an unprecedented step forward in our knowledge of the Solar System, the science scope could be even larger if an appropriate ground-based observation campaign takes place. In this case, more difficult measurements of small perturbations in the asteroid orbital motion (such as the ‘Yarkovsky effect’, due to the small perturbations in the orbital motion of these bodies thermal infrared emission) will become accessible for some objects. Conversely, future ground-based observations will also take profit from Gaia results and open new perspectives for classic techniques. This is the case, for example, of asteroid occultations of stars, whose predictions will be much more accurate and reliable, permitting systematic determinations of size and shapes for asteroids larger than 10 km. In this sense, Gaia heritage will not only be a revolution for Solar System science, but will also durably impact the other related observation activities.

¹ OCA/Cassiope, BP 4229, 06304 Nice cedex 04, France

POSTERS

- Gaia, materiel pour l'animation scientifique auprès du grand public – F. Arenou & C. Turon
- Multi-step VLBI Observations of weak extragalactic radio sources to align the ICRF and the future Gaia frame - G. Bourda et al.
- Radial velocity standards for the Gaia-RVS – F. Crifo et al
- Ground-based observations of Solar System bodies in complement to Gaia – D. Hestroffer et al.
- Ground-based observations for Gaia (GBOG) – C. Soubiran et al.
- Activities of the ICRS product centre (SYRTE, Paris Observatory) – J. Souchay et al.
- Radial velocities with the Gaia RVS spectrometer – Y.P. Viala et al.
- Simulating charge transfer inefficiency effects on future Gaia data – M. Weiler M. and C. Babusiaux

Arenou F., Turon C. (GÉPI/Observatoire de Paris) pour l'Action Spécifique Gaia & E.S.A.

L'année 2009 sera celle de l'Astronomie. Gaia est une mission particulièrement bien placée pour illustrer la discipline en direction de la jeunesse et du grand public. Gaia touche à de nombreux domaines de l'astrophysique, depuis le système solaire jusqu'aux galaxies extérieures, la mesure des distances et les effets relativistes, en passant par la détection de planètes extrasolaires. L'ESA a préparé un matériel de présentation assez vaste, disponible en ligne, dont la traduction est présentée ci-dessous.

Prospectus (A4)

Petits livres (A4 → A7)

Maquette



Gaia - l'arpenteur de la Voie Lactée

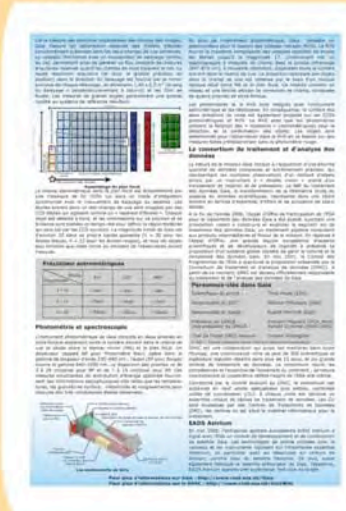
Après une mission spatiale dédiée au Soleil et à son système planétaire, l'ESA lance en 2013 la mission Gaia, la plus précise jamais réalisée. Elle va mesurer la position, le mouvement et la luminosité de plus de 100 milliards d'étoiles dans notre galaxie, la Voie Lactée.

Un projet spatial et l'instrument astronomique

La mission Gaia est une mission spatiale de grande précision. Elle va mesurer la position, le mouvement et la luminosité de plus de 100 milliards d'étoiles dans notre galaxie, la Voie Lactée.

Phénométrie et spectroscopie

La mission Gaia va mesurer la position, le mouvement et la luminosité de plus de 100 milliards d'étoiles dans notre galaxie, la Voie Lactée.



La opportunité de l'instrument et d'analyse des données

La mission Gaia va mesurer la position, le mouvement et la luminosité de plus de 100 milliards d'étoiles dans notre galaxie, la Voie Lactée.

Phénométrie et spectroscopie

La mission Gaia va mesurer la position, le mouvement et la luminosité de plus de 100 milliards d'étoiles dans notre galaxie, la Voie Lactée.



HISTOIRE DE L'ASTRONOMIE

LA RECHERCHE DE PLANÈTES

LA NAISSANCE D'UNE NOUVELLE MOUSSE SCIENTIFIQUE



CE QU'IL Y A DANS LES ÉTOILES

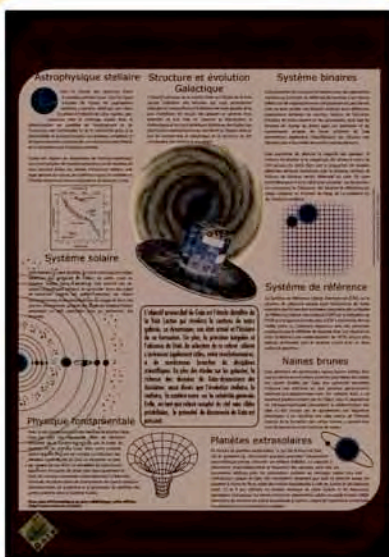
LES ÉTOILES ET LES PLANÈTES

LES ÉTOILES ET LES GALAXIES



- Le but**
 - Répondre à la curiosité du public
 - Rendre la science attractive et accessible
 - Recueillir des vocations
 - Donner de la visibilité à nos Établissements et à l'ESA
- Une situation très favorable**
 - L'astrophysique (Gaia touche à de nombreux domaines)
 - L'aspect technique (un satellite)
 - Un projet Européen et où la France est bien positionnée
 - L'appui technique de l'ESA

Posters (A2/A3)



Astrophysique stellaire

Structure et évolution Galactique

Système solaire

Système de référence

Naines brunes

Planètes extrasolaires



DPAC

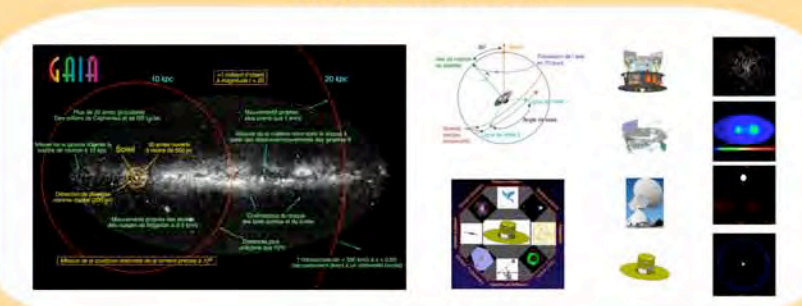
DPAC



GAIA, l'univers en 3 dimensions

Images et courtes vidéos

Présentations




Liens utiles

Ce matériel est disponible sur les sites de :
L'ESA: <http://www.rssd.esa.int/index.php?project=Gaia>
L'A.S. Gaia: <http://www.hip.obspm.fr/gaia/AS>

MULTI-STEP VLBI OBSERVATIONS OF WEAK EXTRAGALACTIC RADIO SOURCES TO ALIGN THE ICRF AND THE FUTURE GAIA FRAME

Bourda, G.¹, Charlot, P.¹, Porcas, R.² and Garrington, S.³

Abstract. The space astrometry mission Gaia will construct a dense optical QSO-based celestial reference frame. For consistency between optical and radio positions, it will be important to align the Gaia frame and the International Celestial Reference Frame (ICRF) with the highest accuracy. Currently, it is found that only 10% of the ICRF sources (70 sources) are suitable to establish this link, either because they are not bright enough at optical wavelengths or because they have significant extended radio emission which precludes reaching the highest astrometric accuracy. In order to improve the situation, we have initiated a VLBI survey dedicated to finding additional suitable radio sources for aligning the two frames. The sample consists of about 450 sources, typically 20 times weaker than the current ICRF sources, which have been selected by cross-correlating optical and radio catalogues. This paper presents the observing strategy to detect, image, and measure accurate positions for these sources. It also provides results about the VLBI detectability of the sources, as derived from initial observations with the European VLBI Network in June and October 2007. Based on these observations, an excellent detection rate of 89% is found, which is very promising for the continuation of this project.

1 Context

The International Celestial Reference Frame (ICRF) is the realization at radio wavelengths of the International Celestial Reference System (ICRS; Arias et al. 1995), through Very Long Baseline Interferometry (VLBI) measurements of extragalactic radio source positions (Ma et al. 1998; Fey et al. 2004). It was adopted by the International Astronomical Union (IAU) as the fundamental celestial reference frame during the IAU 23rd General Assembly at Kyoto, in 1997. The ICRF currently consists of a catalogue with the VLBI coordinates of 717 extragalactic radio sources (from which 212 are defining sources), with sub-milliarcsecond accuracy.

The European space astrometry mission Gaia, to be launched by 2011, will survey about (i) one billion stars in our Galaxy and throughout the Local Group, and (ii) 500 000 Quasi Stellar Objects (QSOs), down to an apparent optical magnitude V of 20 (Perryman et al. 2001). Optical positions with Gaia will be determined with an unprecedented accuracy, ranging from a few tens of microarcseconds (μ as) at magnitude 15–18 to about 200 μ as at magnitude 20. Unlike Hipparcos, Gaia will permit the realization of the extragalactic reference frame directly at optical bands, based on the QSOs that have the most accurate positions (i.e. those with $V \leq 18$ (Mignard 2003); it is expected to detect at least 10 000 of such QSOs (Mignard 2002)). A preliminary Gaia catalogue is expected to be available by 2015 with the final version released by 2020.

In the future, aligning the ICRF and the Gaia frame will be crucial for ensuring consistency between the measured radio and optical positions. This alignment, to be determined with the highest accuracy, requires several hundreds of common sources, with a uniform sky coverage and very accurate radio and optical positions. Obtaining such accurate positions implies that the link sources must have (i) an apparent optical magnitude V brighter than 18 (for the highest Gaia astrometric accuracy), and (ii) no extended VLBI structures (for the highest VLBI astrometric accuracy). In a previous study, we investigated the current status of this alignment based on the present list of ICRF sources (Bourda et al. 2008). We showed that although about 30% of the ICRF sources have an optical counterpart with $V \leq 18$, only one third of these are compact enough on VLBI

¹ Laboratoire d’Astrophysique de Bordeaux, Université de Bordeaux, CNRS UMR 5804, BP89, 33271 Floirac Cedex, France

² Max-Planck-Institute for Radio Astronomy, P.O. Box 2024, 53010 Bonn, Germany

³ Jodrell Bank Observatory, The University of Manchester, Macclesfield, Cheshire, SK11 9DL, UK

scales for the highest astrometric accuracy. Overall only 10% of the current ICRF sources (70 sources) are available today for the alignment with the future Gaia frame. This highlights the need to identify additional suitable radio sources, which is the purpose of the project described here.

2 Strategy to identify new VLBI radio sources for the ICRF–Gaia alignment

Searching for additional radio sources suitable for aligning accurately the ICRF and the Gaia frame could rely on the VLBA Calibrator Survey (VCS; Petrov et al. 2008 and references therein), a catalogue of more than 3000 extragalactic radio sources observed with the VLBA (Very Long Baseline Array). This investigation is currently underway. Another possibility is to search for new VLBI sources, which implies going to weaker radio sources that have a flux density typically below 100 mJy. This can now be envisioned owing to the recent increase in the VLBI network sensitivity (i.e. recording now possible at 1Gb/s) and by using a network with big antennas like the EVN (European VLBI Network). A sample of about 450 radio sources that mostly have never been observed with VLBI (i.e. not part of the ICRF or VCS) has been selected for this purpose by cross-identifying the NRAO VLA Sky Survey (NVSS; Condon et al. 1998), a deep radio survey (complete to the 2.5 mJy level) that covers the entire sky north of -40° , with the Véron-Cetty & Véron (2006) optical catalogue of QSOs. This sample is based on the following criteria: $V \leq 18$ (for an accurate position with Gaia), $\delta \geq -10^\circ$ (for possible observing with northern VLBI arrays), and NVSS flux density ≥ 20 mJy (for possible VLBI detection). The observing strategy to identify the appropriate link sources in the sample includes three successive steps: (1) to determine the VLBI detectability of these weak radio sources, mostly not observed before with VLBI; (2) to image the sources detected in the previous step, in order to reveal their VLBI structure; and (3) to determine an accurate astrometric position for the most point-like sources of the sample.

3 VLBI results

Initial VLBI observations for this project were carried out in June and October 2007 (during two 48–hours experiments), with a network of 4 or 5 VLBI antennas from the EVN. The purpose of these two experiments was to determine the VLBI detectability of the 447 weak radio sources in our sample based on snapshot observations. Our results indicate excellent detection rates of 97% at X band and 89% at S band. Overall, 398 sources were detected at both frequencies. The overall mean correlated flux densities were determined for each source and band by the mean over all scans and baselines detected. At X band, 432 sources were detected and the mean correlated fluxes range from 1 mJy to 190 mJy, with a median value of 26 mJy. At S band, 399 sources were detected and the mean correlated fluxes range from 8 mJy to 481 mJy, with a median value of 46 mJy. A comparison between the X-band flux density distribution for our sources, those from the VCS and the ICRF shows that the sources of our sample are indeed much weaker. On average, they are 27 times weaker than the ICRF sources and 8 times weaker than the VCS sources. The spectral index α ($S \propto \nu^\alpha$, S being the source flux density and ν the frequency) was determined for the 398 radio sources detected at both frequencies; the sources with a compact core are expected to have $\alpha > -0.5$. The median value of α in our sample is -0.34 and about 70% of the sources have $\alpha > -0.5$, hence indicating that they must have a dominating core component, which is very promising for the future stages of this project. The next step will be targeted at imaging the 398 sources that we have detected at both frequencies, by using the global VLBI network (EVN+VLBA), in order to identify the most point-like sources and therefore the most suitable ones for the ICRF–Gaia link.

References

- Arias, E. F., Charlot, P., Feissel, M., & Lestrade, J.-F. 1995, *A&A*, 303, 604
 Bourda, G., Charlot, P., & Le Champion, J.-F. 2008, *A&A* (in press)
 Condon, J. J., Cotton, W. D., Greisen, E. W., Yin, Q. F., Perley, R., et al. 1998, *AJ*, 115, 1693
 Fey, A. L., Ma, C., Arias, E. F., Charlot, P., Feissel-Vernier, M., et al. 2004, *AJ*, 127, 3587
 Ma, C., Arias, E. F., Eubanks, T. M., Fey, A. L., Gontier, A.-M., et al. 1998, *AJ*, 116, 516
 Mignard, F. 2002, In: *Gaia: A European space project*, O. Bienaymé & C. Turon (eds.), EAS Publications series, 2, 327
 Mignard, F. 2003, In: *IAU XXV, Joint Discussion 16*, R. Gaume, D. McCarthy & J. Souchay (eds.), 133
 Perryman, M. A. C., de Boer, K. S., Gilmore, G., Hog, E., Lattanzi, M. G., et al. 2001, *A&A*, 369, 339
 Petrov, L., Kovalev, Y., Fomalont, E., & Gordon, D. 2005, *AJ*, 129, 1163
 Véron-Cetty, M.-P., & Véron, P. 2006, *A&A*, 455, 773

RADIAL VELOCITY STANDARDS FOR THE GAIA-RVS

Crifo, F.¹, Jasniewicz, G.², Soubiran, C.³, Veltz, L.⁴, Hestroffer, D.⁵, Katz, D.¹, Siebert, A.⁶ and Udry, S.⁷

Abstract. The ESA GAIA mission (launch expected end 2011), besides the 5 astrometric parameters and photometry for some 10^9 objects, will also produce radial velocities and short spectra for a few 10^8 stars, with a 1 to 15 km/s accuracy.

The calibration of radial velocities in the integral-field spectrograph will rely on a set of some 1000 bright RV-stable stars already observed with a much higher accuracy from the ground, on a few bright enough asteroids, and a set of some 10^5 stable stars selected later from the RVS measurements themselves. We present here a status report on the ongoing effort to construct the basic list with ground-based observations.

1 The RVS and the need for ground-based standards

The Radial Velocity Spectrometer (RVS) onboard GAIA is designed mainly for measuring radial velocities of the brightest GAIA targets. It is a slitless spectrograph, without onboard calibration device. It covers the spectral range (847 - 874) nm. The brightest stars ($V \leq 10$) will be observed with a resolution of 11500; and the fainter ones with a resolution of about 4000.

The RVS is a self-calibrating instrument relying on a set of about 1000 bright, stable objects with well-known RVs. This sample must be well-distributed over the sky to set the RV zero-point and is included in the iterative reduction process. As these objects will be regularly observed by GAIA (some 40 observations each, over the 5 years of mission), they will also allow a permanent check of the state and performances of the instrument.

2 Star selection

Bright asteroids and single stars with a good observational history are selected and re-observed before the start of the mission to insure a stability at the level of 300m/s until the end of mission (2017). Selection criteria for stars have been already given with some details (see Crifo et al, 2007) (HIP stars; $V \geq 6$; $G_{RVS} \leq 10$; F5-K; M dwarfs; not variable, not double or multiple; no disturbing neighbour in the selection window, i.e. within 80 arcsec; already well observed).

The stars are selected within the 3 following published lists: Nidever et al. (2002); Nordström et al. (2004; mostly CORAVEL data); Famaey et al. (2005; CORAVEL data). A provisional list of about 1400 stars is now defined, and used for the observations.

¹ GEPI (UMR 811 du CNRS; Université Paris 7), Observatoire de Paris, 92195 MEUDON Cedex, France

² UMR CNRS/UM2 GRAAL, CC 72, Université Montpellier2, 34095 MONTPELLIER Cedex 05, France

³ Université Bordeaux 1, CNRS, LAB, F-33270 FLOIRAC, France

⁴ Astrophysikalisches Institut Potsdam, POTSDAM, Germany

⁵ IMCCE (UMR 8028 du CNRS), Observatoire de Paris, 77 av. Denfert-Rochereau, 75014 PARIS, France

⁶ Observatoire de Strasbourg (Université Louis Pasteur et CNRS), 11 rue de l'Université, 67000 STRASBOURG, France

⁷ Observatoire de Genève, 51 Ch. des Maillettes, 1290 SAUVERNY, Switzerland

3 On-going ground-based observations

Each candidate is re-observed at least once before launch to eliminate evident variables. Supplementary observations are made, depending on the observational history of the star, and for follow-up during the mission. The observing programme is running on the echelle spectrographs SOPHIE (OHP), NARVAL (TBL, Pic du Midi), and CORALIE (Swiss Euler telescope, La Silla), for a total of about 9 nights per semester. The observations started in 2006. The new data are stored in an on-purpose database, presently hosted at AIP-Potsdam.

NARVAL is the only spectrograph covering totally the RVS spectral interval, and these spectra will therefore also be used for comparing the velocities obtained either over the full spectral range, or only over the RVS range.

Figure 1 shows for asteroids the difference (O-C) between data and calculated predictions, as a function of the S/N ratio during the observation, for SOPHIE and previous ELODIE. Figure 2 shows for stars the comparison between the Sophie data and and previous data as published by Famaey (Coravel), Nordström (Coravel) or Nidever: the larger dispersion for Famaey and Nordström is due to lower Coravel accuracy.

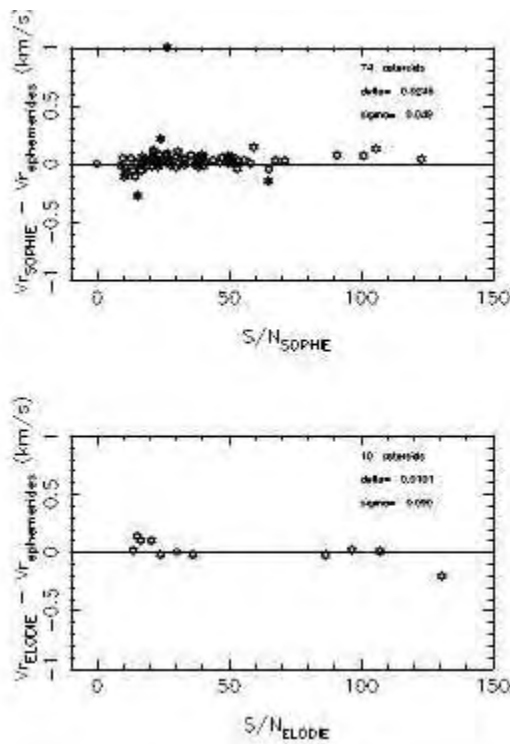


Fig. 1. Asteroids: O-C vs S/N, Sophie & Elodie

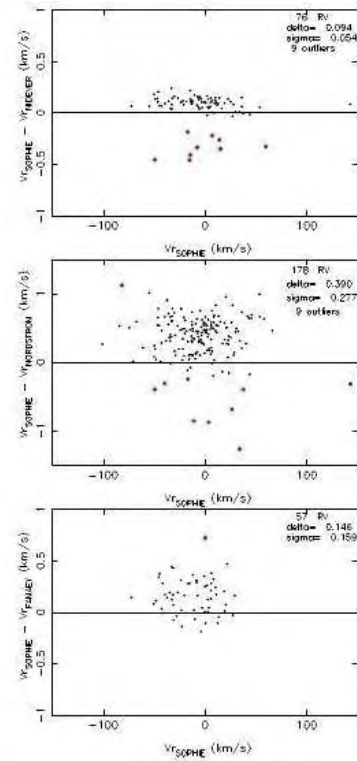


Fig. 2. Stars: Sophie vs Nidever, Nordström and Famaey

4 Conclusion

Good RV standards for the RVS, stable over a long period, must be used to control the accuracy of the RVS instrument zero point. Such a sample can be defined using bright, well-known stars and asteroids, and an important observational effort is underway to verify the stability of about 1000 such objects over the full sky.

References

- Crifo, F., Jasniewicz, G., Soubiran, C., Hestroffer, D., Siebert, A., Guerrier, A., Katz, D., Thévenin, F., & Turon, C. 2007, 2007sf2a.conf..459C
- Famaey, B., Jorissen, A., Luri, X., et al. 2005, A&A, 430, 165
- Nidever, D. L., Marcy, G. W., Butler, R.P., et al. 2002, ApJS, 141, 503
- Nordström, B., Mayor, M., Andersen, J., et al. 2004, A&A, 418, 989

GROUND-BASED OBSERVATIONS OF SOLAR SYSTEM BODIES IN COMPLEMENT TO GAIA.

Hestroffer, D.¹, Thuillot, W.¹, Mouret, S.^{1,2}, Colas, F.¹, Tanga, P.³, Mignard, F.³, Delbò, M.³ and Carry, B.⁴

Abstract. The ESA cornerstone mission Gaia, to be launched during end-2011, will observe $\approx 250,000$ small bodies. These are mostly main belt asteroids, but also Near-Earth objects, Trojans, and a few comets, or planetary satellites. The scientific harvest that Gaia will provide – given the high astrometric accuracy (at sub-milli-arcsec level), valuable photometric measurements (at milli-mag level), and moderate imaging (about 2,000 objects will be resolved) – will have a major impact on our knowledge of this population in terms of composition, formation and evolution (Mignard et al. 2007). There are nevertheless some intrinsic limitations in particular due to the unavoidable limited duration of the mission (5 years), the peculiar observing strategy that is not optimised to the observation of solar system objects, and last, the limited imaging possibilities. We can thus identify two kind of complementary data and ground-based observations, whether they are part of the Gaia Data Processing and Analysis Consortium (DPAC), or not, but provide a strong leverage to the Gaia science.

We discuss different aspects of additional observations from ground (yet not exclusively) either in preparation to the Gaia mission, in alert during the mission, or after the mission as additional complementary information. Observations of a set of well defined and selected targets, with different telescopes and instrumentation, will increase the scientific output in three particular and important topics: mass of asteroids, their bulk density and possible link to their taxonomy, and non-gravitational forces.

1 Gaia an ESA cornerstone astrometric mission

Gaia is the next space mission from the European Space Agency dedicated to astrometry. It is much more ambitious compared to its precursor Hipparcos, considering either the number of targets, the astrometric and photometric precision reached, or last the potential scientific outputs. For instance Gaia will enable the determination of asteroids taxonomy, spin state, and – for a smaller set – sizes, and masses. Nevertheless, the limiting magnitude and scanning law as well as the modest imaging resolution power, make that not all category of objects can be observed optimally. It is then interesting to complement such space data with dedicated ground-based observations. Such observations can be made on alert during the Gaia mission, but also either before or after the mission completion. Ground-based observations of asteroids and small bodies can be used a) for practical reasons during the data reduction itself, b) as supplementary data over larger time span, or c) as complementary data because out of the accessibility of the Gaia instruments.

2 Ground-based complements

Here we focus on a few points of interest:

1. Observations in alert will enable to trigger ground-based observations in short time (but not less than ≈ 24 hours) to ensure a good threading of the object, avoid its loss (and potential hazard), and complete

¹ IMCCE, Observatoire de Paris, UPMC, USTL, CNRS, 77 av. Denfert-Rochereau 75014 Paris, France – <mailto:hestro@imcce.fr>

² Univ. of Helsinki observatory, Helsinki, Finland

³ OCA, CNRS, Le Mont Gros 06000 Nice, France

⁴ ESO, Vitacura, Chile. LESIA, Observatoire de Paris, UMR CNRS/INSU 8109, place J. Janssen, 92195 Meudon, France

the Gaia observations limited at $V \leq 20$ Tanga et al. (2008). These are delicate observations due to the possible low solar elongation, and the large parallax of the satellite located at the Sun-Earth L2 Lagrangian point;

2. High angular-resolution observations for selected asteroids will provide precise size and shape estimate and, once combined to good mass knowledge, their bulk density. Because there are no particular bias toward the binary asteroid population, and many taxonomic classes will be sampled, we will test for a possible link between asteroids' taxonomy and their interior (see Table 1). Additionally, these observations will be useful to calibrate the size determination from the Gaia imaging itself, and to calibrate the photocenter correction modelling to apply during the astrometric reduction;
3. Astrometric observations before and after Gaia of about more than 50 target asteroids will increase the number of derived asteroids masses (Mouret 2007) adding more than 25 bodies to the list of approx. 150 from Gaia observations alone. Moreover, astrometry and radiometric size measurements of several selected NEOs will enable the detection of the Yarkovsky effect and possibly give an indication on their thermal inertia. These additional information will also enable us to better understand and model possible bias in the global adjustment of the complex model to the Gaia observations, avoiding hence a degradation of the general quality of any global parameter estimation (test of General Relativity, link of the dynamical reference frame to the optical ICRF, etc.);
4. Last, the availability of the Gaia stellar catalogue – together with better orbits of asteroids – will enable a much better prediction of stellar occultations, and their path on the surface of the Earth (see Fig. 1).

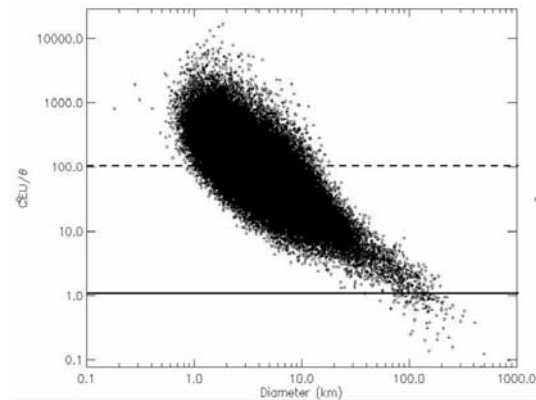


Fig. 1 Asteroids accessible to stellar occultations, as a function of their prediction precision and size. This is given by the ratio of the asteroids ephemeris uncertainty (CEU) to angular diameter θ as a function of the asteroid size. Good predictions are provided when $CEU/\theta \leq 1$ thus an increase of one dex on the CEU precision would yield an increase of two dex in the number of potential asteroids, and also enable to sample smaller bodies (diameter $\gtrsim 10$ km). Compared to what can be achieved today with the Tycho catalogue, Gaia will yield a much larger number of interesting events; which in turn will be observed with a larger number of chords and not for only one snapshot, and consequently provide a completely scaled 3-dimensional view of the whole body.

Table 1. Taxonomic type sampling of asteroids with expected known masses (and apparent diameter ≥ 80 mas) observable at the VLT during forthcoming ESO observations periods (covering 2 years).

| Type | A | B | C | K | L | Q | R | S | T | X |
|-------|---|---|----|---|---|---|---|----|---|----|
| P83 | – | 1 | 6 | 1 | – | 1 | – | 10 | – | 5 |
| P84 | 1 | – | 7 | – | – | – | – | 4 | – | 4 |
| P85 | – | 1 | 5 | 1 | 1 | – | 1 | 9 | 1 | 2 |
| P86 | – | 1 | 5 | 1 | – | – | – | 6 | – | 3 |
| Total | 1 | 3 | 23 | 3 | 1 | 1 | 1 | 29 | 1 | 14 |

References

- Mignard F., Cellino A., Muinonen K., et al., Dec. 2007, Earth Moon and Planets, 101, 97
 Mouret S., 2007, Investigations on the dynamics of minor planets with Gaia, Ph.D. thesis, Observatoire de Paris
 Tanga P., Hestroffer D., Delbò M., et al., 2008, Planetary and Space Science, In press

GROUND-BASED OBSERVATIONS FOR GAIA (GBOG)

Soubiran, C.¹, Allende Prieto, C.², Altmann, M.³, Bragaglia, A.⁴, Clementini, G.⁴, Frémat, Y.⁵, Heiter, U.⁶, Joliet, E.⁷, Pancino, E.⁴, Sartoretti, P.⁸, Smart, R.⁹ and Thuillot, W.¹⁰

Abstract. This contribution gives an overview of the ground-based observing efforts organized to collect the auxiliary data mandatory for the calibrations and tests of the Gaia data processing.

1 Introduction

Gaia is an ambitious space astrometry mission of ESA the main objective of which is to map the sky in astrometry down to $V=20$ mag with unprecedented accuracy. Additionally, photometry of all objects and spectroscopy down to $V=17$ will be obtained. The final catalogue will include distances, motions and astrophysical parameters of one billion stars, a fundamental dataset for unravelling the structure, formation and evolution of our Milky Way. The challenging task of the data processing is under the responsibility of 320 scientists from 15 countries organised in the DPAC consortium: a major project for the European astronomical community (Mignard et al. 2008).

The Gaia data processing requires reference data in photometry and spectroscopy in order to tie the instrumental system to physical units. The GBOG Working Group is responsible for the coordination of the joint ground-based observing efforts to collect the auxiliary data mandatory for Gaia's calibrations.

2 The major on-going observations

- For the spectrophotometric calibration of the RP-BP and G bands, it is planned to collect the absolute fluxes of 250 spectrophotometric standard stars at 1% accuracy within 330-1050 nm. The targets will be monitored for variability. The facilities used are : REM/ROSS+REMIR, TNG/DOLORES, San Pedro Martir 1.5m/LARUCA, CAHA 2.2-m/CAFOS, Loiano 1.52m/BFOSC, ESO-NTT/EFOSC2 (Large Programme).
- For the radial velocity calibration, it is planned to qualify 1000 reference stars to fix the zero point of radial velocities and to validate a method of calibration with asteroids. This implies to gather ~ 3500 RV measurements (Crifo et al. 2008). The observing programmes, supported by PNG and PNPS, are conducted on OHP/SOPHIE and TBL/NARVAL for the Northern part. An agreement was obtained with Geneva Observatory for the Southern part on the Swiss 1.2-m Leonard Euler telescope / CORALIE, with support from AS-Gaia.

¹ Laboratoire d'Astrophysique de Bordeaux

² MSSL, University College London

³ Zentrum für Astronomie der Universität Heidelberg

⁴ INAF - Osservatorio Astronomico di Bologna

⁵ Observatoire Royal de Belgique

⁶ Uppsala Astronomical Observatory

⁷ ESAC/ESA European Space Astronomy Centre

⁸ Observatoire de Paris Meudon

⁹ INAF - Osservatorio Astronomico di Torino

¹⁰ IMCCE, Observatoire de Paris

- The calibration of the classification / parametrization algorithms needs to establish a grid of reference stars for astrophysical parameter determination across the HR diagram. The corresponding spectra at high and low resolution will also be used to correct synthetic spectra. A part of the programme is made on TBL/NARVAL with support of PNPS, while a Large Programme is to be submitted on ESO-NTT/EFOSC2.
- Calibration fields are built at the Ecliptic Poles for the in-orbit test of the data processing. It is requested to assemble astrometry, photometry and spectroscopy in 1 sq. deg around each ecliptic pole. The imaging part is done on CFHT/Megaprime and ESO-MPI 2.2m/WFI, while some spectroscopy is planned on VLT/FLAMES.

3 Other on-going or foreseen observing programmes for Gaia

- Benchmark stars for critical tests of stellar atmosphere models (ESO 3.6m/HARPS, TNG/SARG)
- Library of solar analogs for Solar System studies (VLT/UVES)
- Primary standards for the flux calibration of RVS spectra 847-874 nm (La Palma 2.5m INT/IDS)
- Time-series photometry of specific classes of variable stars (network already in place)
- Spectroscopy of asteroids (TNG/DOLORES)
- ICRF link with the European VLBI Network (Bourda et al. 2008)
- Optical tracking of the satellite (network to be organised)

4 General considerations

New observations are needed because no pre-existing dataset fulfills the Gaia requirements in terms of homogeneity, precision, sky coverage, magnitude range and spectral interval.

Most of the observations must be done right now because the calibration data must be ready when the data processing will start in 2012.

All data and resulting libraries will be made available to the astronomical community and will offer excellent possibilities for various research programmes.

The GBOG observing programmes are mostly long term ones : follow-up observations will continue during the mission to ensure the stability (photometric or spectroscopic) of the sources. It implies that facilities will be needed until 2017.

The GBOG observing programmes face the problem of being in competition, for the allocation of telescope time, with programmes that are more directly scientifically related.

The GBOG observing programmes have already started with a good support of national facilities but there are still some difficulties covering the southern hemisphere.

The GBOG WG is mandated to coordinate observing programmes required to support the Gaia mission. Follow-up ground based observations resulting from Gaia science alerts are not included under this mandate.

References

- Bourda, G., Charlot, P., Porcas, R.; Garrington, S. 2008, in SF2A-2008: Proceedings of the Annual meeting of the French Society of Astronomy and Astrophysics held in Paris, France, July 2-6, 2008, Eds.: C. Charbonnel, F. Combes and R. Samadi
- Crifo, F., Jasniewicz, G., Soubiran, C., Hestroffer, D., Katz, D., Siebert, A., Veltz, L., Udry, S. 2008, in SF2A-2008: Proceedings of the Annual meeting of the French Society of Astronomy and Astrophysics held in Paris, France, July 2-6, 2008, Eds.: C. Charbonnel, F. Combes and R. Samadi
- Mignard, F., Bailer-Jones, C., Bastian, U., Drimmel, R. et al. 2008, in "A Giant Step: from Milli- to Micro-arcsecond Astrometry", Proceedings of the International Astronomical Union, IAU Symposium, Volume 248, p. 224-230

ACTIVITIES OF THE ICRS PRODUCT CENTRE (SYRTE, PARIS OBSERVATORY)

Souchay, J.¹, Bouquillon, S.¹, Barache, C.¹, Gontier, A.-M.¹, Lambert, S. B.¹, Le Poncin-Lafitte, C.¹, Taris, F.¹, Arias, E.F.², Fienga, A.³ and Andrei, A.H.⁴

Abstract.

We present the various activities of the International Celestial Reference System Product Center (ICRS-PC) hosted jointly at Paris Observatory and US Naval Observatory (Washington) in the frame of the IERS (International Earth Rotation and Reference System Service)

1 Introduction

At its 23rd General Assembly in August 1997, the International Astronomical Union (IAU) decided that starting from 1 January 1998, the IAU celestial reference system shall be the International Celestial Reference System (ICRS), in replacement of the FK5 (Fricke et al. 1988). The ICRS is accessible by means of coordinates of reference extragalactic radio sources (Arias et al. 1995), the International Celestial Reference Frame (ICRF). The ICRS complies with the conditions specified by the 1991 IAU Recommendations. Its origin is located at the barycenter of the solar system through appropriate modelling of VLBI observations in the framework of General Relativity. Its pole is in the direction defined by the conventional IAU models for precession (Lieske et al. 1977) and nutation (Wahr 1981). Its origin of right ascensions was implicitly defined by fixing the right ascension of 3C 273B (see Arias et al. (1995) for more details).

2 The activities of the ICRS Product Centre

In the following we present the various activities of the ICRS Product Centre of the IERS which is hosted both by the SYRTE at Paris Observatory and by the US Naval Observatory (Washington DC). It has two directors, one from each institution, presently R. Gaume(USNO) and J. Souchay (SYRTE), and the sharing of tasks is shared among the two institutions. They can be listed as in the following (for full bibliography, see IERS Annual report 2006, 2007).

2.1 Reference system and frame

- **Maintenance and extension of the ICRF**

We publish extensions to the ICRF consistent to the currently adopted ICRF, e.g. without changes in the positions of the 212 defining sources representing the core sources of the ICRF (Ma et al. 1998). Moreover we compare on a regular basis the VLBI catalogues of quasars obtained by different networks.

- **Investigation of future VLBI realizations of the ICRS**

Fundamental revisions to the ICRF will occur only when improvements in the quantity of data, together with modeling and data analysis strategies are sufficient to justify a complete reconstruction of the standard frame. The responsibility for this decision lies with the appropriate IAU and IVS groups of experts, of which four reserchers of the ICRS PC at the SYRTE are members.

¹ SYRTE, Observatoire de Paris, 61, av. de l'observatoire, 75014 Paris

² BIPM

³ Observatoire de Besançon

⁴ Observatorio Nacional/MCT, Rio de Janeiro // Observatorio do Valongo;UFRJ, Rio de Janeiro

- **Investigation of future non VLBI realizations of the ICRS**

Future astrometric satellite missions such as J-MAPS, SIM and GAIA, may provide fundamental reference frames more accurate than the current VLBI-based ICRF. Members of the ICRS Product Centre have direct ties to these programs, and are in a unique position to study these prospective reference frames.

2.2 Extragalactic radio-sources

- **Monitoring of structure to assess astrometric quality**

The task of imaging the sources (essentially quasars) from VLBI observations and evaluating their astrometric quality is shared between the USNO and Bordeaux observatory.

- **Maintenance of the time stability of the ICRF** Members of the SYRTE address the time stability of the celestial reference frames and the effect on geodetic products. To do so they provide the time variation of the sources astrometric coordinates (Lambert & Gontier 2008)

2.3 Link of other reference frames to the ICRS

- **Maintenance of the link to Hipparcos catalogue**

The location of Hipparcos axes is an object of particular attention, as well as the effect of Hipparcos proper motion uncertainties. An example is the UCAC program which provides a link at the level of 1 mas.

- **Maintenance of the link to the solar dynamical reference frame through millisecond pulsar analysis**

Pulsar timing is a very accurate way to position the ecliptic with respect to the ICRF. Efforts have been recently developed in the frame of a PPF (Plan Pluri Formation) led by A. Fienga (Besançon Observatory), in association with the Nancay radiotelescope where pulsars are observed in a very regular basis, the SYRTE and the IMCCE (Paris Observatory).

- **Maintenance of the link to the solar system dynamical reference frame through observations of asteroids and planets**

Following the asteroids trajectories with respect to quasars enables one to get direct link between the dynamical system and the ICRF. Studies are done recently in order to make statistics of the close approaches between these two classes of objects and to observe these close approaches with middle size telescopes.

- **Maintenance of the link to the solar system dynamical reference frame through Lunar Laser Ranging analysis** The SYRTE has a long history of analysis of the Lunar Laser Ranging (LLR) observations done at CERGA (Grasse). When combined with VLBI technique, the LLR technique is one of the most efficient ways to determine the orientation of the planetary reference frame relative to the ICRF. The ICRS PC gather the various data coming from LLR measurements.

3 Discussion and conclusion

Recent studies in the frame of the ICRS Product Centre at the SYRTE-USNO have begun in the scope of the GAIA mission. One of them is the preparation of a Large Quasar Astrometric Catalogue (Souchay et al. 2008), which contains 113 663 objects. It could serve as a kind of input catalogue for GAIA, to make statistics and to cross-identify the objects with the 200 000 quasars or more which will be observed by the astrometric space mission. Another study is the follow-up of the WMAP satellite which is located at the L_2 Lagrange point, as GAIA. Applying the same methods will allow a very accurate astrometric determination of GAIA.

References

- Arias, E. F., Charlot P., Feissel M., & Lestrade J.-F. 1995 *Astron. Astrophys.*, 303, p. 604
 Fricke, W., Schwan, H., & Lederle, T. 1988: FK5, Part I. Verff. *Astron. Rechen Inst.*, Heidelberg.
 IERS Annual report 2006 or 2007, Verlag des Bundesamts für Kartographie und Geodäsie (BKG), Frankfurt, Main
 Lieske, J. H., Lederle, T., Fricke, W., and Morando, B., *Astron. Astrophys.*, 58, pp. 1-16.
 Ma, C., & Arias, E.F., Eubanks, M., et al. 1998, *AJ*116,516
 Wahr, J.M., Geophys. J.R. *Astron. Soc.*, 64, 705

RADIAL VELOCITIES WITH THE GAIA RVS SPECTROMETER

Viala, Y.P.¹, Blomme, R.², Damerdji, Y.³, Delle Luche, C.¹, Frémat, Y.², Gosset, E.³, Jonckheere, A.², Katz, D.¹, Martayan, C.², Morel, T.³, Poels, J.³ and Royer, F.¹

Abstract. Four different methods are used to derive radial velocities from spectra observed by the Gaia Radial Velocity Spectrometer (RVS). They are briefly presented here together with very preliminary results.

1 Introduction

The main aim of the Gaia Radial Velocity Spectrometer (RVS) is to determine the radial velocities of nearly 100 to 200 millions of stars, with an expected accuracy of 1 km/s up to magnitude $V = 13$ and 15 km/s down to $V = 16$. These data will be a very useful tool for kinematics and dynamics studies of our Galaxy.

The Gaia data will be processed and analyzed by an international consortium (DPAC) including ESA and European institutes participating to the mission (Mignard & Drimmel 2007). Within DPAC nine coordination units CU have in charge a specific scientific or management problem. The processing of spectroscopic data provided by the RVS is devoted to CU6. The aim of this paper is to briefly present the work done within the development unit (DU) "Single transit analysis (STA)" in charge of analysing the data obtained during a unique transit of an object through the RVS field of view.

2 Radial velocity determination of single stars during a single transit

Deriving radial velocities of the observed object is an important task of DU STA. We restrict here to radial velocity determination of single stars. Four different algorithms have been developed using Java programming language : i) Cross-correlation between the object spectrum and a template spectrum in direct space, ii) Cross-correlation between the object spectrum and a template spectrum in Fourier space, iii) Cross-correlation between the object spectrum and a template spectrum in Fourier space using the Chelli's method (Chelli 2000), iv) Method of minimum distance between the object spectrum and a series of templates. A detailed description of these methods can be found in (Viala et al. 2007).

For a given set of astrophysical parameters/magnitude, Monte-Carlo simulations (provided by CU2) led to 1000 spectra differing only by noise realisation but all shifted by 20 km/s. Radial velocities from the series of spectra were derived by the 4 algorithms. As an example, figure 1 shows histograms of the radial velocities for solar type stars of magnitude 8.6, 10.6 and 12.6. The mean value of the distribution slightly differ from 20 km/s : this small bias is due to different slopes of the continuum between the object and the template spectrum. The dispersion of the distribution gives the error on the radial velocity determination. Preliminary error derivations are listed in table 1 for several spectral types.

3 Conclusion

For a single transit and for the three methods discussed, radial velocities can be determined with a fairly good accuracy in the range 1 to 8 km/s down to magnitude $G_{RVS} \leq 14$ for F-G-K spectral types. Accuracies and magnitude limit are much less good for hotter stars (Spectral types O, B and A). Tests have not yet been done for cool M stars. Tentative determination of the projected rotational velocities, using the three algorithms developed within DU STA is planned for a near future.

¹ Observatoire de Paris, GEPI, 92195 Meudon Cedex

² Observatoire Royal de Belgique, Avenue circulaire 3, B 1180 Uccle(Bruxelles)

³ Institut d'Astrophysique et de Géophysique, Université de Liège, Allée du 6 août, B-4000 Liège

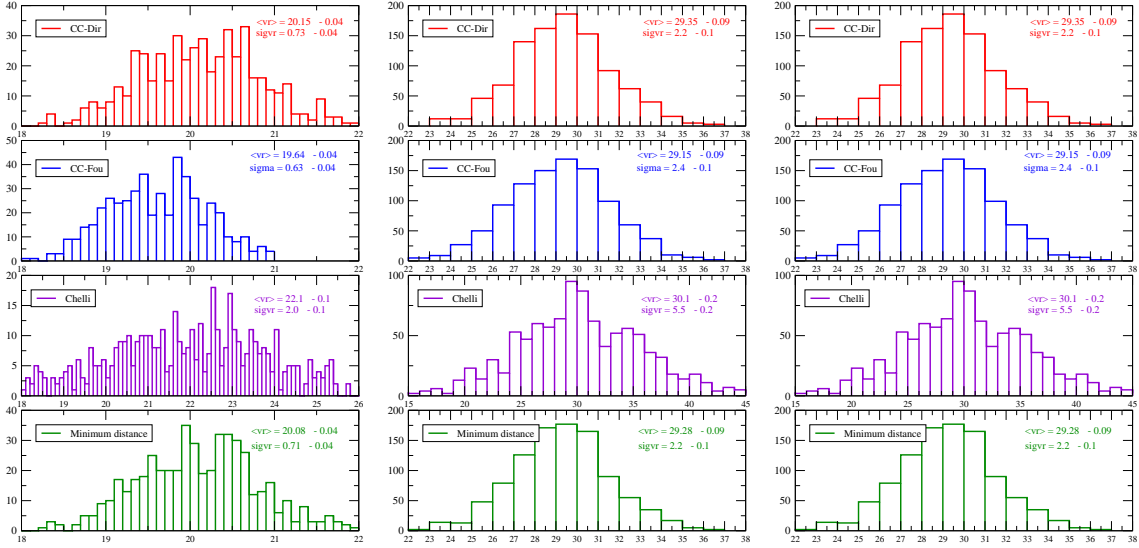


Fig. 1. Histograms derived radial velocities by the 4 algorithms for a G5V star of RVS magnitude 8.6, 10.6 and 12.6

Table 1. Errors from Monte Carlo simulations on radial velocity derivation for single stars of various spectral types

| Sp. type | T_{eff} | log g | Fe/H | RVS magnitude | error on vrاد in km/s | | | |
|----------|-----------|-------|------|---------------|-----------------------|-------|--------|---------|
| | | | | | CCDir | CCFou | Chelli | MinDist |
| K5V | 4000 K | 4.0 | 0.0 | 8.7 | 0.63 | 0.63 | 1.8 | 0.62 |
| | | | | 12.7 | 7.1 | 7.5 | 22.2 | 7.4 |
| G5V | 5500 K | 4.0 | 0.0 | 8.6 | 0.73 | 0.63 | 2.0 | 0.71 |
| | | | | 12.6 | 7.9 | 8.1 | 26.6 | 8.1 |
| F5V | 7500 K | 4.0 | 0.0 | 8.2 | 0.87 | 0.85 | 3.7 | 0.86 |
| | | | | 12.2 | 8.6 | 8.8 | 46.2 | 8.5 |
| A5V | 10000 K | 4.0 | 0.0 | 7.5 | 0.94 | 0.92 | 5.9 | 0.96 |
| | | | | 11.5 | 11.1 | 12.9 | 46.2 | 10.6 |
| B2V | 20000 K | 4.0 | 0.0 | 6.8 | 3.0 | 3.1 | 15.5 | 2.4 |
| | | | | 10.8 | 31.9 | 33.7 | 315 | 24.8 |
| B0V | 30000 K | 4.0 | 0.0 | 6.4 | 2.7 | 2.8 | 17.0 | 2.3 |
| | | | | 9.9 | 33.5 | 18.3 | 204 | 28.9 |
| O6V | 39000 K | 4.0 | 0.0 | 6.4 | 4.1 | 0.5 | 14.5 | 53.0 |

References

- Chelli, A. 2000, AA, 358, L59
Mignard, F., & Drimmel, R. 2007, ESA Note, GAIA-CD-SP-DPAC-FM-030-2
Viala, Y., Blomme, R., Dammerdji, Y., et al. 2007, ESA Note, GAIA-C6-SP-OPM-YV-004-1
Viala, Y., Blomme, R., Dammerdji, Y., et al. 2008, ESA Note, GAIA-C6-SP-OPM-YV-002-3

SIMULATING CHARGE TRANSFER INEFFICIENCY EFFECTS ON FUTURE GAIA DATA

Weiler, M.¹ and Babusiaux, C.¹

Abstract. Gaia is an ESA cornerstone mission to perform high-accuracy astrometry as well as photometry of about 10^9 objects in the sky down to 20^{mag} . For the brightest objects also spectroscopic observations will be obtained. To reach the accuracy aimed for, the data calibration has to correct for Charge Transfer Inefficiency effects in the CCDs, resulting from particle irradiation in space. This work presents first attempts to simulate the influence of such effects upon the expected data Gaia will provide - an essential step towards the development of calibration procedures.

1 Introduction

The Gaia spacecraft will scan the whole sky continuously during five years. All non-extended astronomical sources brighter than 20^{mag} will be automatically detected and the CCD data within a window allocated to the source will be sent to ground. The CCDs will be operated in Time Delay and Integration mode (TDI), shifting the electrical charges produced by the light of the source with the same velocity towards the read-out register as with which the source moves over the focal plane due to the scanning. From the windows allocated to a source on different CCDs, the position of the center of the Point-Spread-Function (PSF), the brightness of the source, and, using the spectroscopic instrument, the position of spectral lines will be determined (Lindegren et al. 2008).

2 What is Charge Transfer Inefficiency?

In the space environment, the CCDs will be subject to particle irradiation, mainly by protons of solar origin. The particles can cause displacements of atoms from their regular position within the CCD semiconductor lattice. Such vacancy defects result in localized electronic energy levels between the valence band and the conduction band. Electrons from the conduction band can enter these energy levels and getting thus excluded from the charge transfer until a re-emission to the conduction band. The defects are therefore called "traps", while the full effect is called Charge Transfer Inefficiency (CTI). It leads to a "smearing" of the PSF, complicating the data analysis.

Since electron release time scales can reach up to hundreds of seconds, sources that have passed over the CCD before a particular other source can influence the CTI effects. Traps may still be filled by electrons from the preceding source, or electrons captured from the source before are released into the PSF of the following source.

3 How are Charge Transfer Inefficiency Effects Modeled?

The current modeling approach, a certain number of electrons inside a CCD pixel access a certain number of traps and fill these traps completely, while the remaining number of traps inside the pixel remains empty. It is assumed that the electrons are captured instantaneously by the traps (i.e. the capture time constant is much smaller than the residence time inside one pixel), and that the electrons are re-emitted according to a sum of five exponentials. Each exponential represents a particular type of trap, characterized by its release time constant. Such different types of traps could be realized by complexes of two or more vacancy defects in the lattice, or by

¹ Observatoire de Paris-Meudon, GEPI, 92195 Meudon, France

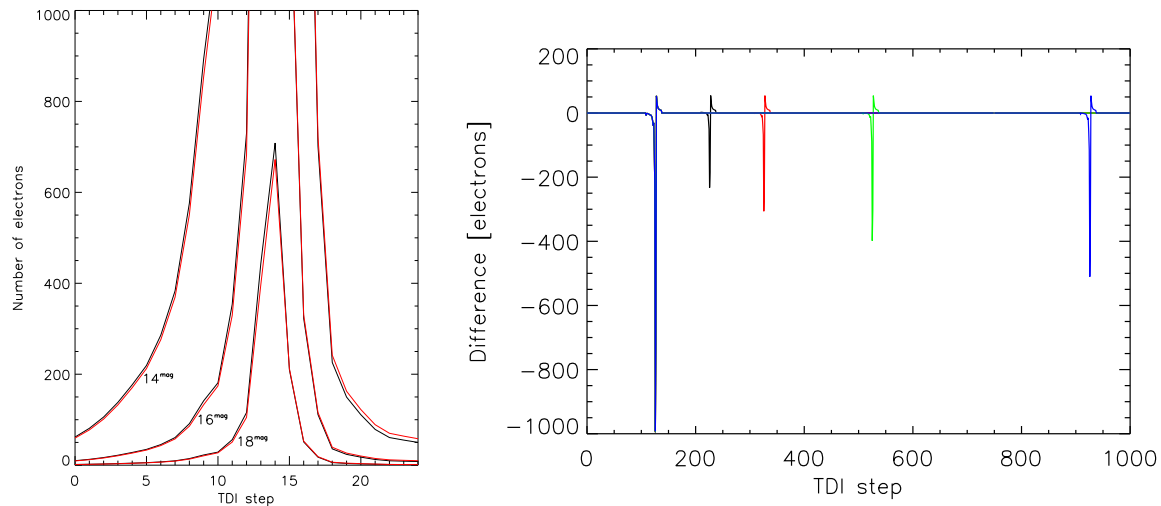


Fig. 1. Left: Cut through the central part of the PSF of stars with three different magnitudes. Black lines: without CTI effects, red lines: with CTI effects. **Right:** Difference in electrons between simulations with and without CTI effects for two consecutive stars. The different colours represent the results for different separations of the stars. In both images pixels were read out in the order of increasing numbers of TDI steps.

complexes of vacancy defects and dopants. The model keeps track of the amounts of electrons that have passed through a CCD pixel before, and thus allows to compute the fraction of empty traps and the release probability of electrons from filled traps at any TDI step. The model is included in the Gaia Instrument and Basic Image Simulator, GIBIS, that allows to simulate Gaia data, taking the physical properties of the sources as well as the optical, electronic, and mechanical properties of the Gaia spacecraft and instruments into account (Babusiaux 2005).

4 Simulation Results

First results of the modeling of CTI effects for simple source configurations are presented in Fig. 1. The left shows the central row of the PSF of stars of three different magnitudes with and without CTI effects. One can see a loss of electrons on the leading edge of the PSF and the center due to electron capture, and an excess of electrons on the trailing edge due to re-emission. The right shows the difference in electrons between a simulation without and with CTI effects for two consecutive stars of the same brightness (14^{mag}). In all cases one sees again the typical loss of electrons on the leading edge of the PSF and an excess of electrons on the trailing edge. For the trailing star, the charge loss is reduced compared to the leading star since traps are filled by electrons captured from the leading star. The larger the distance between the leading and the trailing star is, the less effective is the reduction of CTI effects for the trailing star.

5 Outlook

For more effective simulations of CTI effects, more realistic models are currently developed. These models will release strong assumptions such as the instantaneous capture of electrons. Furthermore, new models aim for faster computations in order to simulate the CCD read-out over longer times. For a more accurate modeling of the CTI effects, better constrained trap parameters (number, release time constants) are required.

References

- Babusiaux, C. 2005, ESASP 576, 417
 Lindegren, L., et al. 2008, IAU Symposium, Vol. 248, 217-223